NAVAL POSTGRADUATE SCHOOL

MONTEREY, CALIFORNIA

THESIS

TRIBOELECTRIC NANOGENERATOR WITH OCEAN WAVE ENERGY

by

Sarah G. Reilly

June 2019

Thesis Advisor: Young W. Kwon
Second Reader: Jarema M. Didoszak

Approved for public release. Distribution is unlimited.

THIS PAGE INTENTIONALLY LEFT BLANK

REPORT DOCUMENTATION PAGE				*Form Approved OMB No. 0704-0188*

1. AGENCY USE ONLY ***(Leave blank)***	**2. REPORT DATE** June 2019	**3. REPORT TYPE AND DATES COVERED** Master's thesis

4. TITLE AND SUBTITLE TRIBOELECTRIC NANOGENERATOR WITH OCEAN WAVE ENERGY	**5. FUNDING NUMBERS**
6. AUTHOR(S) Sarah G. Reilly	
7. PERFORMING ORGANIZATION NAME(S) AND ADDRESS(ES) Naval Postgraduate School Monterey, CA 93943-5000	**8. PERFORMING ORGANIZATION REPORT NUMBER**
9. SPONSORING / MONITORING AGENCY NAME(S) AND ADDRESS(ES) N/A	**10. SPONSORING / MONITORING AGENCY REPORT NUMBER**

11. SUPPLEMENTARY NOTES The views expressed in this thesis are those of the author and do not reflect the official policy or position of the Department of Defense or the U.S. Government.

12a. DISTRIBUTION / AVAILABILITY STATEMENT Approved for public release. Distribution is unlimited.	**12b. DISTRIBUTION CODE** A

13. ABSTRACT (maximum 200 words)

This research successfully developed and tested an improved triboelectric nanogenerator (TENG) with water waves at the Naval Postgraduate School (NPS). The copper electrode holder and track to which the PTFE tape was attached were printed at NPS via a 3D printer. Both the original and improved TENGs were successfully tested with a linear reciprocating motor at two different speeds and with three different weight conditions. In addition, the improved TENG was also tested with thinner PTFE tape. It was found that the biggest influence on the alternating current (AC) output voltage for the TENG was the frequency at which it was operated. The improved TENG was then simply modeled to predict a peak AC output voltage based on input TENG frequency. Finally, the improved TENG was attached to the side of an acrylic column with the ability to operate only in the vertical (heave) direction. It was tested in a wave tank with seven different frequencies and we found that the improved TENG was successful in producing AC voltage output from the waves of the wave tank.

14. SUBJECT TERMS blue energy, triboelectric nanogenerator, oscillating column, wave energy	**15. NUMBER OF PAGES** 127
	16. PRICE CODE

17. SECURITY CLASSIFICATION OF REPORT Unclassified	**18. SECURITY CLASSIFICATION OF THIS PAGE** Unclassified	**19. SECURITY CLASSIFICATION OF ABSTRACT** Unclassified	**20. LIMITATION OF ABSTRACT** UU

NSN 7540-01-280-5500

Standard Form 298 (Rev. 2-89)
Prescribed by ANSI Std. 239-18

THIS PAGE INTENTIONALLY LEFT BLANK

Approved for public release. Distribution is unlimited.

TRIBOELECTRIC NANOGENERATOR WITH OCEAN WAVE ENERGY

Sarah G. Reilly
Ensign, United States Navy
BS, U.S. Naval Academy, 2018

Submitted in partial fulfillment of the
requirements for the degree of

MASTER OF SCIENCE IN MECHANICAL ENGINEERING

from the

NAVAL POSTGRADUATE SCHOOL
June 2019

Approved by: Young W. Kwon
Advisor

Jarema M. Didoszak
Second Reader

Garth V. Hobson
Chair, Department of Mechanical and Aerospace Engineering

THIS PAGE INTENTIONALLY LEFT BLANK

ABSTRACT

This research successfully developed and tested an improved triboelectric nanogenerator (TENG) with water waves at the Naval Postgraduate School (NPS). The copper electrode holder and track to which the PTFE tape was attached were printed at NPS via a 3D printer. Both the original and improved TENGs were successfully tested with a linear reciprocating motor at two different speeds and with three different weight conditions. In addition, the improved TENG was also tested with thinner PTFE tape. It was found that the biggest influence on the alternating current (AC) output voltage for the TENG was the frequency at which it was operated. The improved TENG was then simply modeled to predict a peak AC output voltage based on input TENG frequency. Finally, the improved TENG was attached to the side of an acrylic column with the ability to operate only in the vertical (heave) direction. It was tested in a wave tank with seven different frequencies and we found that the improved TENG was successful in producing AC voltage output from the waves of the wave tank.

THIS PAGE INTENTIONALLY LEFT BLANK

TABLE OF CONTENTS

LIST OF FIGURES

THIS PAGE INTENTIONALLY LEFT BLANK

LIST OF TABLES

THIS PAGE INTENTIONALLY LEFT BLANK

LIST OF ACRONYMS AND ABBREVIATIONS

AC	alternating current
NOAA	National Oceanic and Atmospheric Administration
OC	oscillating column
OWC	oscillating water column
PENG	piezoelectric nanogenerator
PTFE	polytetrafluoroethylene
TENG	triboelectric nanogenerator

THIS PAGE INTENTIONALLY LEFT BLANK

ACKNOWLEDGMENTS

I would like to thank my family and friends for their support throughout my time of study at the Naval Postgraduate School. In addition, I would like to thank Dr. Kwon and Professor Didoszak for their guidance and assistance throughout this project. Also, I would like to thank Lieutenant Katherine Mann for her help in developing this triboelectric nanogenerator. Finally, I would like to thank John Mobley in the Mechanical Engineering Machine Lab, STG1 Cauffiel in the RoboDojo, and Professor Sakoda for their help in fabricating parts for this project.

THIS PAGE INTENTIONALLY LEFT BLANK

I. INTRODUCTION

A. MOTIVATION

The world uses more and more technology and devices that require electricity every single day. This leads to the increasing desire for further ways to generate this electricity. For a long time, humans have depended on the use of fossil fuels for electrical power. As a result, one of the greatest global threats has emerged: global warming.

In response to the impacts of global warming there have been advances in green energy (wind and solar energy) adding to the power grids of many nations. All across the world, people are using solar panels on top of their roofs and wind farms can be found alongside highways. The use of these innovative technologies has helped decrease the burning of fossil fuels. Yet, there is still a lot of room for improvement to find additional alternate energy sources that have lower environmental impact than fossil fuels.

Nearly 71% of the world is covered in water. Of this 71%, about 96.5% of this water is found in the oceans [1]. This equates to 68.5% of the world being water found in the ocean. In addition, about 44% of the population of the world lives within 150 kilometers of the coast [2]. The world revolves around the use of the ocean for trade and travel. According to the National Oceanic and Atmospheric Administration (NOAA), “In 2014, the ocean economy, which includes six economic sectors that depend on the ocean and Great Lakes, contributed more than $352 billion to the U.S. GDP and supported 3.1 million jobs” [3]. In addition, “In 2016, the U.S. maritime transportation system carried $1.5 trillion of cargo through U.S. seaports to and from our international trading partners” [3]. The ocean is powerful for the world economy, but is the power of the ocean being extracted to the fullest capability?

The basis of energy is a wave. Waves are naturally found in the oceans due to wind and the gravitational pull of the sun and the moon [3]. In theory, the world could entirely be powered by the energy found in the waves of the oceans without adding any pollution to the atmosphere. The solution to the energy crisis seems to be obvious with the power found in the ocean being a natural source. Yet, the technology to garner this energy is still in the early stages of development.

There are some challenges in the way of letting this huge source of energy to be used. The main issues arise from the powerful and chemical nature of the ocean. Some of the biggest problems are due to the lack of sustainability and durability of the devices proposed to harness the ocean's energy. The continuous and repetitive nature of waves is great for consistency and reliability, yet, the roughness of the seas can cause issues in sustainability. In addition, the ocean consists of salt water, therefore, specific materials are required to prevent corrosion and increase durability of the devices used. However, the tremendous benefit is that the waves of the ocean offer the highest energy density of any renewable energy source [4]. This research focuses on finding a way to extract the mechanical energy naturally found in ocean waves and convert it into electrical energy with a device that is sustainable and affordable.

B. LITERATURE REVIEW

1. Blue Energy Systems

Blue energy is the name given to the energy found in the waves of the ocean. A multitude of different advances have been made in the systems to extract blue energy. The use of blue energy offers many benefits such as minimal environmental impact, the ability of waves to travel long distances without losing much energy, and the accessibility of being able to use wave energy devices about 90% of the time (compared to availabilities of about 20–30% of the time with solar and wind energy devices). The technology to harvest this energy has over 1,000 patents in Japan, North America and Europe. These technologies are usually differentiated by their location and type [5].

The three main locations for blue energy devices are shoreline, nearshore and offshore. Shoreline is considered to be in the shallow water near the shore. The shoreline devices have the advantages of being close to land and easier to maintain. In addition, they have a lower chance of being damaged in extreme weather conditions as they could be removed if harsh seas are predicted [5]. One disadvantage is that as a result of being in shallow water, the waves tend to have less power near the shore. Nearshore devices are located a bit farther out into the water, but still have the ability to be attached to the seabed. Nearshore devices tend to have the same disadvantage as the shoreline devices of not being able to take advantage of more powerful waves due to their shallow water location. Offshore devices are generally found in deep water. Deep water devices tend to be more expensive, difficult to construct, and maintain due to being further from the shore and encountering more extreme conditions (greater wave heights and energies). Yet, these more powerful waves can lead to greater power generation [5].

The three major types of wave energy devices are attenuators, point absorbers, and terminators [5]. Attenuators, shown in Figure 1, are positioned parallel to the direction the wave is traveling.

Figure 1. Attenuators in Ocean Waves. Source: [5].

Point absorbers, shown in Figure 2, are small compared to the wavelength they are harvesting the energy from and tend to gather energy from the rising and falling motion of waves.

Figure 2. Point Absorbers in Ocean Waves. Source: [5].

Terminators, shown in Figure 3, are positioned perpendicular to the direction that the wave is traveling.

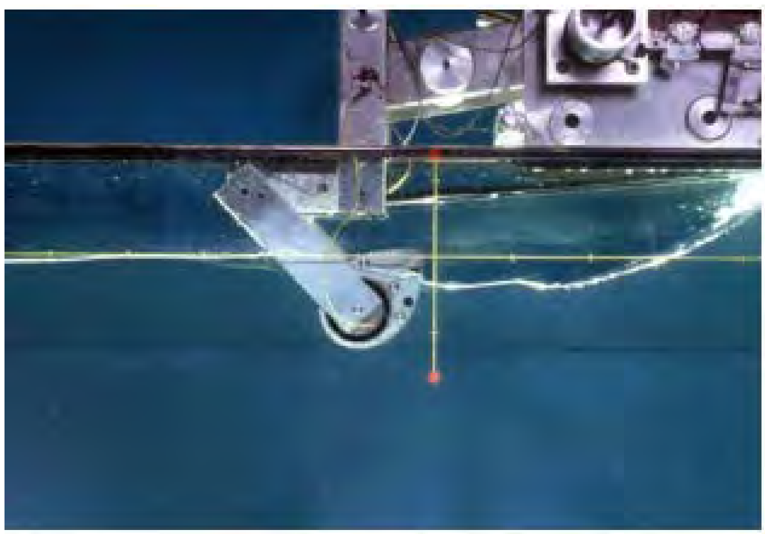

Figure 3. Terminator in Water. Source: [5].

Of the over 1000 different patents, they can all be divided into one of these three locations (shoreline, nearshore, off shore) and one of these three types (attenuators, point absorbers, terminators) [5].

Another way to further classify a wave energy device is by their mode of operation. There is a plethora of modes of operations for wave energy devices, but some of the major ones are submerged pressure differential, oscillating wave surge converter, oscillating water column and overtopping device [5]. A submerged pressure differential device is, “a submerged point absorber that uses the pressure difference above the device between wave crests and troughs” [5]. An oscillating wave surge oscillator is a type of terminator that utilizes the horizontal velocity of waves [5]. An oscillating water column (OWC) could act as either a point absorber or a terminator if it attached to the shoreline [5]. An OWC utilizes a chamber filled with air and the water level that is open to the motion of the wave. As the wave goes through the chamber, pressure is applied to the air through the motion of the wave and is usually pushed through a turbine. An overtopping device has the waves go over it and collects the energy of water the wave through a turbine, which then releases the water back out [5].

The potential to use the power found in the waves of the ocean as a renewable energy is high. There is a wide variety of types and locations for devices with the ability to capture the energy found in ocean waves. Prior reviews of these technologies come to similar conclusions [6], [7]. Those conclusions are that the potential is very high, but it is expensive to make, deploy, test and maintain the devices so progress in the research is slow to develop.

2. Nanoenergy

Electric charges surround everything people do daily. One of these electric charges is called piezoelectricity. The electric charge accumulates in certain materials when mechanical stress is applied to them. It has been proven that one can harness these charges to convert them to usable electricity. The first successful piezoelectric nanogenerator (PENG) converted mechanical energy to electrical energy on a nanoscale with the use of zinc oxide nanowire arrays in 2006 [8]. This device depended on the potential created by the zinc oxide wire to produce the electricity. It was developed with the goal of being able to self-power nanodevices such as portable electronics, wireless sensors, or real-time biomedical monitoring devices [8].

Following the research and analysis of PENGs, there was the evolution of the use of triboelectricity. Triboelectricity is found in the electrostatic phenomenon and commonly found through friction. In the past, this friction has caused a design concern for devices with the presence of charges where they are not beneficial or could be dangerous. Now these charges are being than seen as something that could be utilized to power devices. These charges and potentials found could be a solution to the current need for more clean and renewable energy by utilizing what is already available in our daily life. The first triboelectric nanogenerator (TENG) was introduced in 2012 by the same group that successfully used the piezoelectric nanogenerator [9]. The development of the TENG in 2012 was the beginning of research into harnessing triboelectricity with devices that produce usable electricity from mechanical energy while maintaining low cost and high durability.

The first TENG that was developed in 2012 used two thin polymer films pressed together, Kapton (polyimide) and polyester (PET) [9]. On the nanoscale, these two materials have different roughness, which allows for friction through a relative sliding between the two materials when the TENG is operated. The primary operation of this TENG was achieved through the bending of the stack of materials. On the outside of each of the polymers was a thin layer of aluminum alloy. This aluminum produced equal but opposite charges than the polymer, it was attached to and allowed the TENG to be connected to an external circuit to examine the electrical outputs [9]. The schematic of the first TENG is shown in Figure 4.

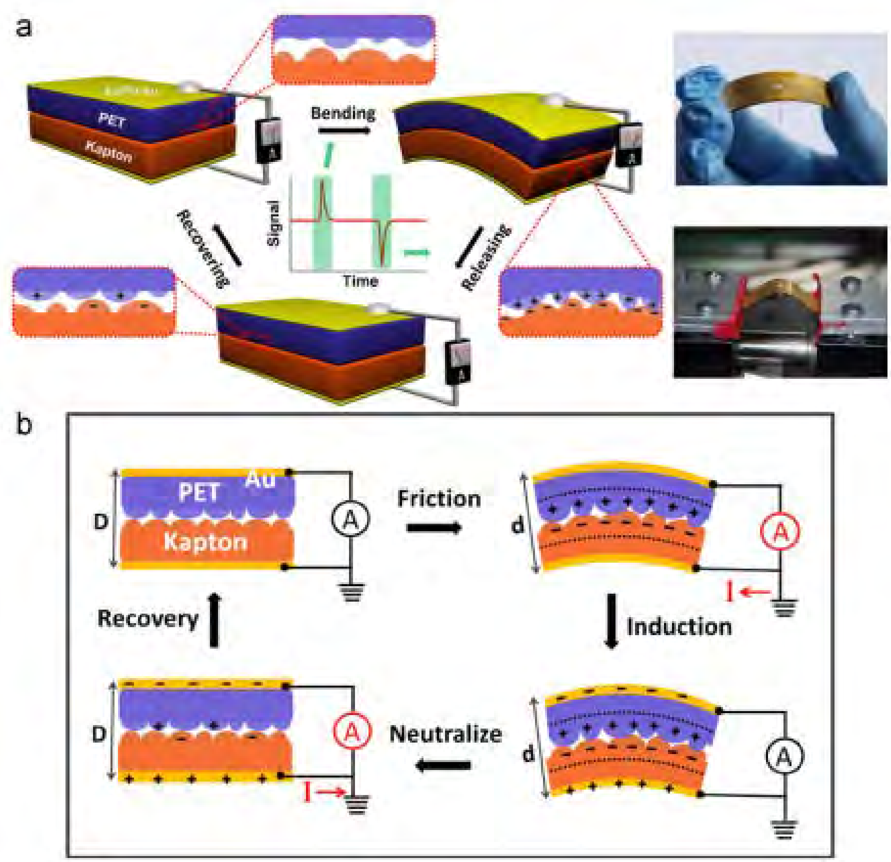

Figure 4. First TENG from 2012. Source: [9].

Since the introduction of the first TENG in 2012, a great deal of different types of TENGS were developed. These TENGS can be classified into four different working modes. These four modes are vertical contact-separation mode, single-electrode mode, freestanding triboelectric-layer mode, and contact-sliding mode [10]. The operation of these modes are shown in Figure 5. The motion of the two contact surfaces with respect to one another are shown with the blue arrow.

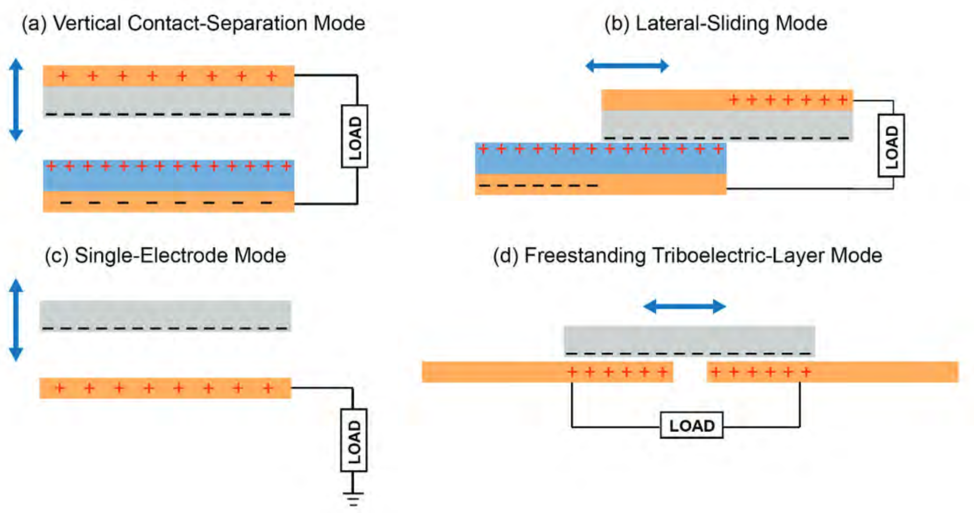

Figure 5. Four Working Modes of the TENG. Source: [10].

The concentration of this research is using the contact-sliding mode of the TENG. The contact-sliding mode operates by these mean. "When two dielectric films are in contact, a relative sliding in parallel to the surface also creates triboelectric charges on the two surfaces. A lateral polarization is thus introduced along the sliding direction, which drives the electrons on the top and bottom electrodes to flow in order to fully balance the field created by the triboelectric charges. A periodic sliding apart and closing generates the AC output" [11]. The current flow depends on how the two materials are matched with each other. More specifically, "When the two surfaces are fully matched there is no current flow, because the positive charges at one side are fully compensated by the negative ones. Once relative displacement is introduced by an externally applied force in the direction parallel to the interface, triboelectric charges are not fully compensated at the displaced/ mismatched areas, resulting in the creating of an effective dipole polarization in parallel to the direction of the displacement. Therefore, a potential difference across the two electrodes is generated" [12]. This sliding TENG has been modeled [13] and proven to work with linear-grating [14] and checker-like interdigital electrodes [15].

In the past seven years since the TENG was first introduced, it has continued to have further developments and uses. The application of the TENG is broken down into two major categories: harvesting from the environment or self-powered devices/sensors [16].

One of the large research areas with the TENG is using the mechanical energy found in water. There are two types of mechanical energy typically found in water, one from the motion of the water flowing, and the other from the motion of the waves [17]. There is a great amount of research that has been completed with the TENG for both capturing the energy from the motion of flowing water [18]-[25] and the motion of water waves [26]-[34]. One TENG has been developed with the ability to harness the water energy from both the motion of the water and the motion of the waves in addition to the wind energy [17]. The focus of this research is on harvesting mechanical energy from the environment, specifically harvesting blue energy from the motion of waves using a lateral-sliding mode TENG.

THIS PAGE INTENTIONALLY LEFT BLANK

II. EXPERIMENTATION PROCESS

A. DEVELOPMENT OF A TENG

The first step was to design, fabricate, and test a TENG. The general design of this TENG was inspired by research out of NASA Ames in Mountain View, California [35]. Their researched focused on having a TENG that was not machined at all, but was made from all printed pieces. The main design concept that was used from this TENG was the interdigitated design of the electrode pieces. One major consideration while developing a TENG is the materials being used. A successful TENG uses two materials that are far away from each other on the triboelectric series so that the electrons will be easily transferred between the two materials [36]. The transfer of these electrons between the two materials is what causes the triboelectricity. The two main materials used in the generation of triboelectricity were copper and Polytetrafluoroethylene (PTFE) tape. The choice of these two materials was inspired by a TENG made of Teflon tape and conductive copper foil tape [37]. These two materials are cost effective and on opposite sides of the triboelectric series.

The block of the TENG where the electrodes were placed into was designed in SolidWorks. The spaces for the fingers of the electrodes were made to a depth of 0.5 millimeters and at the end, the depth was increased slightly to allow for soldering at the end of the electrode. The SolidWorks model for the TENG is shown in Figure 6. The units of this model are in millimeters.

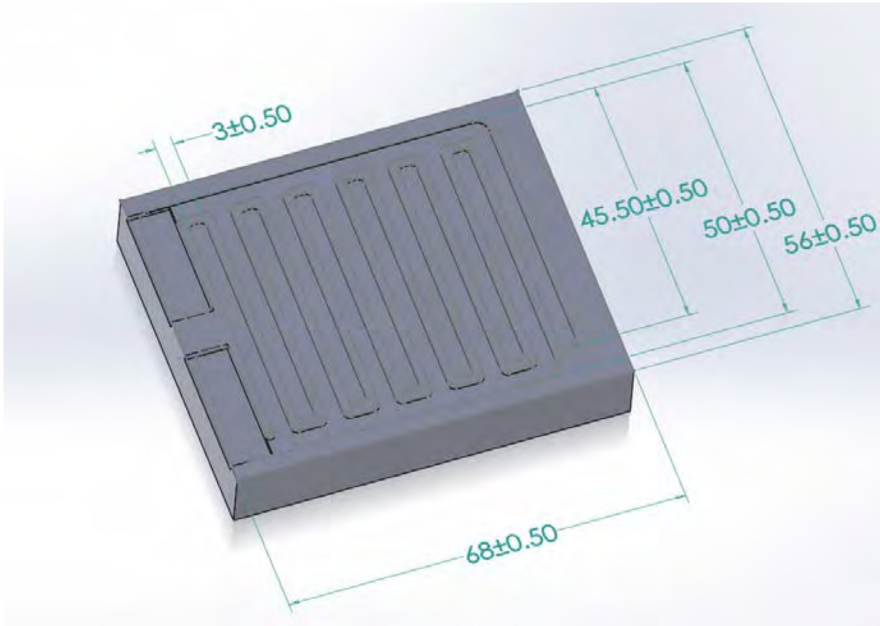

Units in millimeters.

Figure 6. SolidWorks Model for the Electrode Holder of the TENG

This was 3D printed at the RoboDojo at the Naval Postgraduate School in Monterey, California, using an Ultimaker 3 Extended. After the SolidWorks model was established, it was brought to the machine shop to have a copper electrode machined. At the time, a piece of copper readily available in the shop was machined to fit inside the SolidWorks model for the TENG. Wires were then soldered onto the ends of the electrodes to allow for AC voltage readings from the TENG in operation. These copper electrodes are shown in Figure 7.

Figure 7. Copper Electrodes with Wires Soldered On

After the copper electrodes were cut and the wires were soldered on, they were placed into the 3D printed electrode holder. The copper electrodes in the 3D printed electrode holder are shown in Figure 8.

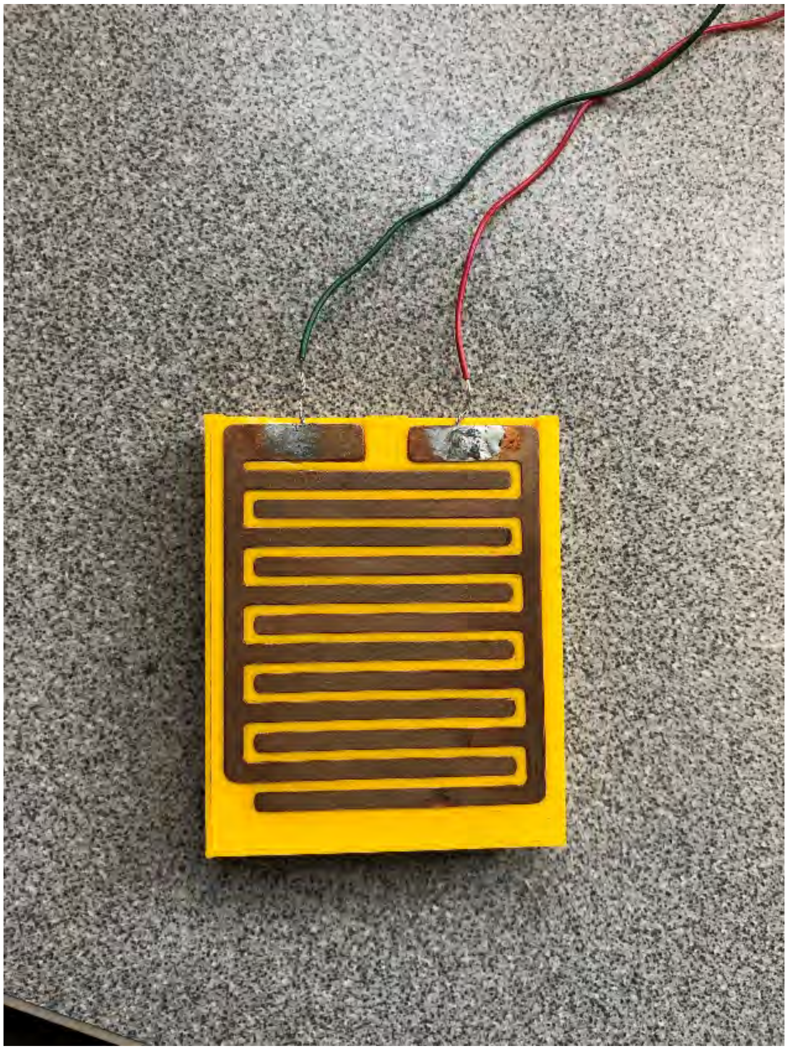

Figure 8. Original TENG Copper Electrodes in Electrode Holder

The track for the TENG to slide on was also modeled and designed in SolidWorks as shown in Figure 9.

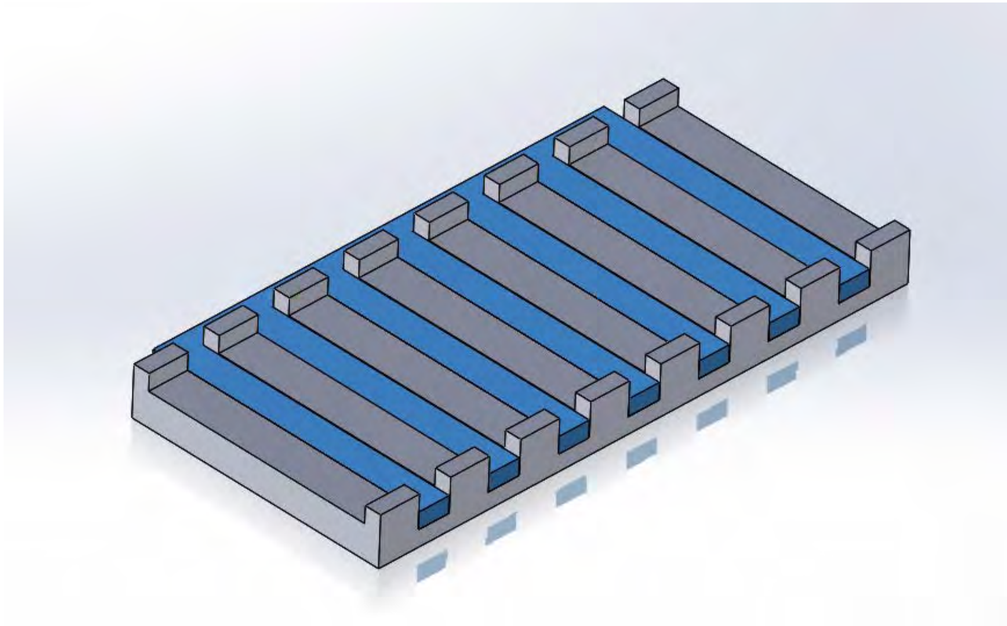

Figure 9. SolidWorks Model for Original “Train Track” Track Setup

This original design was made to allow a 3D printed piece to click in and secure the pieces of PTFE tape because the tape was not adhesive. This piece was 3D printed at the RoboDojo at the Naval Postgraduate School in Monterey, California, using an Ultimaker 3 Extended. The assembly of this track is shown in Figure 10.

Figure 10. 3D Printed Original “Train Track” Track with PTFE Tape

After this track design was constructed, it was determined that it was difficult to perfectly match up the piece that clicked into the TENG track with the TENG track due to the tolerances of the 3D printers. It was decided that it would be better to have individual blocks to fit into the slots of the track to hold the PTFE tape down. The SolidWorks model of this new track design is shown in Figure 11.

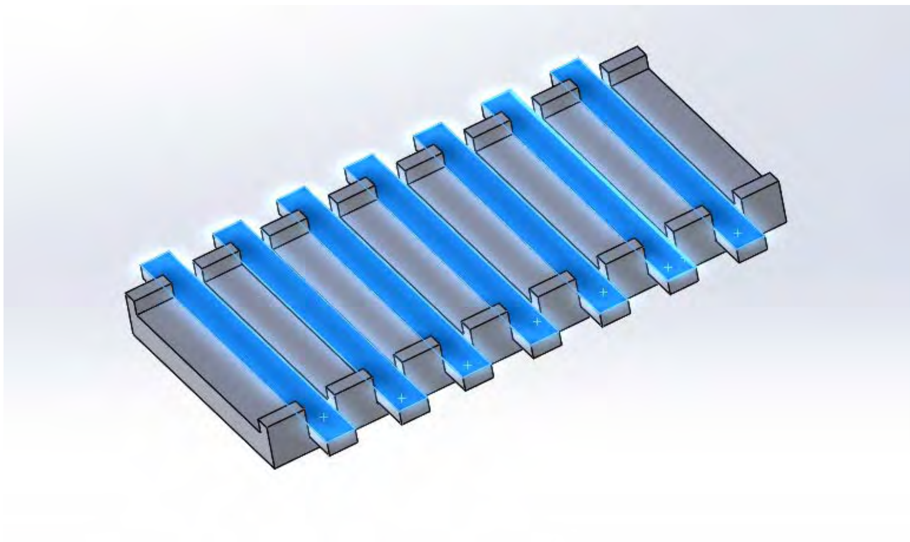

Figure 11. SolidWorks Model for Second “Train Track” Track Setup

The seven individual blocks, shown in blue in Figure 11, were 3D printed at the RoboDojo at the Naval Postgraduate School in Monterey, California, using the Ultimaker 3 Extended. These seven blocks were then clicked into the track, as shown in Figure 12.

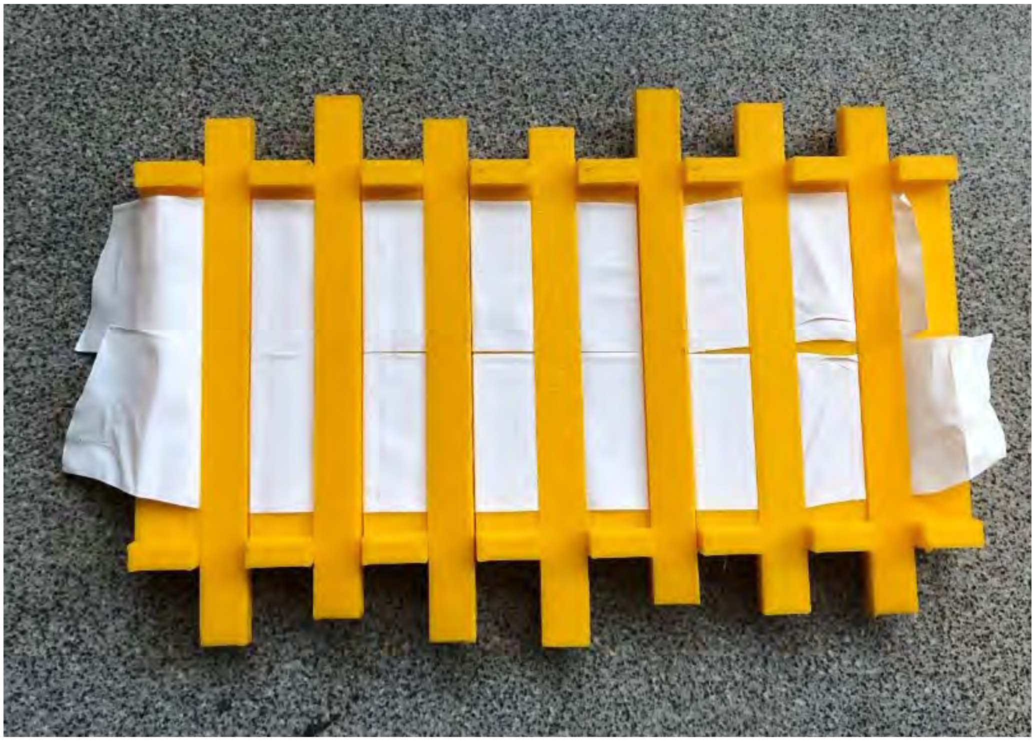

Figure 12. 3D Printed Second “Train Track” Track with PTFE Tape

This design was preliminary tried with the TENG electrodes, but the blocks and tape did not hold securely during operation. It was then decided that it would be more useful to have adhesive PTFE tape for the track and thus eliminate the need for the more intricate block and track design. The new track was designed in SolidWorks and the model is shown in Figure 13, the units shown are in millimeters.

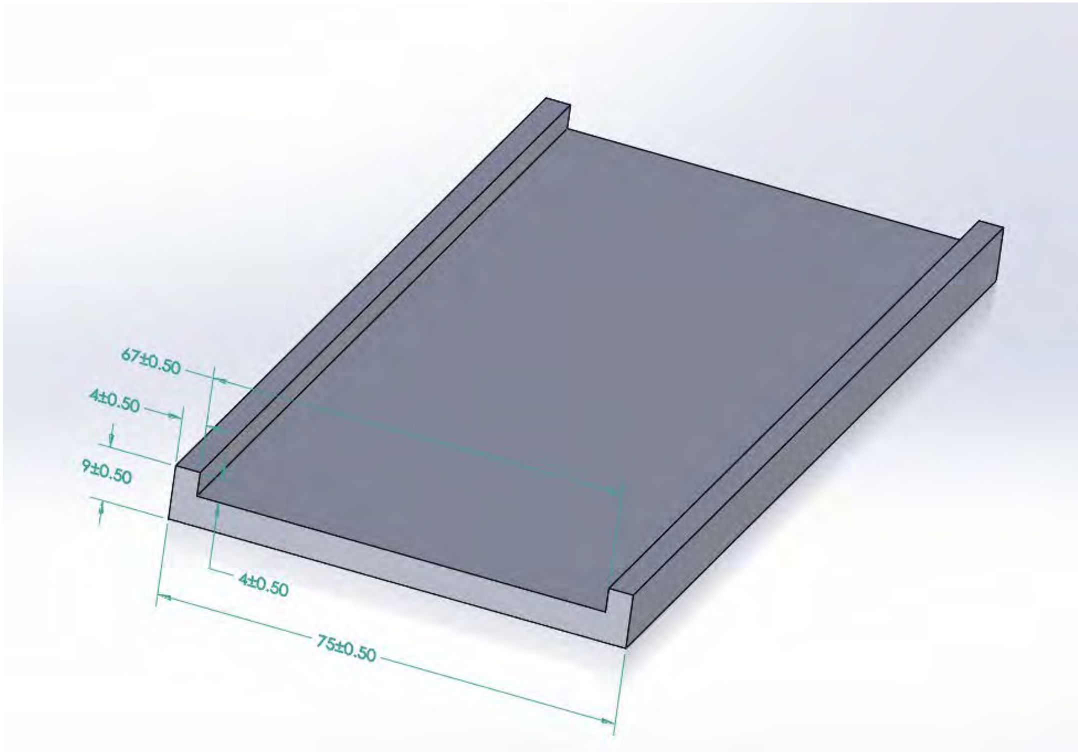

Units in millimeters.

Figure 13. SolidWorks Model of Final Design for the Track

The final track was 3D printed at the RoboDojo at the Naval Postgraduate School in Monterey, California, using an Ultimaker 3 Extended. The adhesive PTFE tape was then added to the track as shown in Figure 14. This track was set to be an inner width of 67 millimeters to prevent any friction on the sides of the TENG and strictly allow friction at the interface of the PTFE tape and the copper electrodes. The length of the track was 155 millimeters to allow a full sliding motion of the TENG electrode length. This was the track used in the testing of the TENG.

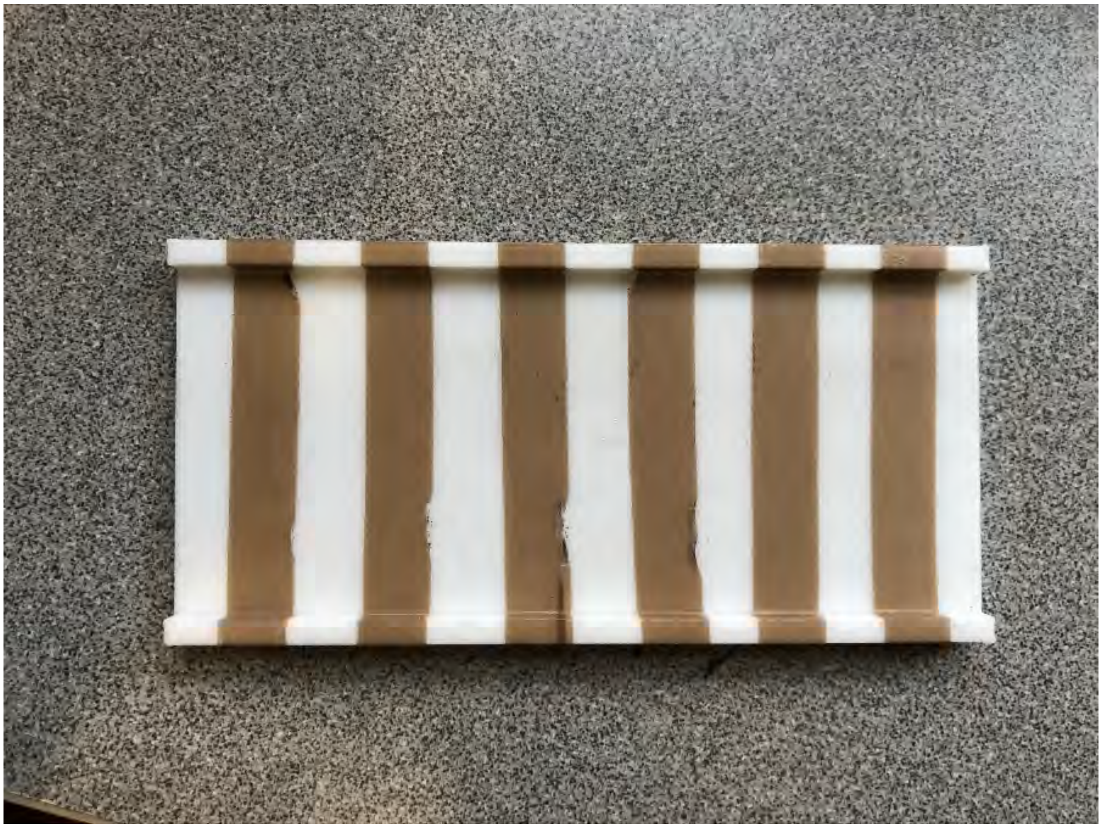

Figure 14. 3D Printed Final Track with Adhesive PTFE Tape

Once the TENG electrodes and track were established, they were set up together and tested by hand to see what the output AC voltages were for the TENG. This simple test proved that the TENG was producing an AC output voltage. Yet, it is hard to produce a consistent speed or contact force with the TENG using a human hand, so the next step was to use a linear reciprocating motor to regulate the testing.

B. TESTING OF ORIGINAL TENG WITH A RECIPROCATING MOTOR

A linear reciprocating motor was wired and set up for the testing of the TENG. It allowed for the speed to be regulated. A small connector piece was made in SolidWorks to connect the TENG to the reciprocating motor as shown in Figure 15.

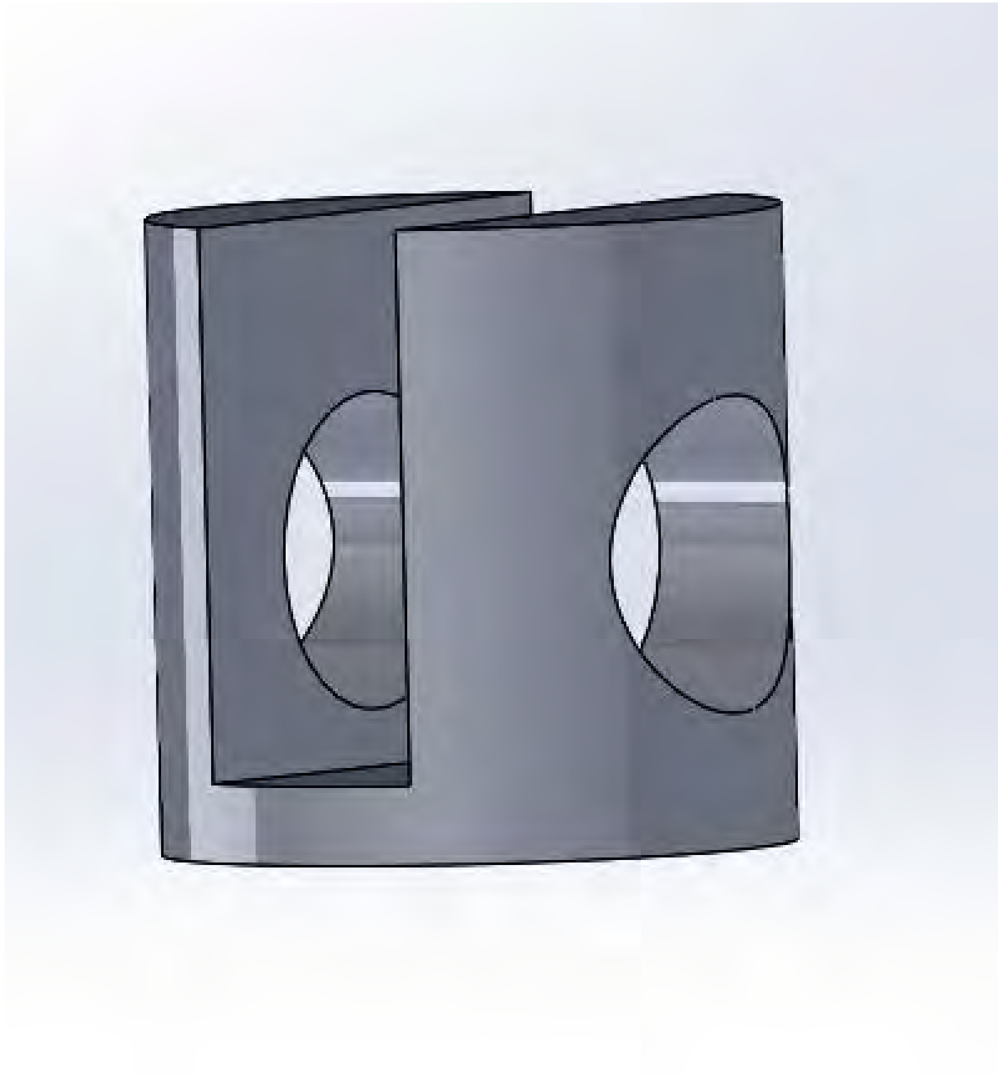

Figure 15. SolidWorks Model of Connector Piece

In addition, a little disk that sat on top of the TENG was created to test the TENG at different contact forces. The SolidWorks model of the weight holder is shown in Figure 16.

Figure 16. SolidWorks Model of Weight Holder

Both of these pieces were 3D printed at the RoboDojo at the Naval Postgraduate School in Monterey, California, using an Ultimaker 3 Extended. The final setup of the TENG with the reciprocating motor, track, connector piece, and weight holder is shown in Figure 17, Figure 18, and Figure 19.

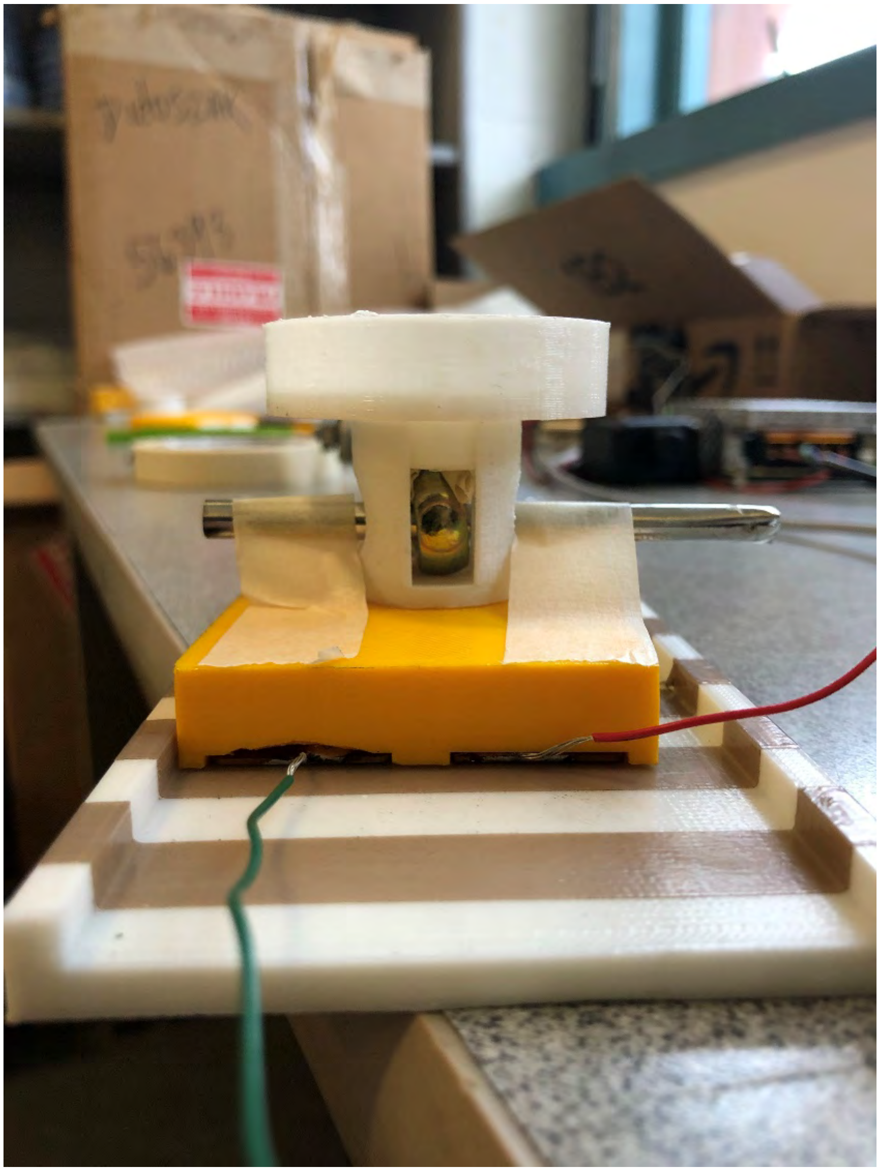

Figure 17. End view of TENG Electrode Holder and Track Setup with Connector Piece and Weight Holder

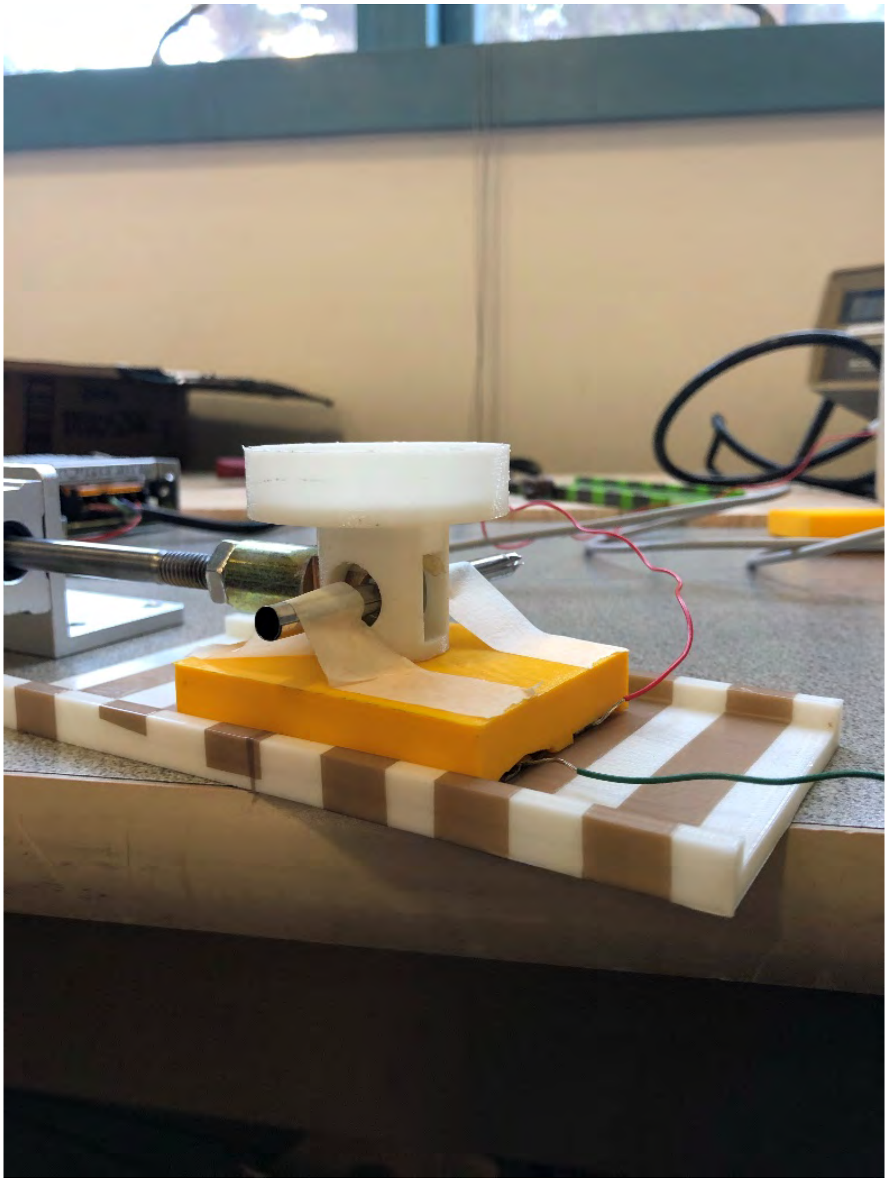

Figure 18. Side View of TENG Electrode Holder and Track Setup with Connector Piece and Weight Holder

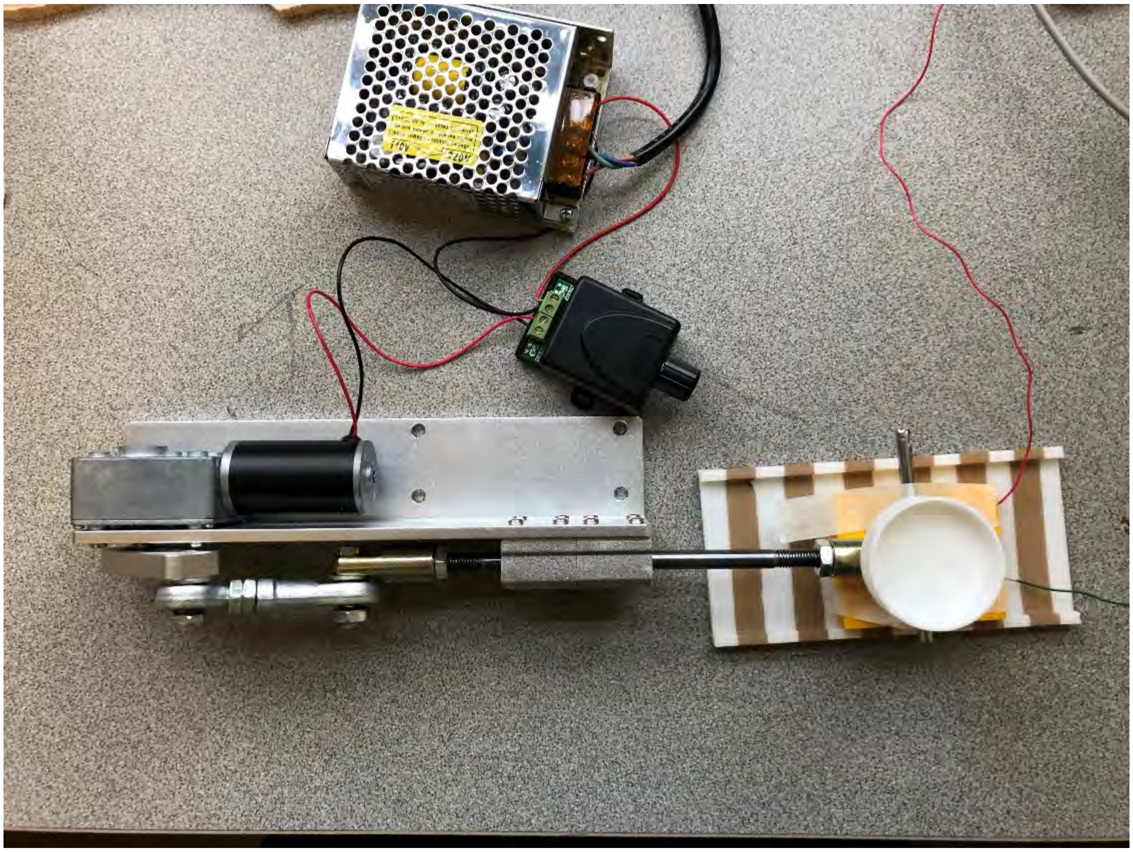

Figure 19. Top View of the TENG Setup Attached to Reciprocating Linear Motor

This setup was then tested at two different speeds with the linear motor, one at 50% speed (TENG frequency of 2.083 hertz) and one at full speed (TENG frequency of 4.167 hertz). Each of these speeds was also tested with three different weight conditions on the weight plate. The first condition was without any additional weight. The next condition that was tested was with one bolt (32 grams) on the weight plate as shown in Figure 20.

Figure 20. TENG Weight Holder with One Bolt (32 grams)

The final condition that was tested was with three bolts (96 grams) on the weight plate and is shown in Figure 21.

Figure 21. TENG Weight Holder with Three Bolts (96 grams)

These two different speeds and three different weight conditions made for a total of six different data collections for each run of the TENG.

C. IMPROVEMENT OF TENG

While the copper piece from the original TENG was being soldered, it was observed that the metal was not heating up as expected for a piece of pure copper. It was then speculated that the current copper electrodes may actually be a piece of copper alloy and not of pure copper. A piece of pure copper was then ordered and machined to make an improved TENG system. Material selection is a huge part of how well a TENG operates so verifying the metal being used for the electrode was pure copper was important for the operability of the TENG. A second TENG block, with the same design as the first TENG was 3D printed at the RoboDojo at the Naval Postgraduate School in Monterey, California, using an Ultimaker 3 Extended. The pure copper electrodes in the TENG block are shown in Figure 22.

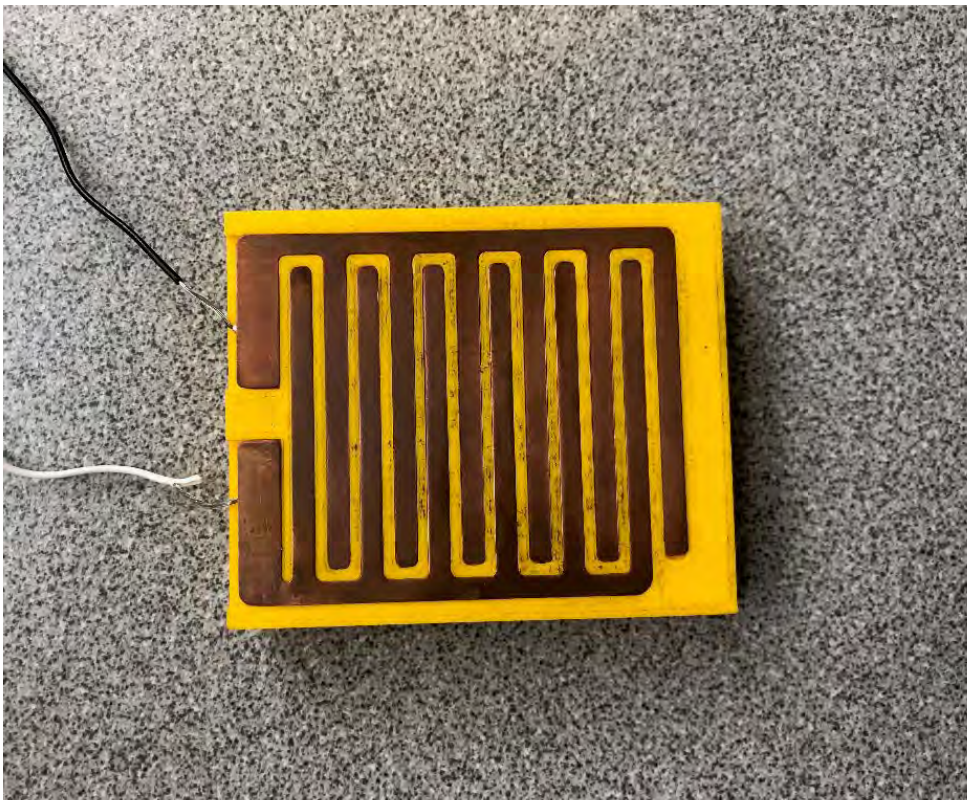

Figure 22. Pure Copper Electrode TENG Block

D. TESTING OF THE IMPROVED TENG WITH A RECIPROCATING MOTOR

The same track was used for the improved TENG from the original TENG testing. This ensured the exact same PTFE tape spacing. In addition, the same connector piece and weight holder were used. Just as was completed with the original TENG, this improved

TENG was tested at two different speeds, one at 50% and one at full speed. In addition, the TENG was tested with three different weight conditions: weightless, one bolt (32 grams), and three bolts (96 grams).

E. TESTING OF THE IMPROVED TENG WITH A RECIPROCATING MOTOR AND THINNER PTFE

A second identical track was then 3D printed at the RoboDojo at the Naval Postgraduate School in Monterey, California, using an Ultimaker 3 Extended. The track had thinner strips (half thickness) of the PTFE tape from the original testing. This track is shown in Figure 23.

Figure 23. Track with Thin Adhesive PTFE Tape

The improved TENG was tested with the thinner PTFE tape strips with no added weight and 3 bolts (96 grams) of added weight. Both of these tests were completed at full speed of the linear reciprocating motor.

III. RESULTS FROM EXPERIMENTATION

The first experimentation that was run was with the original TENG. It was tested with three different weight conditions and two different speeds. These six different runs were each run three times to make sure that the data was repeatable. The AC voltage outputs were measured with a Keysight DSO1052B digital oscilloscope.

A. EXPERIMENTAL RESULTS OF ORIGINAL TENG

1. No Added Weight, Half Speed

The following is the result of the AC output voltages from the original TENG with reciprocating motor run at half speed (frequency of 2.083 for the pulses). This run had no weight added in the weight holder. Shown in Figure 24 is the result from the first run.

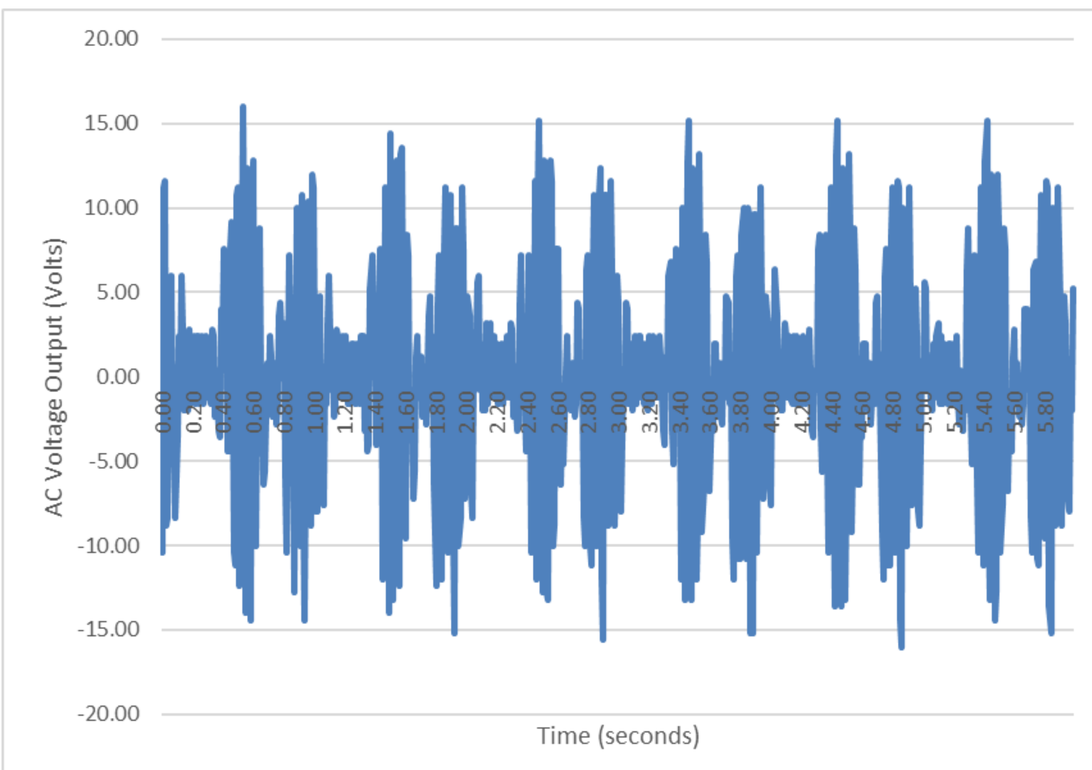

Figure 24. AC Voltage Output from Original TENG with No Additional Weight and 2.083 Hertz TENG Frequency

The AC voltage outputs for this TENG were in a pulsing pattern. For this TENG test, there is a closer gap between the two pulses for a forward and backward movement of the TENG, which was one cycle of the linear motor. As the motor moved forward again, there was a little bit of a longer pause in the data. A zoom in of this pulse pair is shown in Figure 25. From this run, one can see the range of the peak-to-peak is 32 volts.

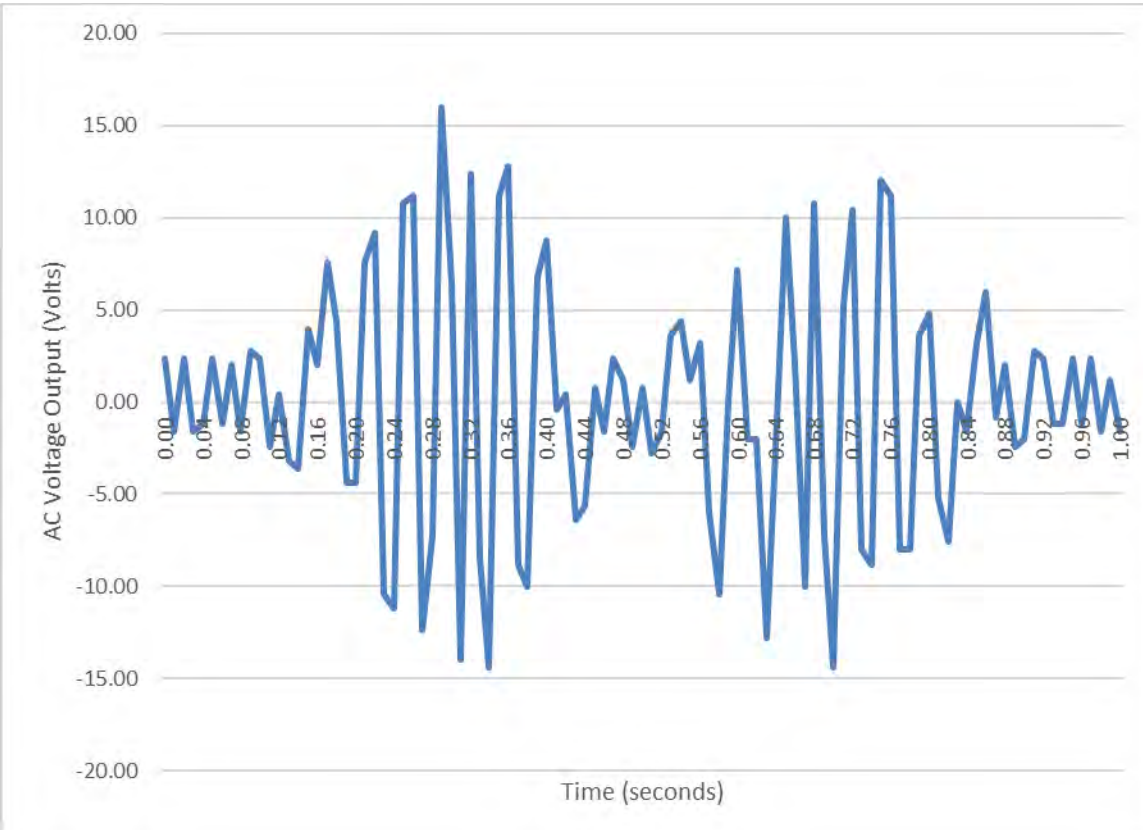

Figure 25. Zoomed in View of AC Voltage Output from Original TENG with No Additional Weight and 2.083 Hertz TENG Frequency

Figure 25 shows how the TENG has the pairs of pulses that are close together which correspond with the complete cycle of the linear motor. One can observe that the first pulse (forward motion) has the most positive maximum and the second pulse (backward motion) has the most negative minimum. This condition was run three separate times to verify that the data was repeatable. The average peak-to-peak for those three runs was 31.47 volts.

2. One Bolt of Added Weight, Half Speed

The next test run was with one bolt of weight added (32 grams) and the linear motor still at the half speed (frequency of 2.083 hertz for the TENG). The results of this run are shown in Figure 26.

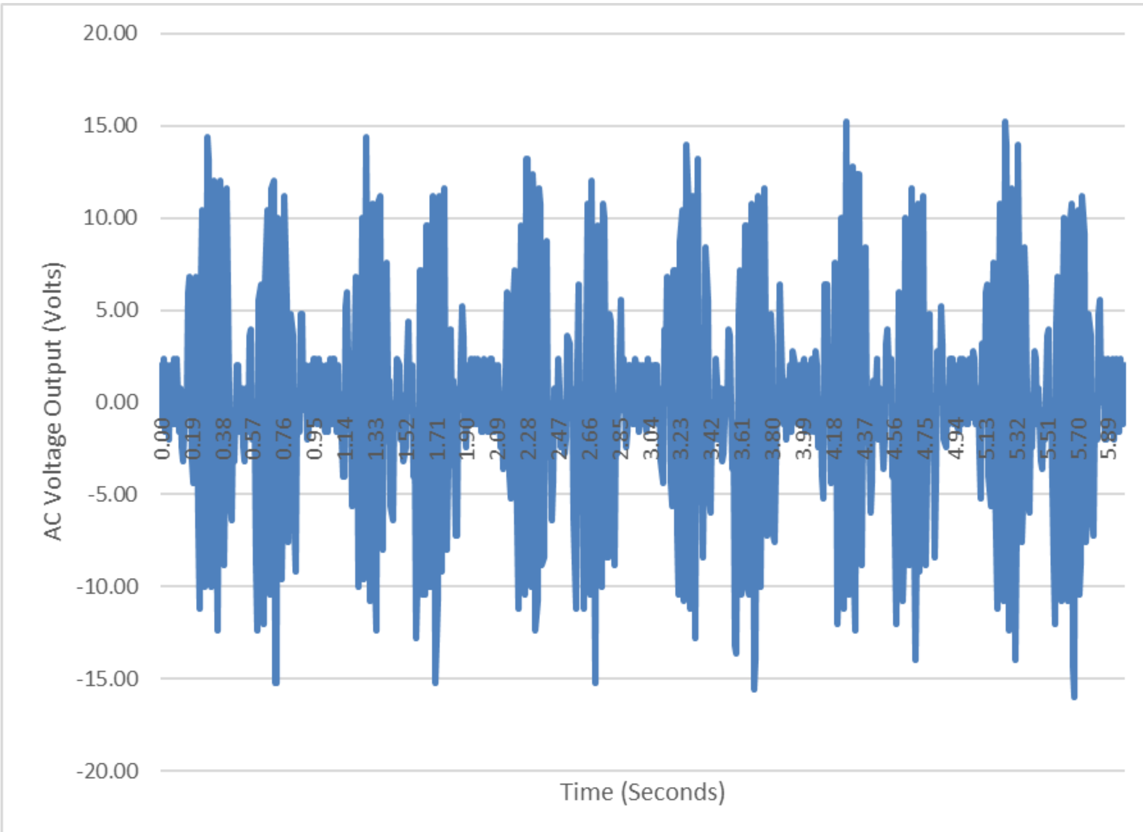

Figure 26. AC Voltage Output from Original TENG with One Bolt (32 grams), Additional Weight, and 2.083 Hertz TENG Frequency

With the one bolt (32 grams) of weight added, there was not much of a difference for the maximum peak-to-peak voltage for the original TENG run compared to the no weight condition. The maximum peak-to-peak for this run was found to be 31.2 volts, slightly smaller than the results found in the no weight condition. A zoom in of this run is shown in Figure 27.

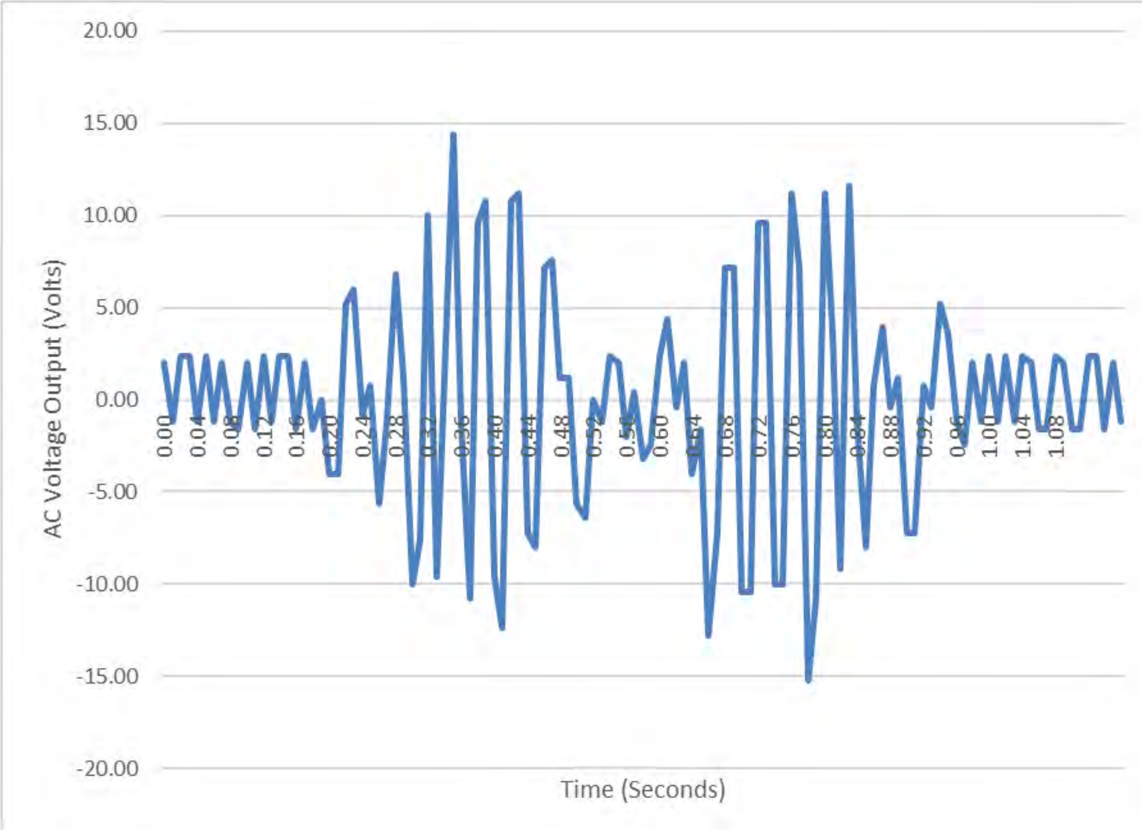

Figure 27. Zoomed in View of AC Voltage Output from Original TENG with One Bolt (32 grams), Additional Weight, and 2.083 Hertz TENG Frequency

As shown in Figure 27, the zoom-in on the pair of pulses for the one bolt (32 gram) weigh condition looks nearly identical to the no weight condition. Similar to what was seen in Figure 25, the first pulse had the most positive maximum and the second pulse had the most negative minimum. Just as was done with the no weight condition, this test was run three times to confirm the repeatability of the data. The average peak-to-peak for those three runs was 30.67 volts.

3. Three Bolts of Added Weight, Half Speed

The final condition run with the original TENG and the linear motor at half speed was with a weight condition of three bolts (96 grams). The results of this run are shown in Figure 28.

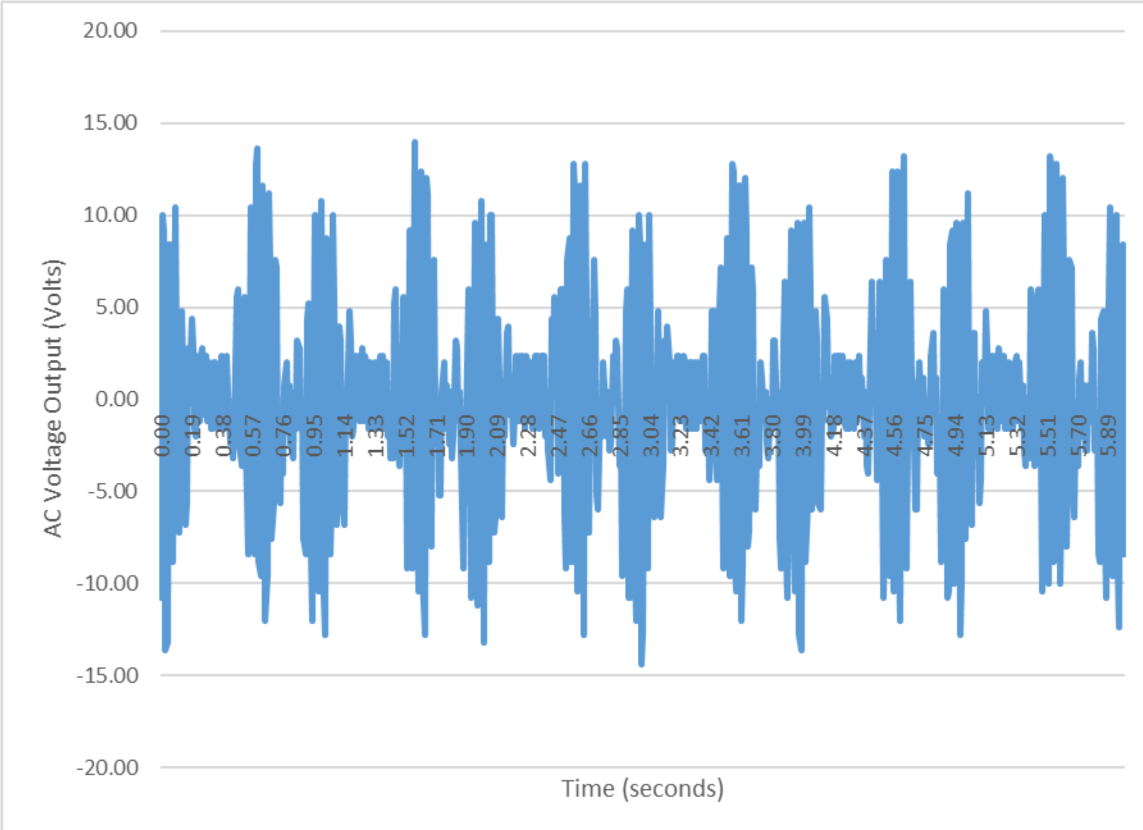

Figure 28. AC Voltage Output from Original TENG with Three Bolts (96 grams), Additional Weight, and 2.083 Hertz TENG Frequency

For this run, the peak-to-peak AC voltage for the three bolts (96 grams) of weight condition was found to be 28.4 volts. This is less than what was found for the no weight and one bolt (32 grams) of weight conditions tested. The zoom in of this test is shown in Figure 29.

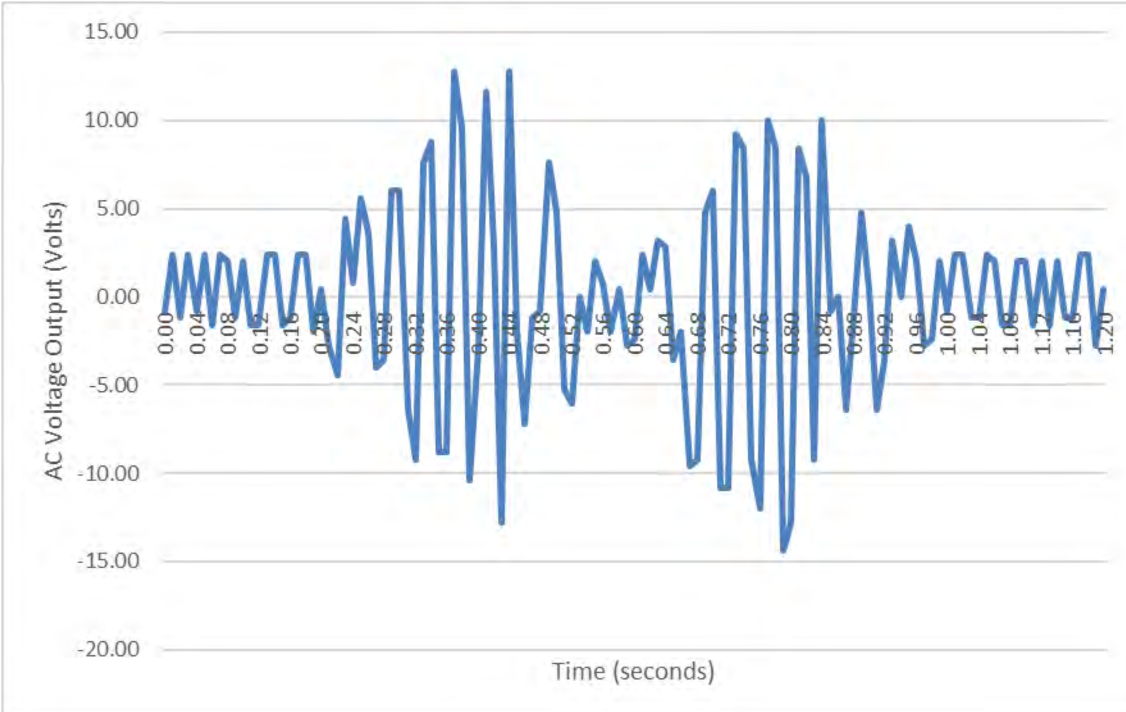

Figure 29. Zoomed In View of AC Voltage Output from Original TENG with Three Bolts (96 grams), Additional Weight, and 2.083 Hertz TENG Frequency

As expected, the first pulse had the most positive maximum, while the second pulse had the most negative minimum. Yet, the maximum and minimum are not as large in magnitude as was found with the first two weight conditions. This condition was run for three tests to confirm the repeatability of the data. The average peak-to-peak for those three runs was 27.33 volts.

4. No Added Weight, Full Speed

The next test that was run was having the original TENG with no weight added at the full speed of the linear reciprocating motor. The frequency of the TENG was 4.167 hertz, double of the first set of tests. The results of the no weight added and full speed linear reciprocating motor are shown in Figure 30.

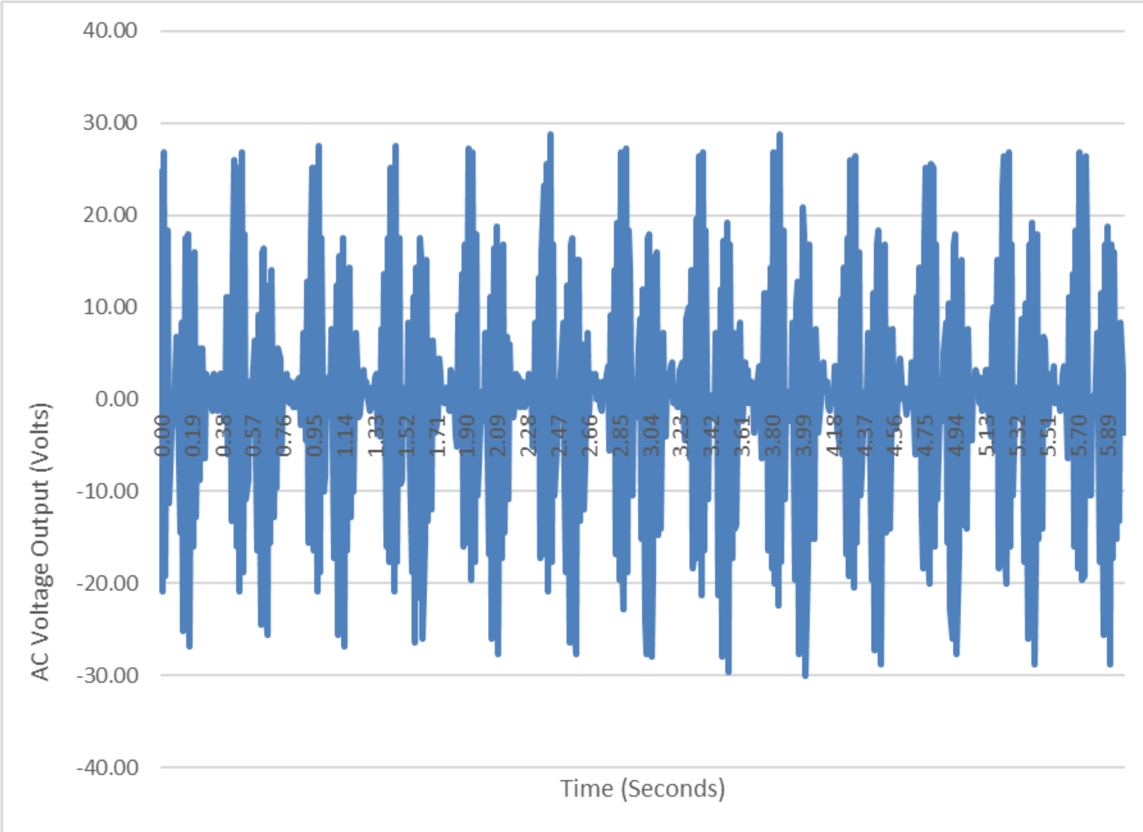

Figure 30. AC Voltage Output from Original TENG with No Additional Weight and 4.167 Hertz TENG Frequency

At the higher speed, the pairs of pulses for the forward and backward motion of the TENG are easier to notice. In addition, the peak-to-peak AC output voltage is greatly increased with the increased frequency. For this run, the peak-to-peak output voltage was found to be 58.8 volts, nearly double the result of the same weight condition at half speed. The zoom in of this run is shown in Figure 31.

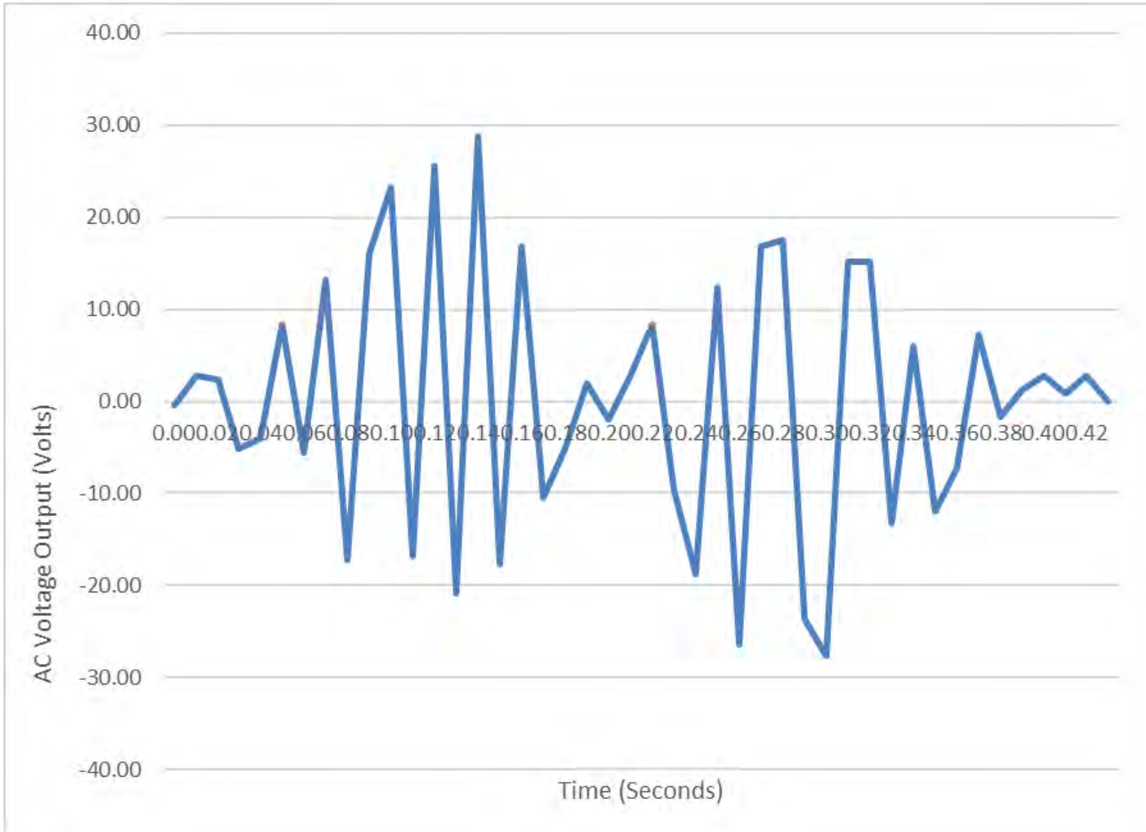

Figure 31. Zoomed In View of AC Voltage Output from Original TENG with No Additional Weight and 4.167 Hertz TENG Frequency

While the zoomed in shape of the full speed run looks similar to that of the half speed run, the time is much shorter and the peak-to-peak is much larger. Yet the same pattern of having the most positive maximum on the first pulse and the most negative minimum on the second pulse remains. This was also run three times to ensure the repeatability of the data. The average of those three runs was found to be 62 volts.

5. One Bolt of Added Weight, Full Speed

The next test run was for the full speed of the linear motor with one bolt (32 grams) of added weight on the weight holder. The results of this test are shown in Figure 32.

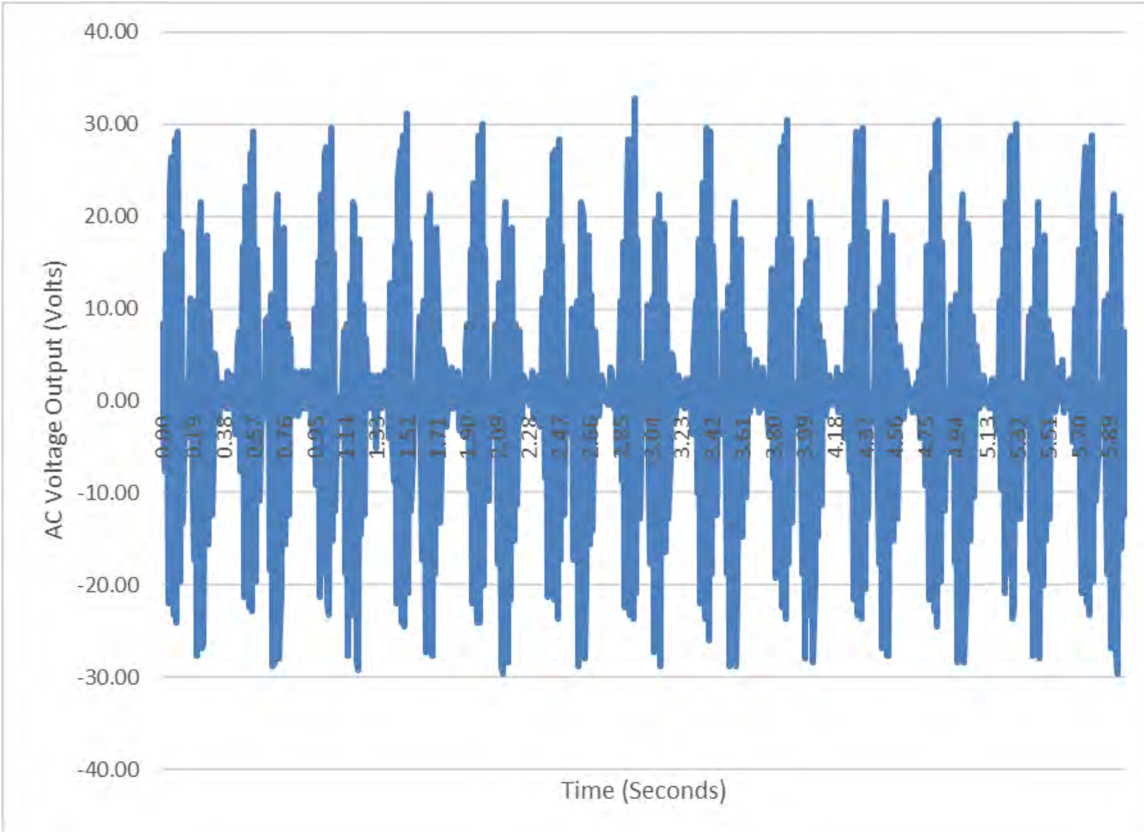

Figure 32. AC Voltage Output from Original TENG with One Bolt (32 grams), Additional Weight, and 4.167 Hertz TENG Frequency

The maximum peak-to-peak AC voltage for this test was found to be 62.3 volts. Similar to the results found in the no weight condition, the peak-to-peak voltage nearly doubled for the one bolt weight condition at the higher frequency. The zoom-in on the results is shown in Figure 33.

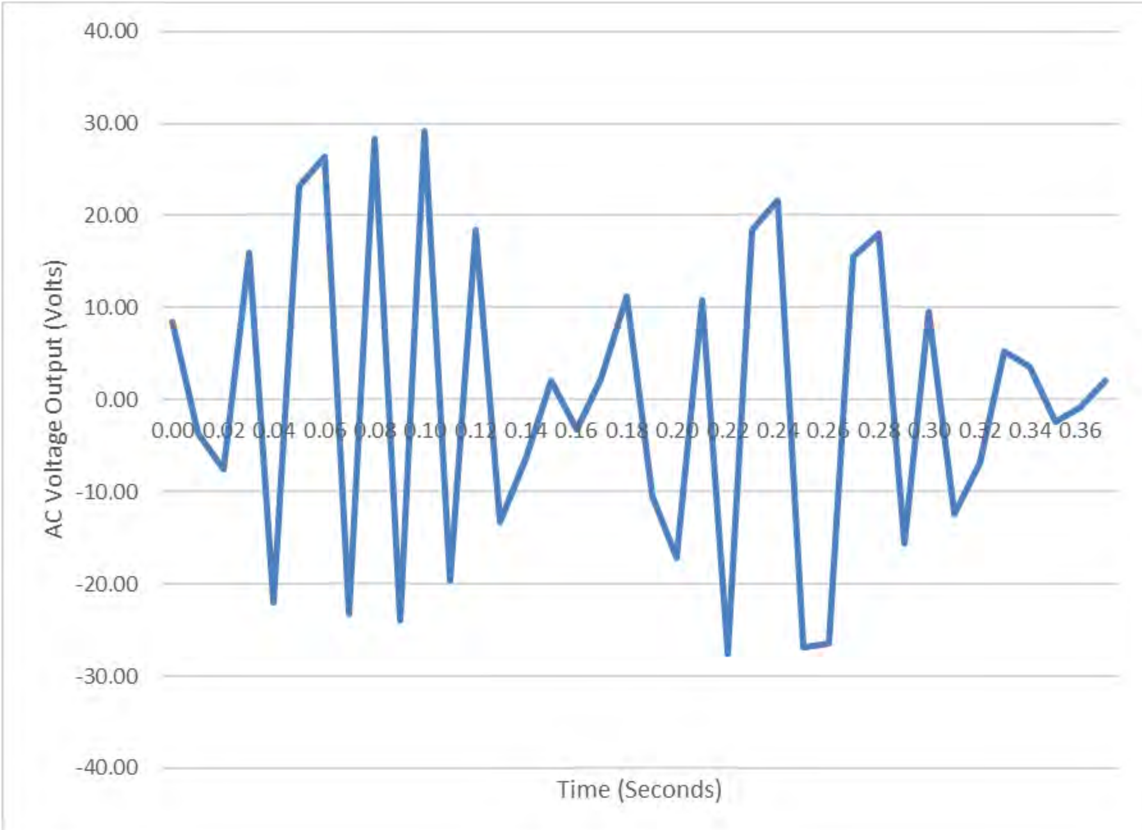

Figure 33. Zoomed In View of AC Voltage Output from Original TENG with One Bolt (32 grams), Additional Weight, and 4.167 Hertz TENG Frequency

This zoom in follows the pattern of all of the zoomed in tests of the past. The most positive maximum is found in the first pulse and the most negative minimum is found in the second pulse. For this test, which was run three times to ensure repeatability of the data, the average maximum peak-to-peak AC voltage was found to be 61.83 volts. This result is very close to the result from the no weight, full speed condition that had an average of 62 volts.

6. Three Bolts of Added Weight, Full Speed

The final condition tested for the original TENG at the full speed of the linear reciprocating motor was with three bolts (96 grams) of weight added to the weight holder. The results of this test are shown in Figure 34.

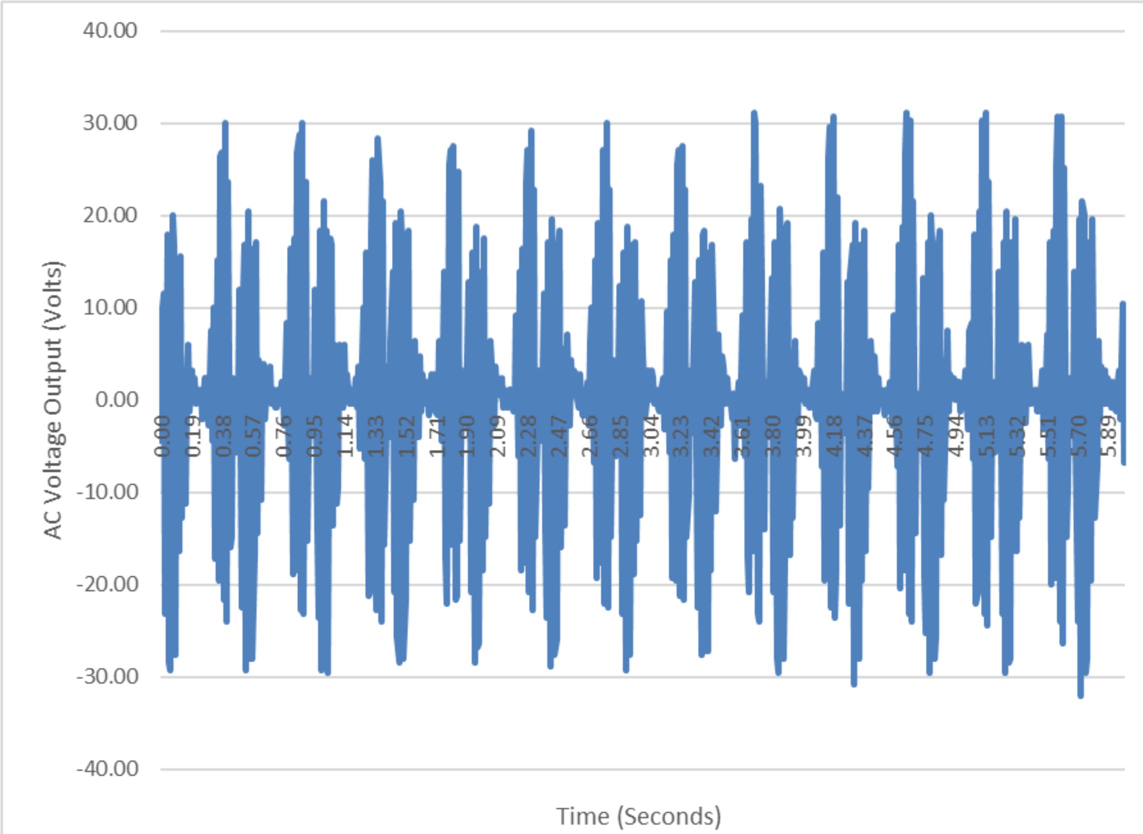

Figure 34. AC Voltage Output from Original TENG with Three Bolts (96 grams), Additional Weight, and 4.167 Hertz TENG Frequency

The maximum peak-to-peak AC voltage output for this test was found to be 63.2 volts. This is slightly higher than the result from the no weight and one bolt (32 grams) of weight conditions. Yet, as shown before, the full speed condition led to almost two times as much peak-to-peak AC voltage output as the half speed condition. The zoom in for this test is shown in Figure 35.

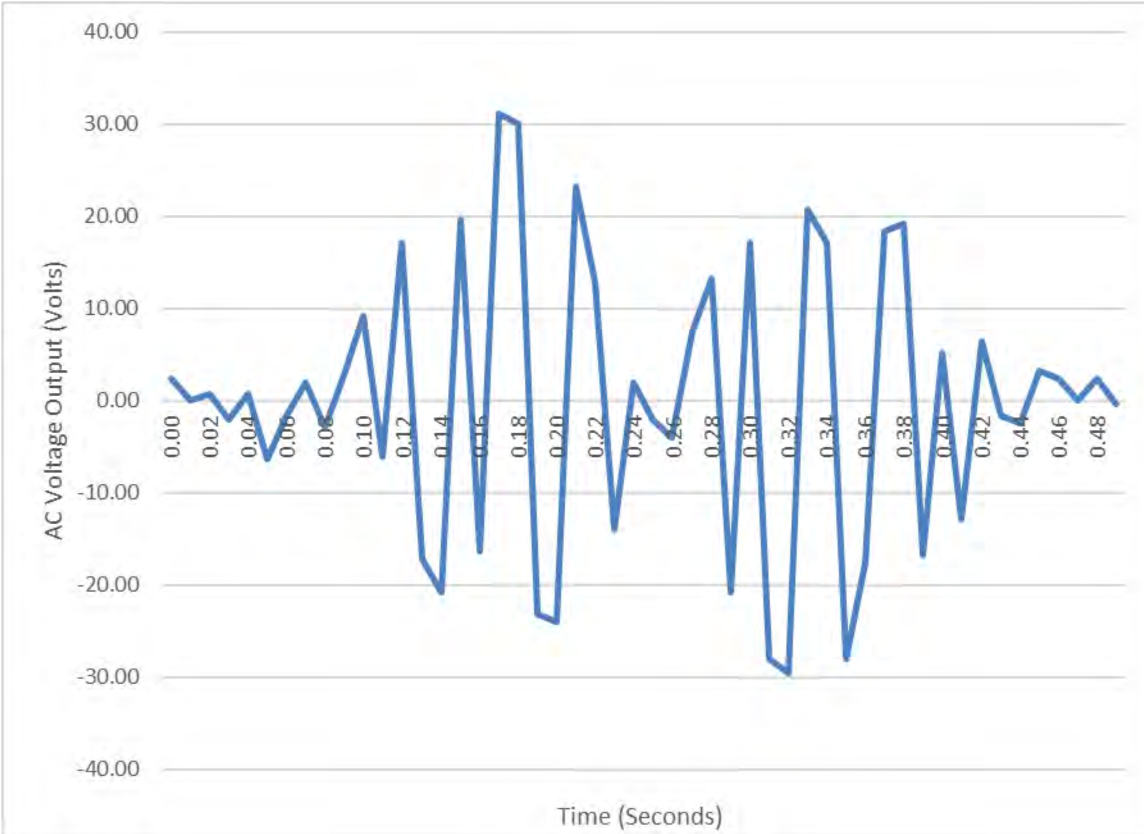

Figure 35. Zoomed In View of AC Voltage Output from Original TENG with Three Bolts (96 grams), Additional Weight, and 4.167 Hertz TENG Frequency

This zoom in continues to show the trend of having the most positive maximum on the first pulse and the most negative minimum on the second pulse. For the three tests completed for this condition to ensure repeatability, the average peak-to-peak voltage was found to be 67.6 volts. This is the highest average of all of the tests run with the original TENG. The data from runs 2 and 3 for the original TENG under all conditions is located in Appendix A.

7. Maximum Output by Hand

After completing the three different weight conditions at two different speeds, the original TENG was then moved by a human hand at a fast speed to find the maximum output the original TENG could possibly create. Although it is not possible to determine the contact force (weight) applied by the hand, it is possible to see the frequency associated with the maximum peak-to-peak AC voltage output. Figure 36 shows the first run to maximize the original TENG.

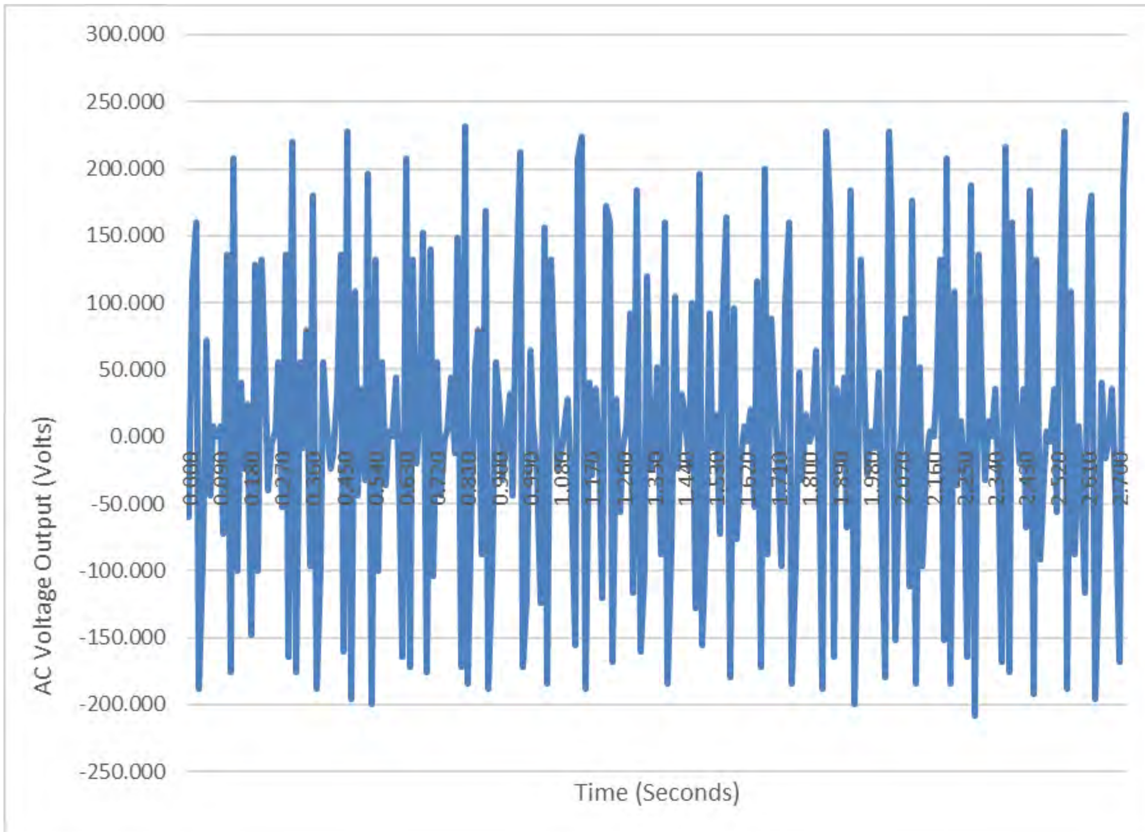

Figure 36. AC Voltage Output from Original TENG with Maximum Output by Hand

For the original TENG, the first run showed that there could be a maximum peak-to-peak AC output voltage of 448 volts. This test was completed at a frequency of 10.42 hertz. For the three tests run, the average maximum peak-to-peak AC output voltage of 446.47 volts. Those three tests had an average frequency of 10.35 hertz. The data for runs 2 and 3 for the maximum output of the original TENG is located in Appendix D.

8. Summary of Original TENG Results

The original TENG testing led to some trends between the frequency the TENG operated at and the maximum peak-to-peak AC output voltage. The overview of the maximum peak-to-peak AC output voltage and its corresponding frequency and added weight is shown in Table 1.

Table 1. Summary of Original TENG Testing with Linear Reciprocating Motor

Frequency (Hertz)	Added Weight (Grams)	Average (for 3 Runs) Maximum Peak to Peak AC Output Voltage (Volts)
2.08	0.00	31.47
2.08	32.00	30.67
2.08	96.00	27.33
4.17	0.00	62.00
4.17	32.00	61.83
4.17	96.00	67.60
10.35	N/A	446.67

The trend with frequency and the original TENG is that as the frequency increased, the maximum peak-to-peak AC voltage output also increased. This is increasing at an exponential rate based on the data points collected, as shown in Figure 37.

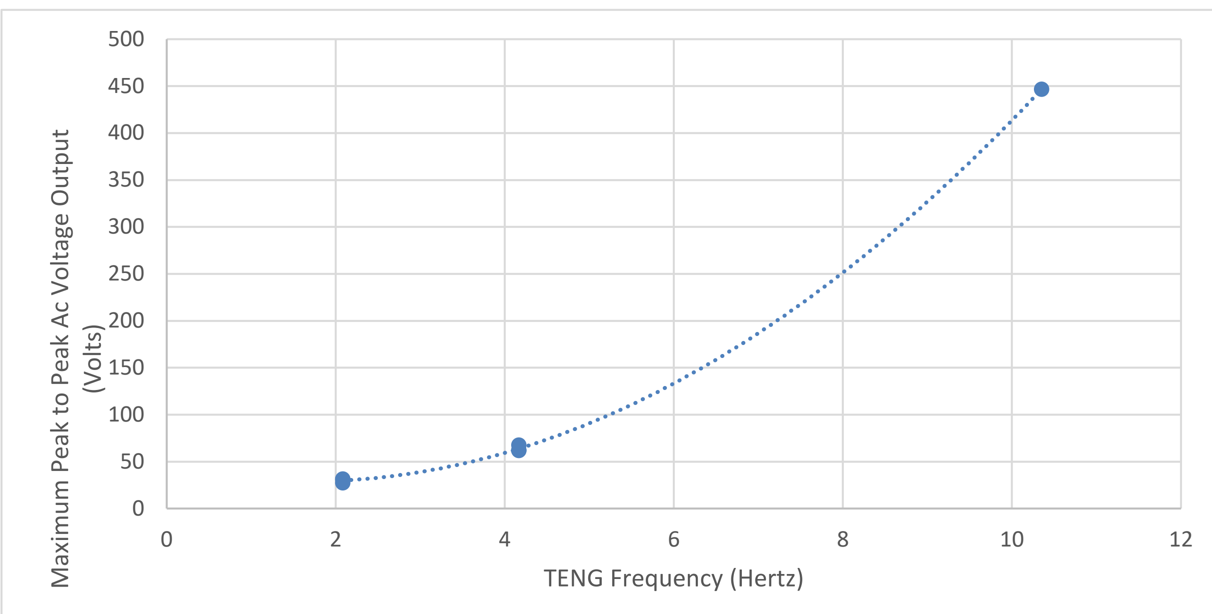

Figure 37. TENG Frequency and AC Voltage for Original TENG

There was not a trend found for the weight added to the original TENG and the AC output voltage. The results from the two different frequencies are shown in Figure 38.

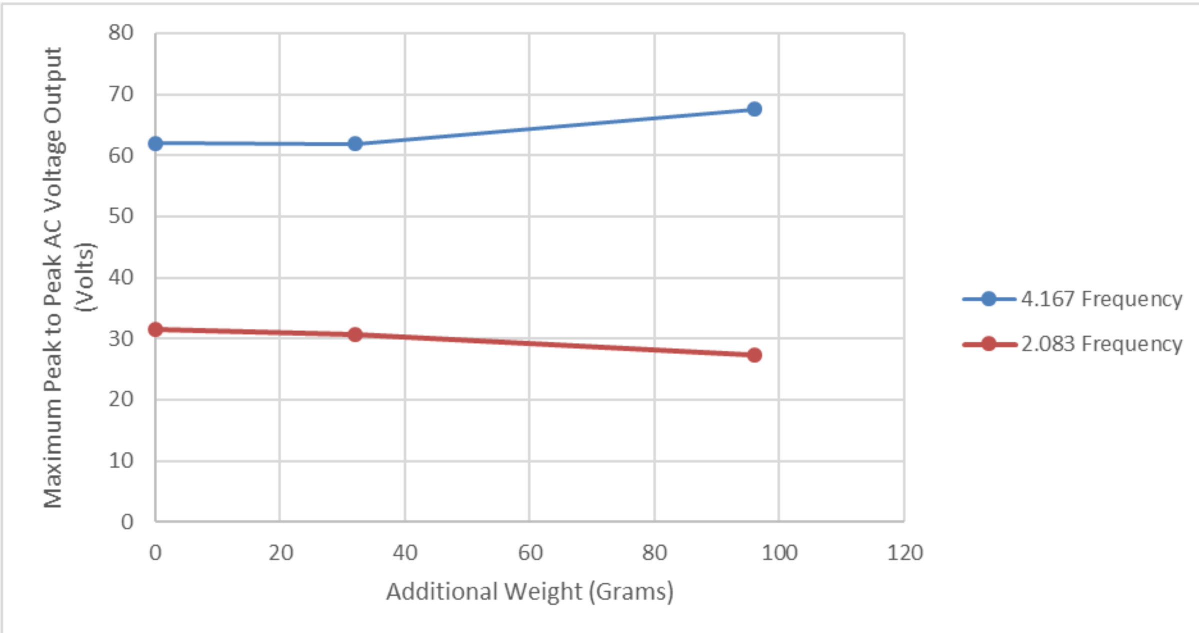

Figure 38. Additional Weight and AC Voltage for Original TENG

For the higher frequency of 4.167 hertz, the maximum peak-to-peak AC output voltage went up with the additional weights added. However, for the lower frequency of 2.083 hertz, the maximum peak-to-peak output voltage decreased with the additional weights added. Therefore, for the original TENG, it was concluded that a higher frequency led to a higher maximum peak-to-peak AC output voltage, but the additional weights did not have a direct impact on the voltage.

B. EXPERIMENTAL RESULTS OF IMPROVED TENG

After testing the original TENG, the improved TENG made of pure copper electrodes was tested under the same three weight conditions and two speed conditions. These different conditions were also each tested three times to make sure the data collected was repeatable.

1. No Added Weight, Half Speed

The first condition with the improved TENG was with no weight in the weight holder and the linear reciprocating motor at half speed. The results of this condition are shown in Figure 39.

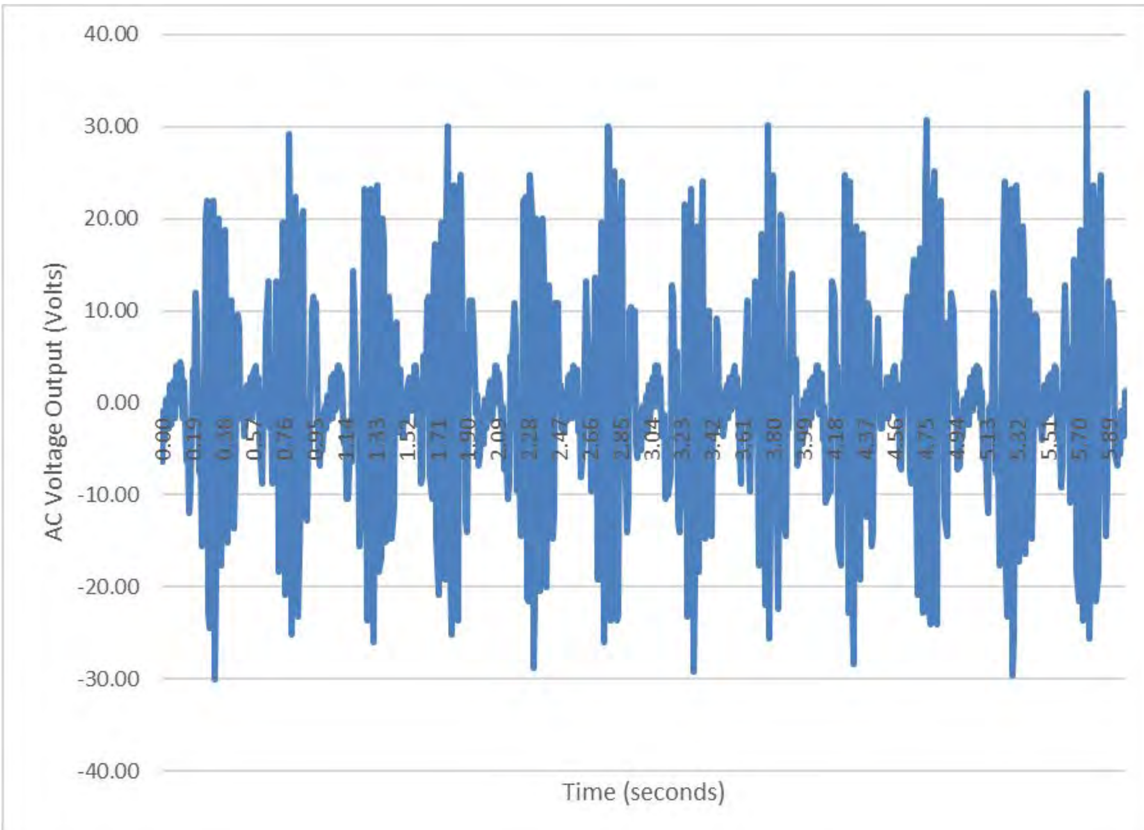

Figure 39. AC Voltage Output from Improved TENG with No Additional Weight and 2.083 Hertz TENG Frequency

For this run, the maximum peak-to-peak AC output voltage was found to be 63.6 volts. Although the pairs of pulses are not as obvious in the improved TENG as they were for the original TENG, there are still pairs of pulses present. These can be seen in the zoomed in view of the voltages. The zoom in for this test is shown in Figure 40.

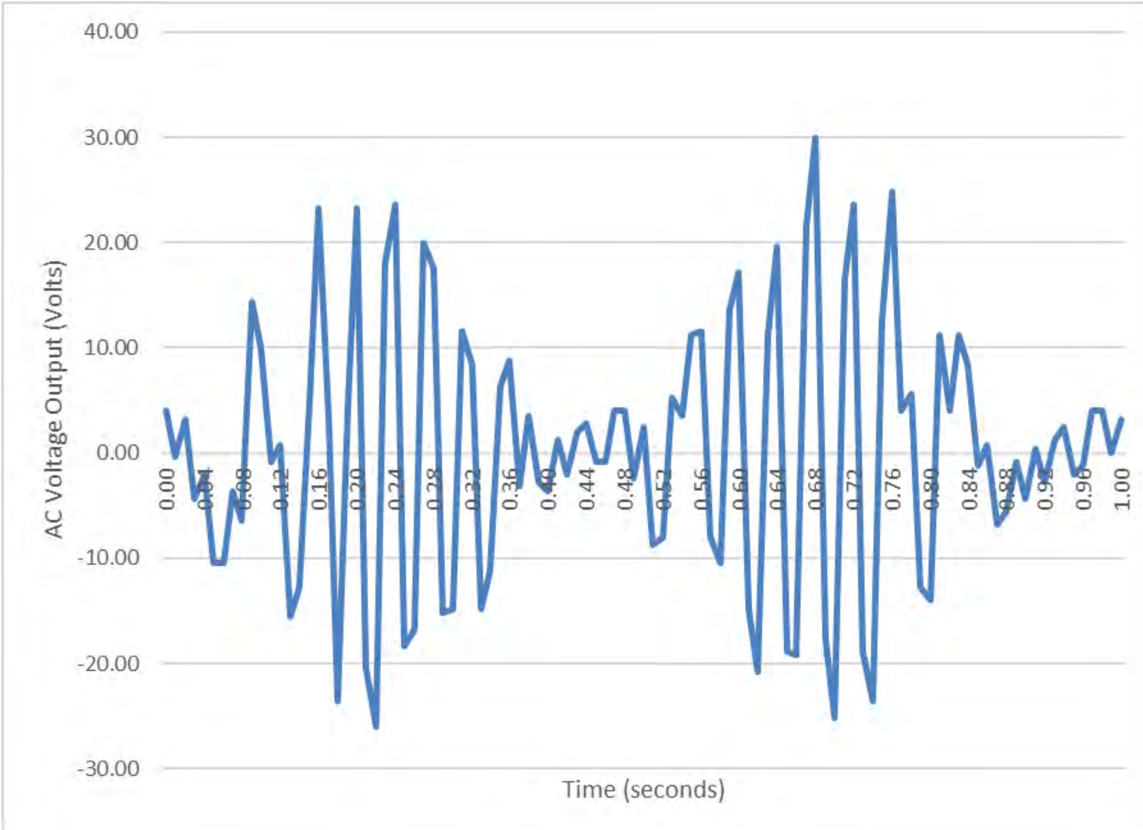

Figure 40. Zoomed In View of AC Voltage Output from Improved TENG with No Additional Weight and 2.083 Hertz TENG Frequency

Just as seen with the original TENG, the improved TENG had the pair of pulses alternating with having either the most positive maximum or the most negative minimum. The average of the three runs for maximum peak-to-peak AC voltage output for the improved TENG with no addition weight and the linear reciprocating motor at half speed was 64.33 volts.

2. One Bolt of Added Weight, Half Speed

Following the no additional weight condition, the improved TENG was tested with one bolt (32 grams) of weight in the weight holder at half speed of the linear reciprocating motor. The results of this run are shown in Figure 41.

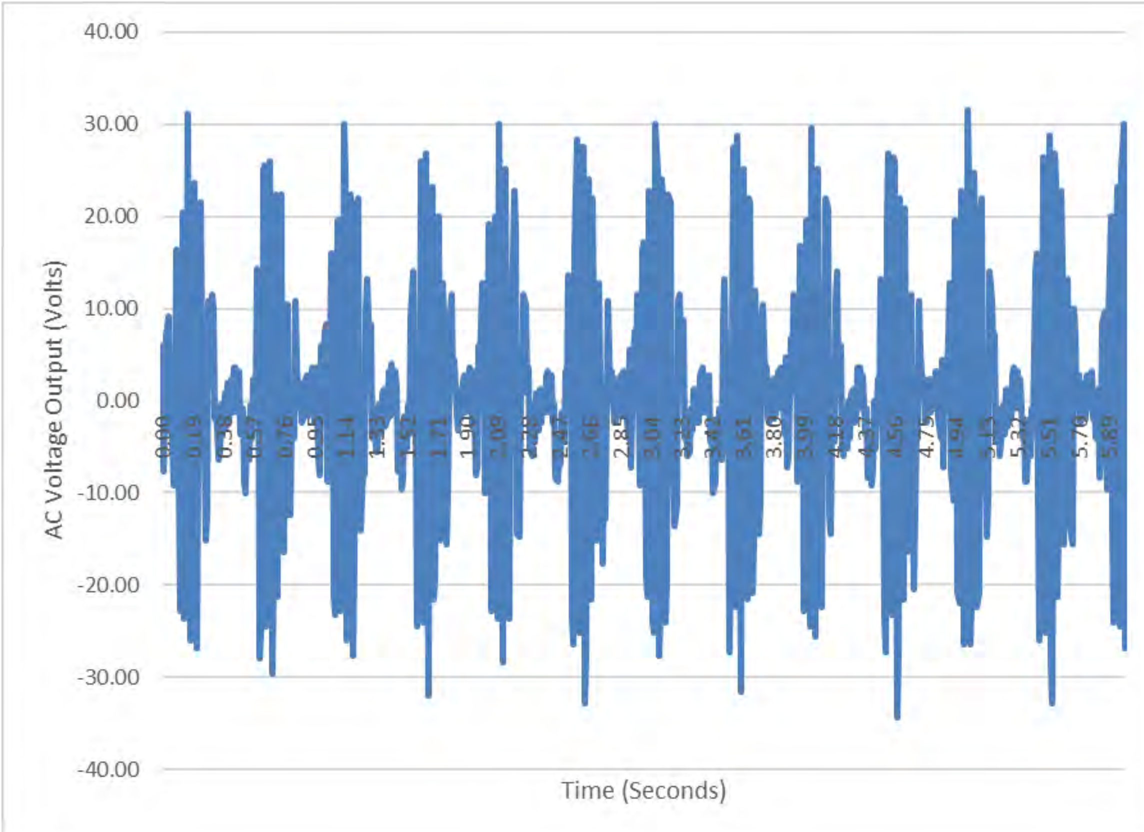

Figure 41. AC Voltage Output from Improved TENG with One Bolt (32 grams), Additional Weight, and 2.083 Hertz TENG Frequency

For this run, the maximum peak-to-peak AC voltage output was 66 volts. This is about double the maximum peak-to-peak AC voltage output of the original TENG under the same conditions. The zoom in view of this test is shown in Figure 42.

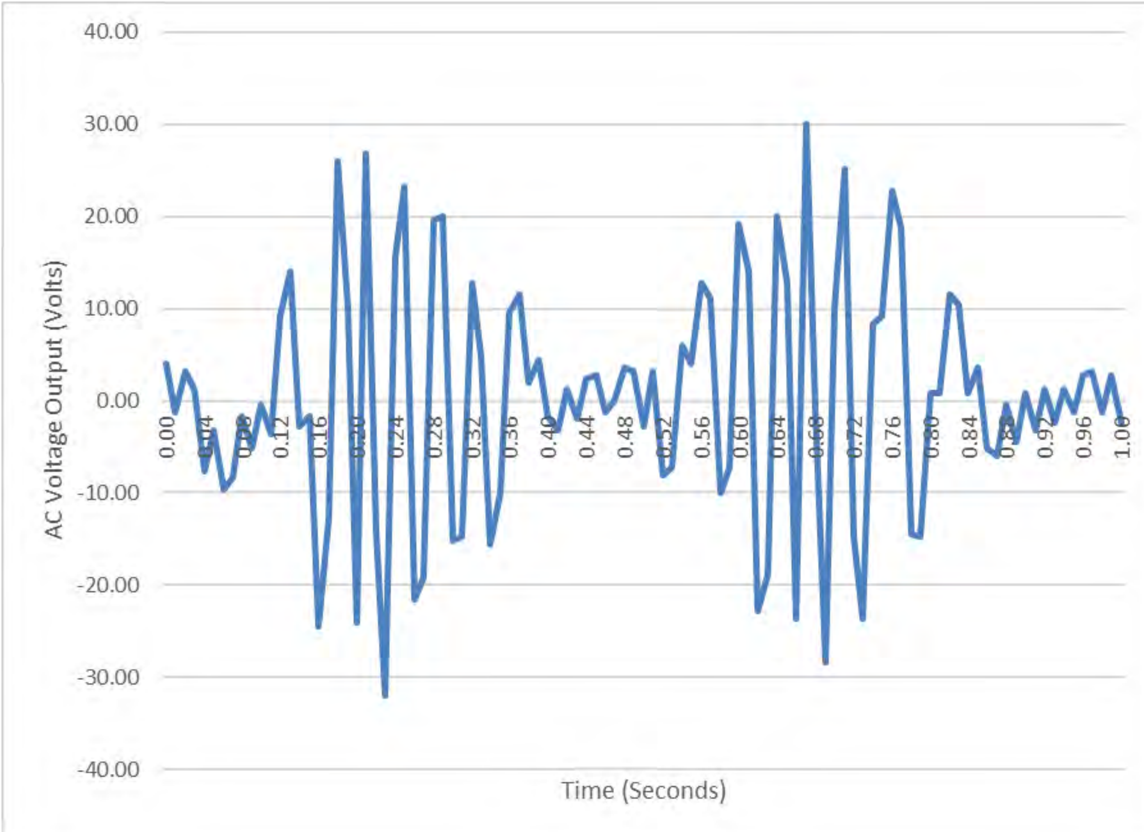

Figure 42. Zoomed In View of AC Voltage Output from Improved TENG with One Bolt (32 grams), Additional Weight and 2.083 Hertz TENG Frequency

This test also followed the same trend of having alternating pulses having a maximum positive voltage followed by a pulse having the minimum negative voltage. The average of the three runs for maximum peak-to-peak AC voltage output for this condition was 71.6 volts. This is higher than the maximum peak-to-peak AC voltage for the no weight added improved TENG tested at the same speed.

3. Three Bolts of Added Weight, Half Speed

The final test run at half speed of the linear reciprocating motor was with the improved TENG and three bolts (96 grams) of added weight to the weight holder. The results from this are shown in Figure 43.

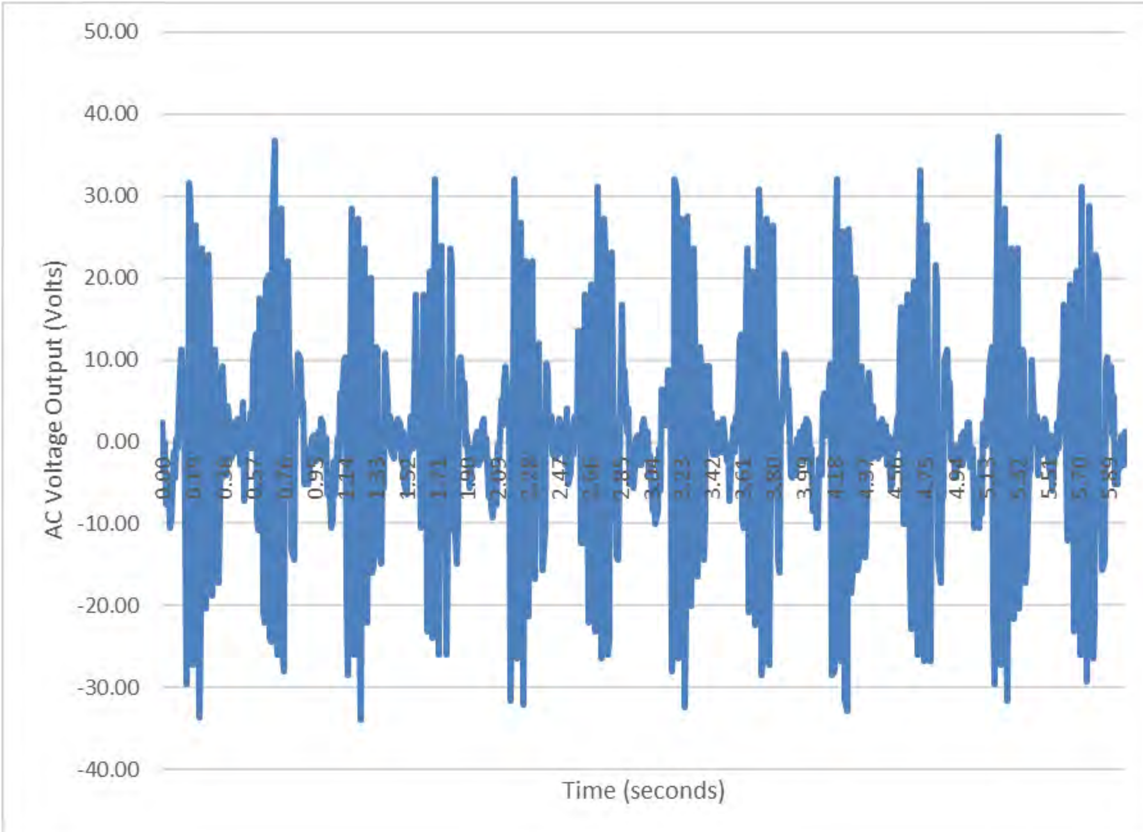

Figure 43. AC Voltage Output from Improved TENG with Three Bolts (96 grams), Additional Weight., and 2.083 Hertz TENG Frequency

For this run, the maximum peak-to-peak AC voltage output was 71.2 volts. This is more than double the amount for the original TENG under the same conditions. A zoomed in view of this run is shown in Figure 44.

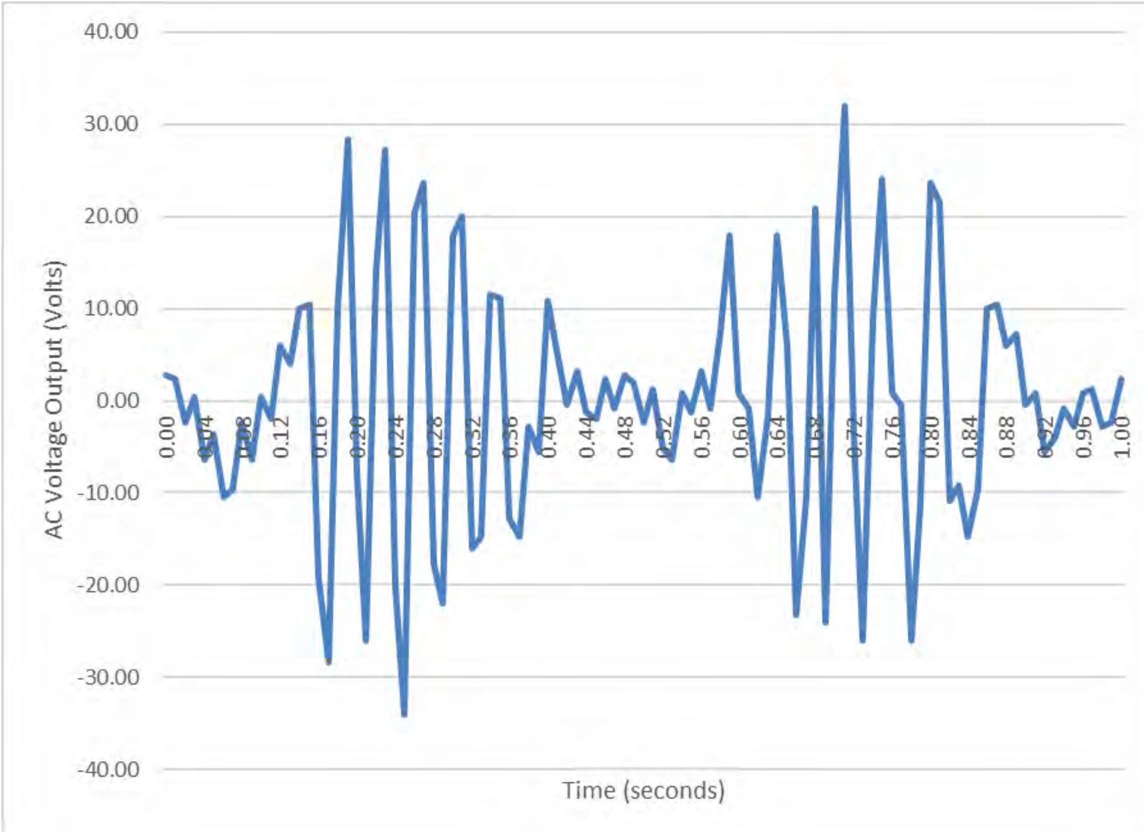

Figure 44. Zoomed In View of AC Voltage Output from Improved TENG with Three Bolts (96 grams), Additional Weight, and 2.083 Hertz TENG Frequency

This follows the same pattern with the pulses and maximums and minimums as shown in every test so far. For this condition, the average of the maximum peak-to-peak AC voltage output was found to be 74.13 volts. This is higher than the results from the no weight and one bolt (32 grams) conditions.

4. No Added Weight, Full Speed

The improved TENG was then tested at the full speed of the linear reciprocating motor with no weight added to the weight holder. The results of this run are shown in Figure 45.

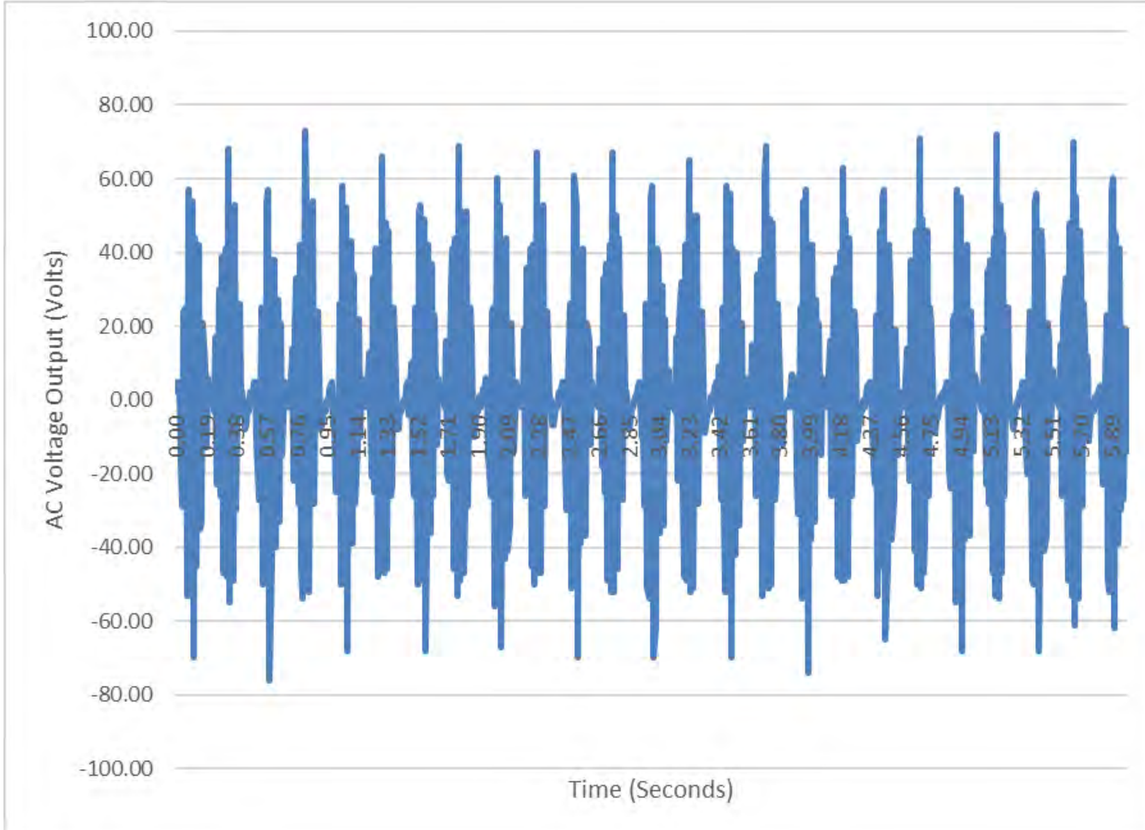

Figure 45. AC Voltage Output from Improved TENG with No Additional Weight and 4.167 Hertz TENG Frequency

The maximum peak-to-peak AC output voltage for this run was 149 volts. This is more than two times the amount of peak-to-peak AC output voltage with the same weight condition at half speed. The zoom in view of this run is shown in Figure 46.

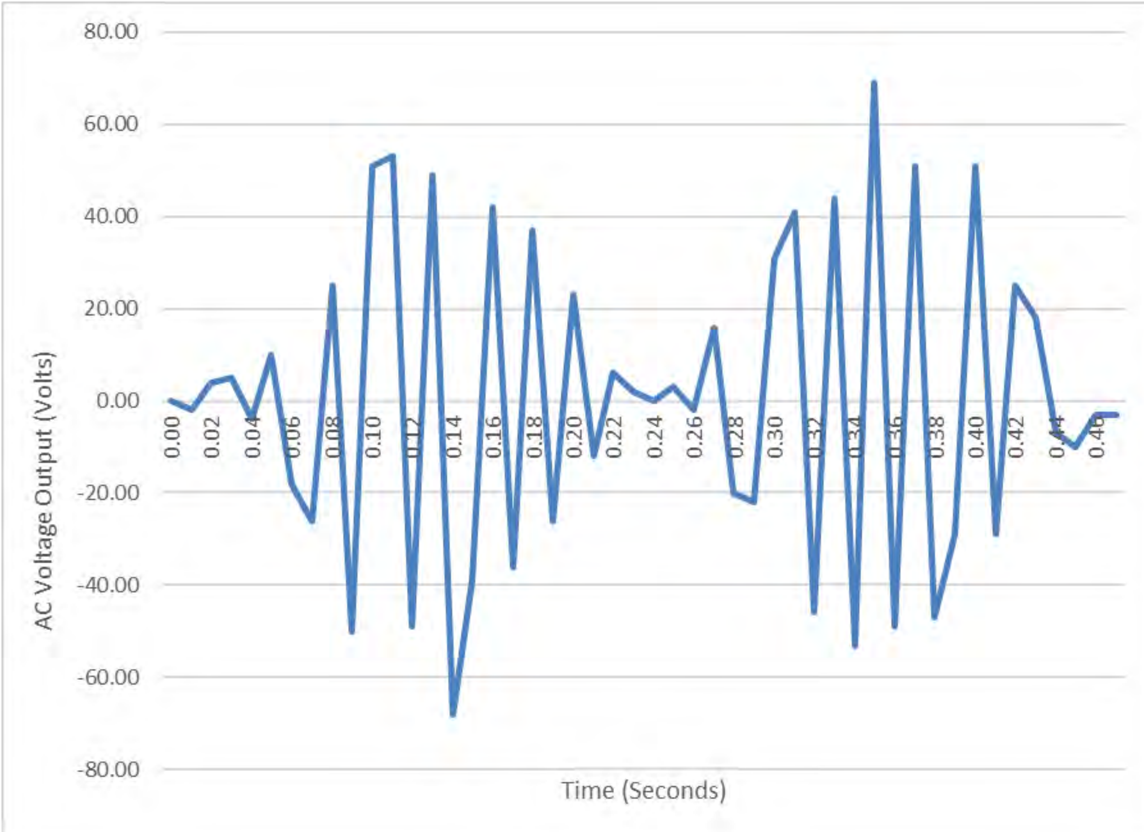

Figure 46. Zoomed In View of AC Voltage Output from Improved TENG with No Additional Weight and 4.167 Hertz TENG Frequency

The zoom in view shows the two pulses from the full speed run. The average peak-to-peak AC voltage output for the three runs at this condition was 151.33 volts. This is the highest peak-to-peak AC output voltage of any of the TENG without any weight added runs.

5. One Bolt of Added Weight, Full Speed

The next condition that was tested was the improved TENG and one bolt (32 grams) of weight added at the full speed of the linear reciprocating motor. The results of this run are shown in Figure 47.

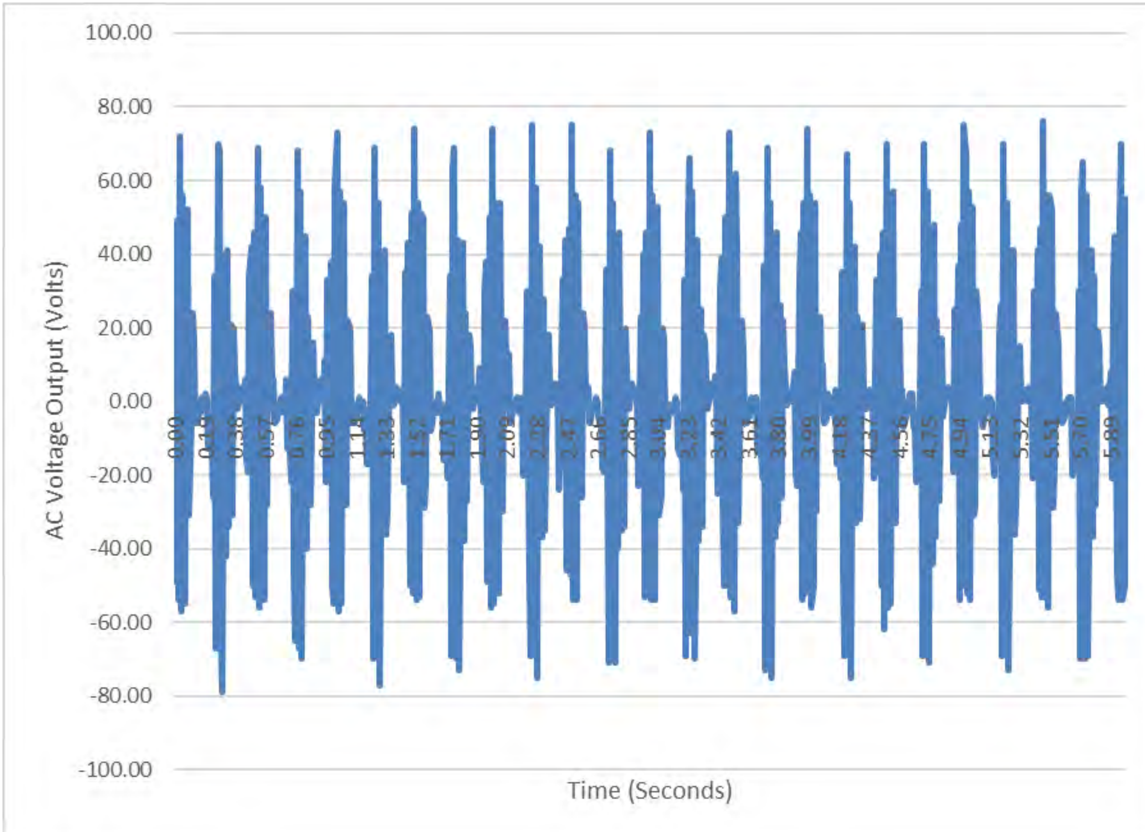

Figure 47. AC Voltage Output from Improved TENG with One Bolt (32 grams), Additional Weight, and 4.167 Hertz TENG Frequency

The maximum peak-to-peak AC output voltage for this run was found to be 155 volts. As shown in other runs compared to the original TENG, this is more than two times the amount of peak-to-peak AC output voltage under the same conditions. The zoomed in view of this run is shown in Figure 48.

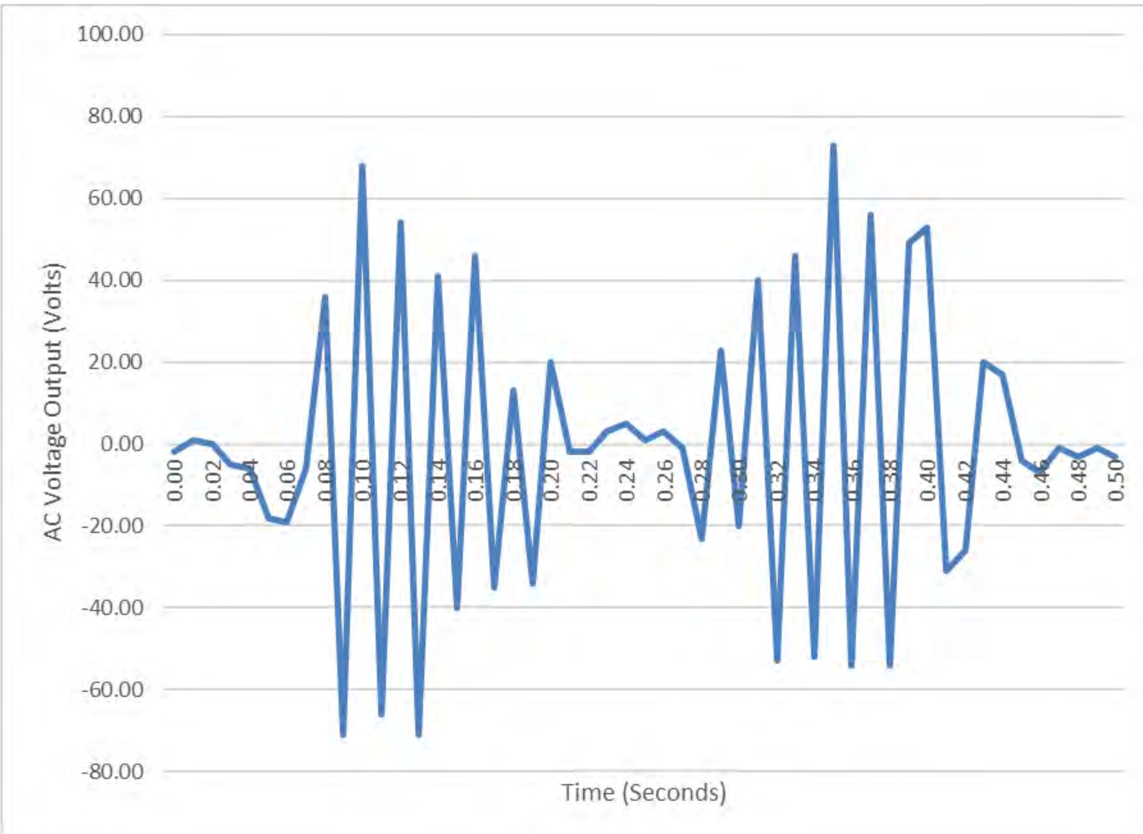

Figure 48. Zoomed In View of AC Voltage Output from Improved TENG with One Bolt (32 grams), Additional Weight, and 4.167 Hertz TENG Frequency

The zoomed in view shows the same pair of pulses as shown in all the previous runs. Of note, the average peak-to-peak AC output voltage for the three runs under these conditions was 166 volts. This is greater than the peak-to-peak AC output voltage for the runs with no weight added.

6. Three Bolts of Added Weight, Full Speed

The final condition for the improved TENG with the linear reciprocating motor was with the motor at full speed and three bolts (96 grams) of weight in the weight holder. The results from one of these runs are shown in Figure 49.

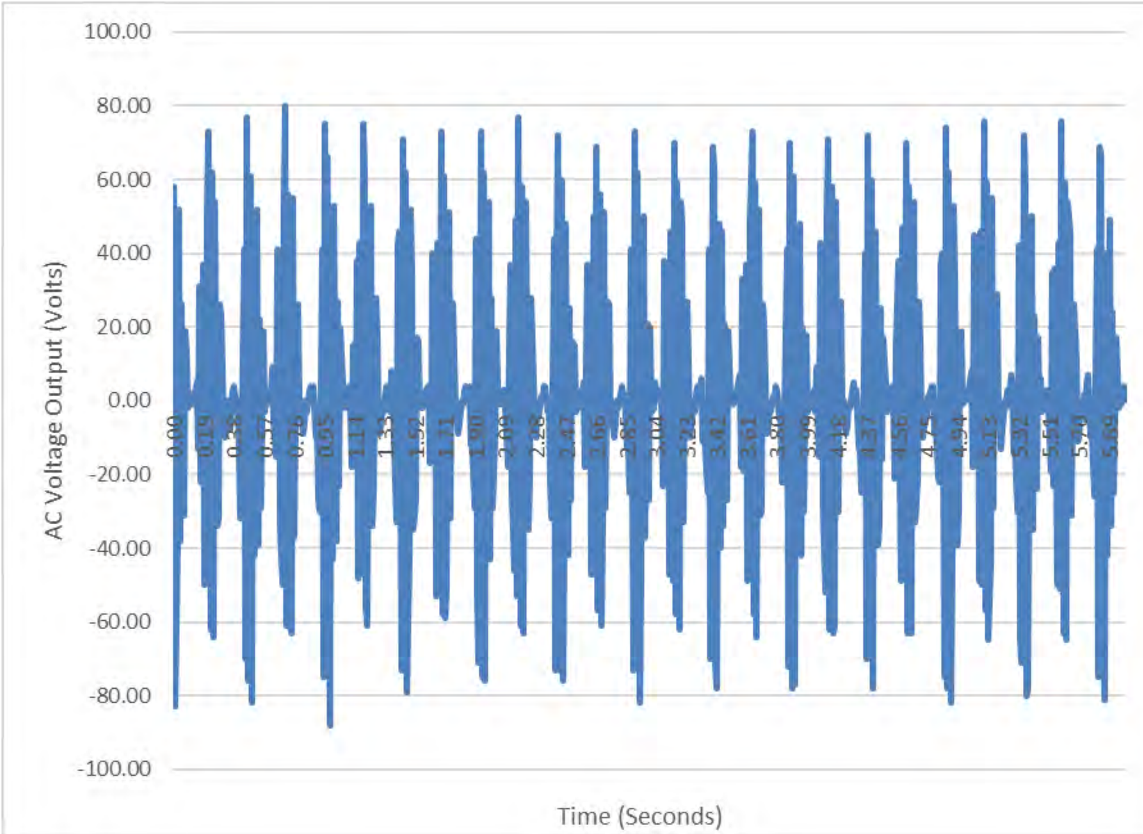

Figure 49. AC Voltage Output from Improved TENG with Three Bolts (96 grams), Additional Weight, and 4.167 Hertz TENG Frequency

The maximum peak-to-peak AC output voltage for this run was 168 volts. The pattern continued with this being more than twice the peak-to-peak AC output voltage of the same conditions run with the original TENG. The zoomed in view of this run is shown in Figure 50.

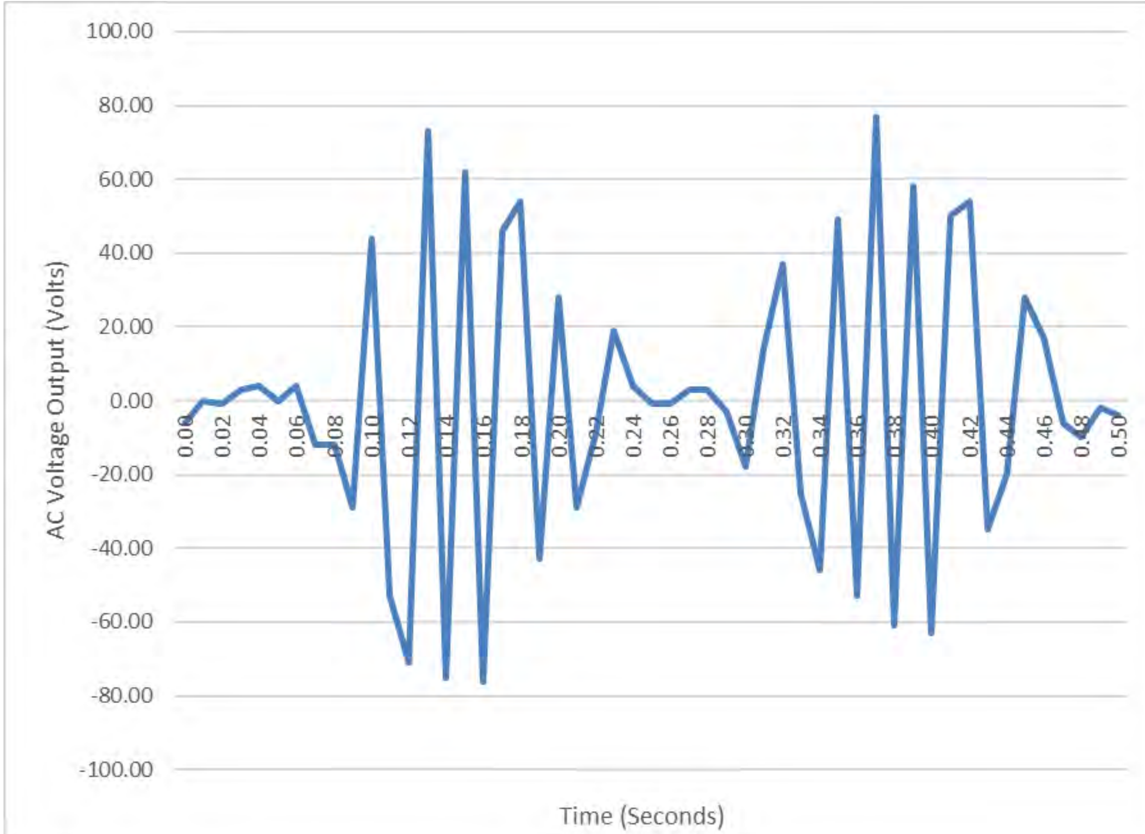

Figure 50. Zoomed In View of AC Voltage Output from Improved TENG with Three Bolts (96 grams), Additional Weight, and 4.167 Hertz TENG Frequency

These two pulses in the zoomed in view also continue to show the pattern of most positive maximum in one pulse followed by the most negative minimum in the next pulse. The average for the three runs under this condition for peak-to-peak AC output voltage was 169.67 volts. This is the highest voltage of any of the runs completed with both the original and improved TENGs and the linear reciprocating motor. The data from runs 2 and 3 for the improved TENG under all conditions is located in Appendix B.

7. Thinner PTFE Tape

For the next testing condition, the major change was with the thickness on the PTFE track as shown in Figure 23. For this new track, the improved TENG was tested with the linear reciprocating motor at full speed. In addition, two weight conditions were tested, one with no added weight and one with three bolts (96 grams) of added weight. This created two new conditions to be completed with the improved TENG. Each of these conditions was run three times to ensure the repeatability of the data.

The first run with the thinner PTFE tape track was with no added weight and the motor at full speed. The results from this test are shown in Figure 51.

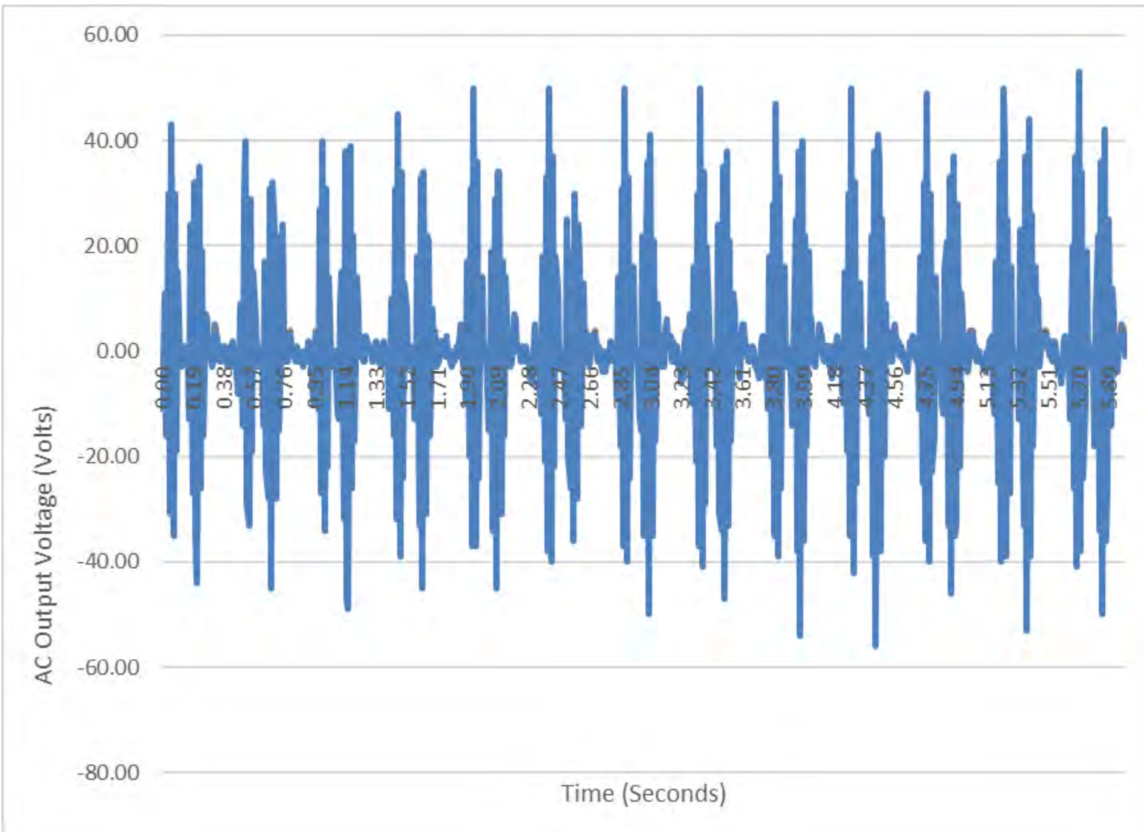

Figure 51. AC Voltage Output from Improved TENG with No Additional Weight, Thinner PTFE Tape on the Track and 4.167 Hertz TENG Frequency

The average maximum peak-to-peak AC output voltages for the three runs with this condition was 121 volts. This is about 30 volts less than the same speed and weight conditions for the improved TENG and the thicker PTFE tape.

The second condition with the thinner PTFE tape was completed with the linear reciprocating motor at full speed and the weight of three bolts (96 grams) in the weight holder. The results from this run are shown in Figure 52.

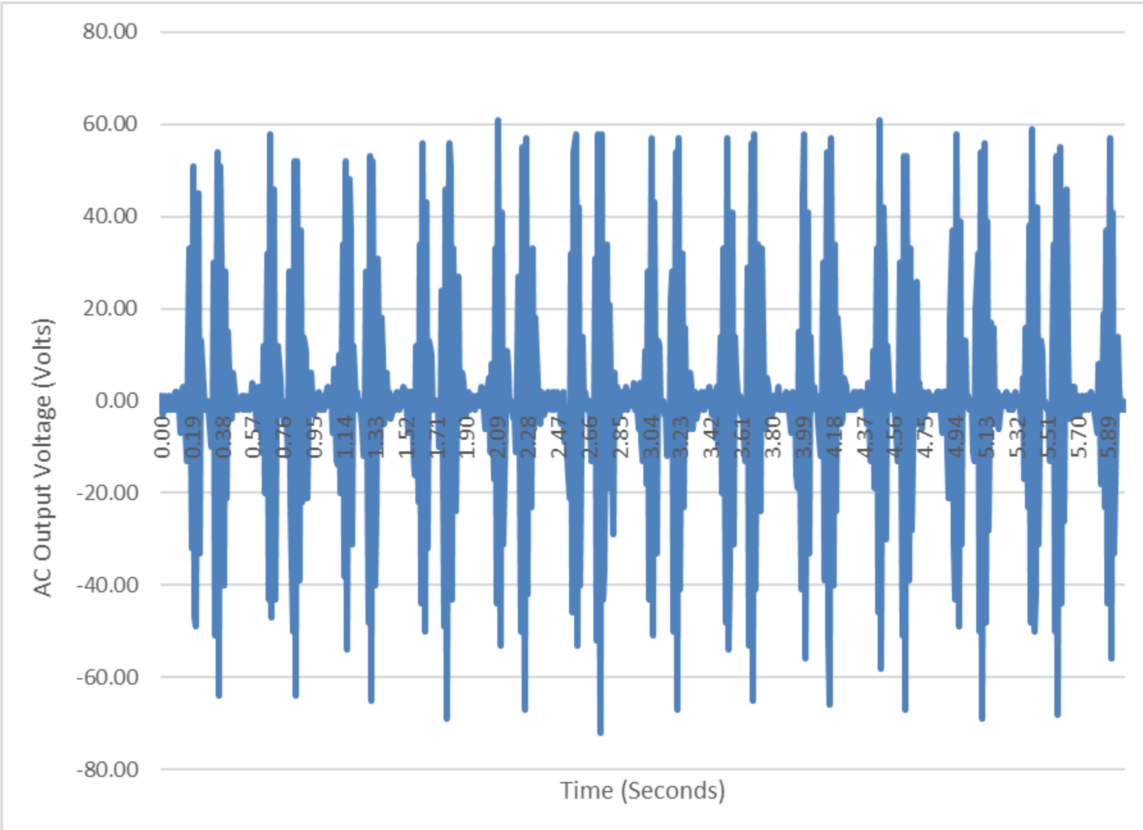

Figure 52. AC Voltage Output from Improved TENG with Three Bolts (96 grams) of Additional Weight, Thinner PTFE Tape on the Track and 4.167 Hertz TENG Frequency

The average maximum peak-to-peak AC output voltage for the three runs at this condition was 146.67 volts. This is about 20 volts less than the improved TENG under the same conditions with the thicker pieces of PTFE tape on the track. It was concluded that having the thinner PTFE tape was not beneficial to get the maximum AC voltage output of the improved TENG. The data from runs 2 and 3 with the thinner PTFE tape is located in in Appendix C.

8. Maximum Output by Hand

The final condition completed with the improved TENG was to get a maximum output AC voltage with the TENG powered by a human hand with the thicker PTFE tape track. This test was completed three times to validate the repeatability of the data. The results from the first run are shown in Figure 53.

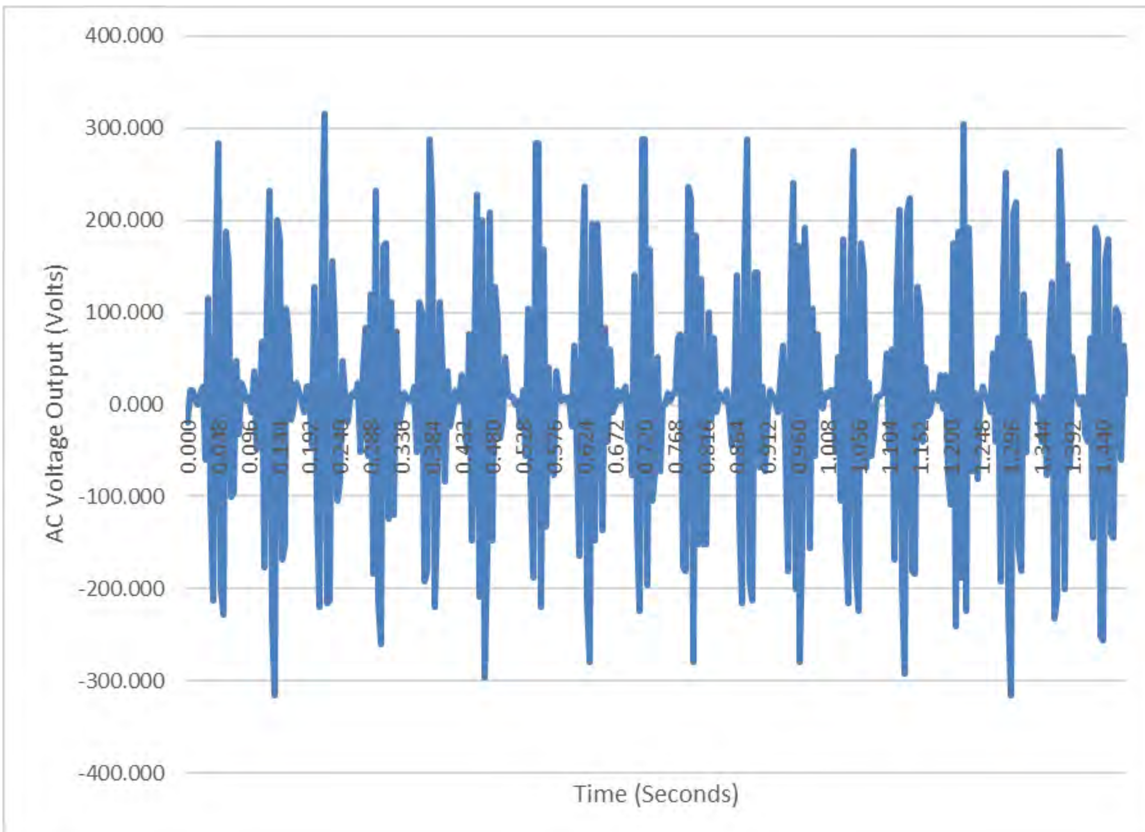

Figure 53. AC Voltage Output of the Improved TENG with Maximum Output by Hand

For this run, the maximum peak-to-peak AC voltage output was 632 volts. It was completed at frequency of the TENG of 9.8 hertz. The average maximum peak-to-peak AC voltage output of the three runs was 641.33 volts and were run at an average TENG frequency of 10.4 hertz. The data from runs 2 and 3 is located in Appendix D.

9. Summary of Improved TENG Results

Similarly, to the comparisons made with the original TENG, the improved TENG was found to have a relationship between the operating frequency of the TENG and the maximum peak-to-peak AC output voltage. The overview of the frequency of the improved TENG, the additional weight, and the maximum peak-to-peak AC voltage output is shown in Table 2.

Table 2. Summary of Improved TENG Testing with Linear Reciprocating Motor

Frequency (Hertz)	Added Weight (Grams)	Average (for 3 Runs) Maximum Peak to Peak AC Output Voltage (Volts)
2.08	0.00	64.33
2.08	32.00	71.60
2.08	96.00	74.13
4.17	0.00	151.33
4.17	32.00	166.00
4.17	96.00	169.67
10.40	N/A	641.33

Just as was observed with the frequency increase with the original TENG, the improved TENG also had an increase in the maximum peak-to-peak AC voltage output. This trend is shown in Figure 54.

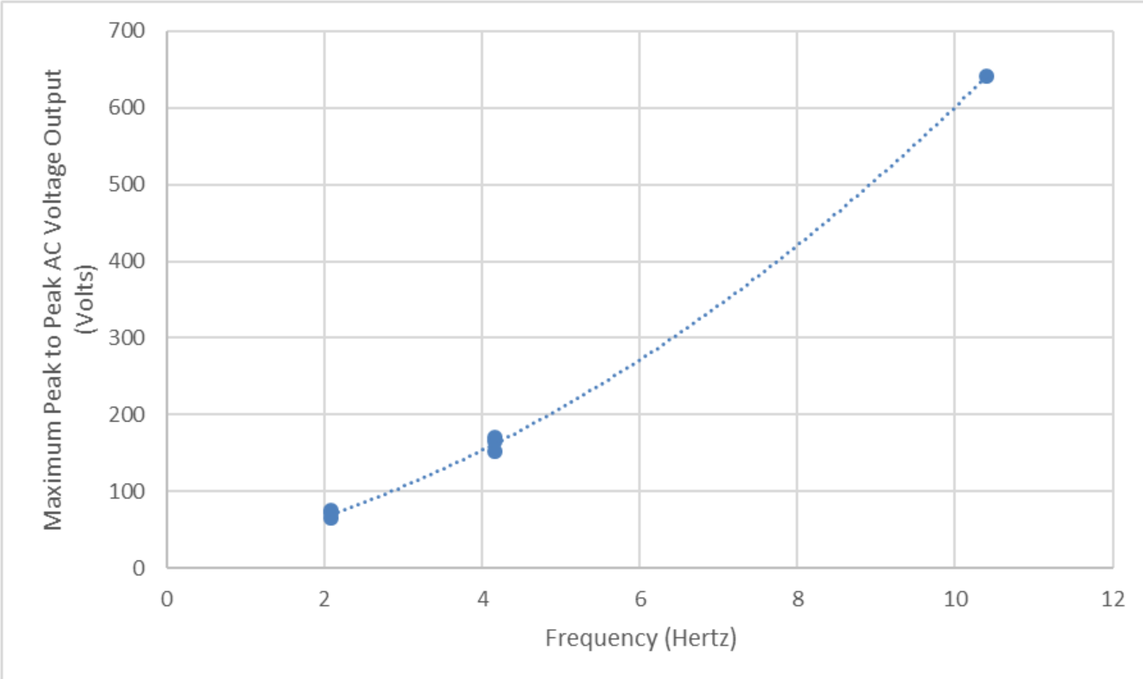

Figure 54. TENG Frequency and AC Voltage for Improved TENG with Thick PTFE Tape

The trend between frequency and maximum peak-to-peak AC voltage output for the improved TENG has a bit more linear, but still polynomial, trend than what was seen with the original TENG. Yet, it was clear that the increase in frequency directly correlated to an increase in AC voltage.

Upon further analyzation of the improved TENG run with the two speeds and three weight conditions, peak-to-peak AC voltage output also increased with the additional weight added. Although the impact of the additional weight was not as significant as the frequency, there was a consistent trend that as the weight was added, the peak-to-peak AC voltage output increased. This is shown in Figure 55.

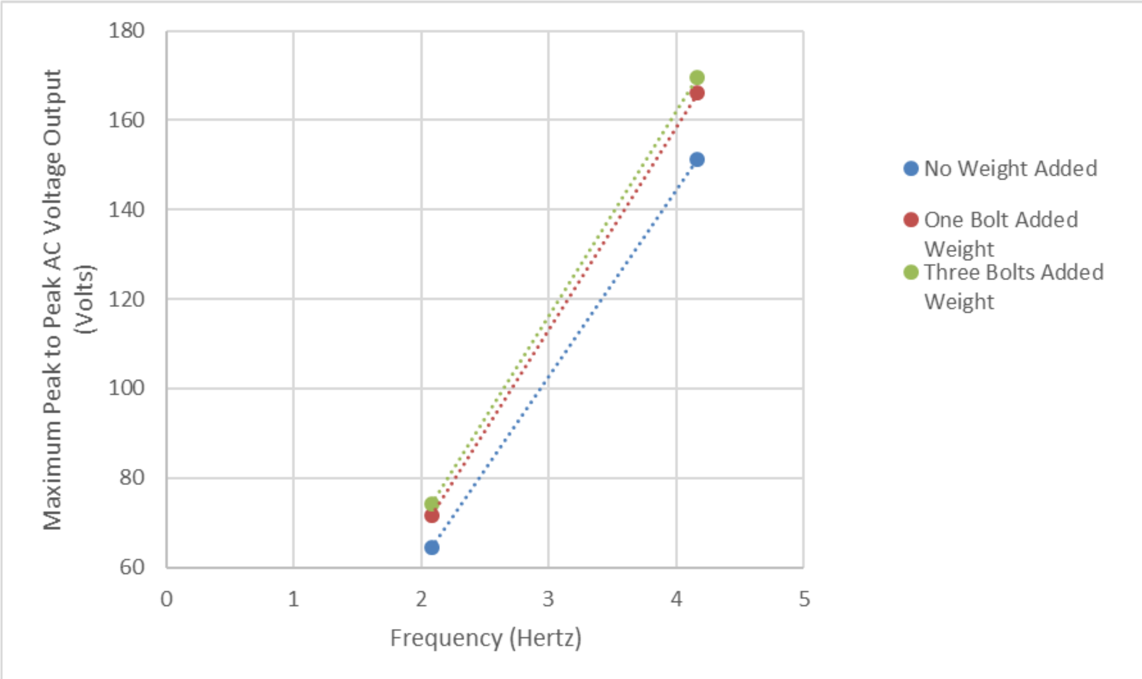

Figure 55. Improved TENG Frequency vs. AC Voltage for Different Weights Added

The direct influence of the additional weight on the maximum peak-to-peak AC output voltage was also analyzed for the improved TENG. The results from this are shown in Figure 56.

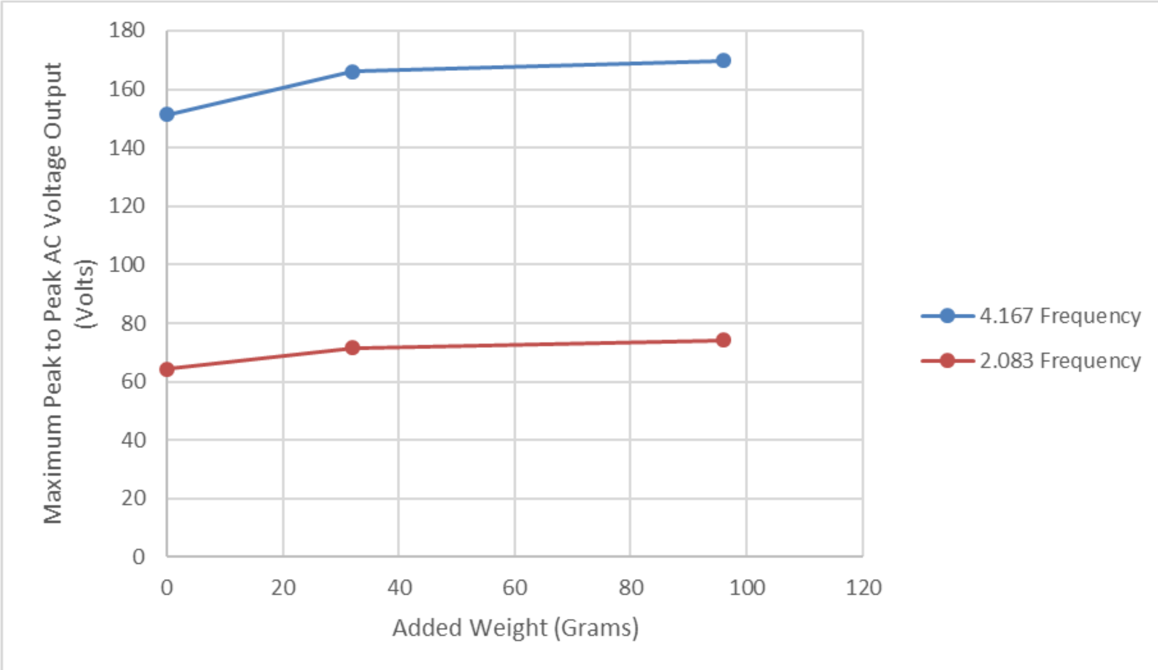

Figure 56. Additional Weight and AC Voltage of Improved TENG

As shown in Figure 55 and Figure 56, there was found to be a trend between the added weight and frequency with the improved TENG. For both the fast frequency (4.167 hertz) and the slow frequency (2.083 hertz), the maximum peak-to-peak AC output voltage increased with the addition of more weight. Although this trend between added weight and AC voltage was found for the improved TENG, the dominating factor for higher AC voltage for both the original and improved TENGS is to have the TENG operating at higher frequencies. The comparison for frequency versus maximum peak-to-peak AC voltage output for both the original TENG and improved TENG are shown in Figure 57.

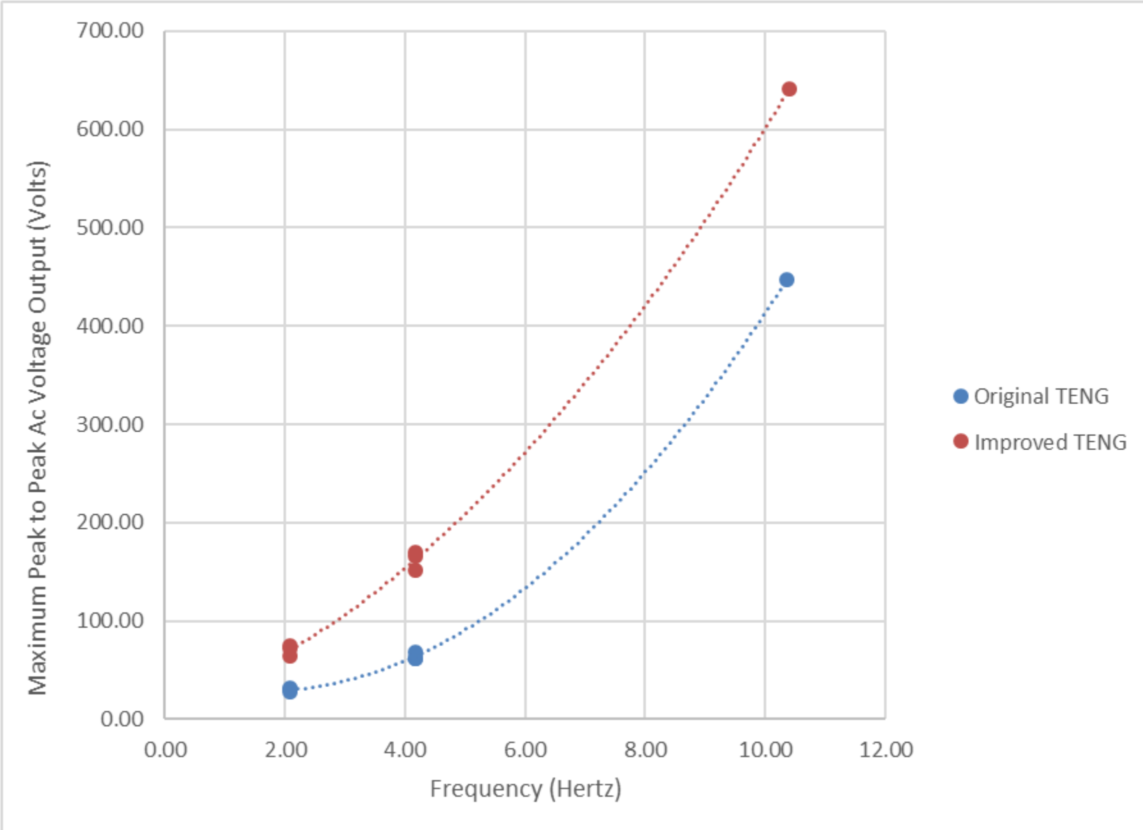

Figure 57. Frequency versus Maximum Peak-to-Peak AC Voltage Output for Original TENG and Improved TENG

C. MODELING TO PREDICT VOLTAGE OUTPUTS OF IMPROVED TENG

Following the testing of the improved TENG with the linear reciprocating motor, it was desired to be able to predict the maximum peak-to-peak AC output voltage for different frequencies. This would allow a user to achieve certain the maximum peak-to-peak AC output voltage by applying a certain frequency to the TENG. The basis of this model was made from the experimental results with the improved TENG and no additional weight condition. The goal of this simplified model was to be able to predict the upper half of the AC voltage signals produced. Equation 1 was used to calculate the model's prediction for AC voltage output for each time step.

$$V(t) = V_{peak} * \sin(\omega * t) \tag{1}$$

In Equation 1, peak voltage, V_{peak}, was determined based on the experimental data from the TENG testing with the linear reciprocating motor. For the slow frequency of 2.083 herrtz, a peak voltage of 32.5 volts was used and for the fast frequency of 4.167 hertz, a peak voltage of 75.5 volts was used. The angular frequency, ω, was calculated by multiplying the frequency of the TENG by 2π. For the frequency of 2.083 hertz, the angular frequency was 13.088 radians per second and for the frequency of 4.167 hertz, the angular frequency was 26.18 radians per second. Finally, the time, t, was set at the same intervals the data was taken experimentally. The results from the model compared to the first run, 2.083 hertz frequency TENG testing with no additional weight is shown in Figure 58.

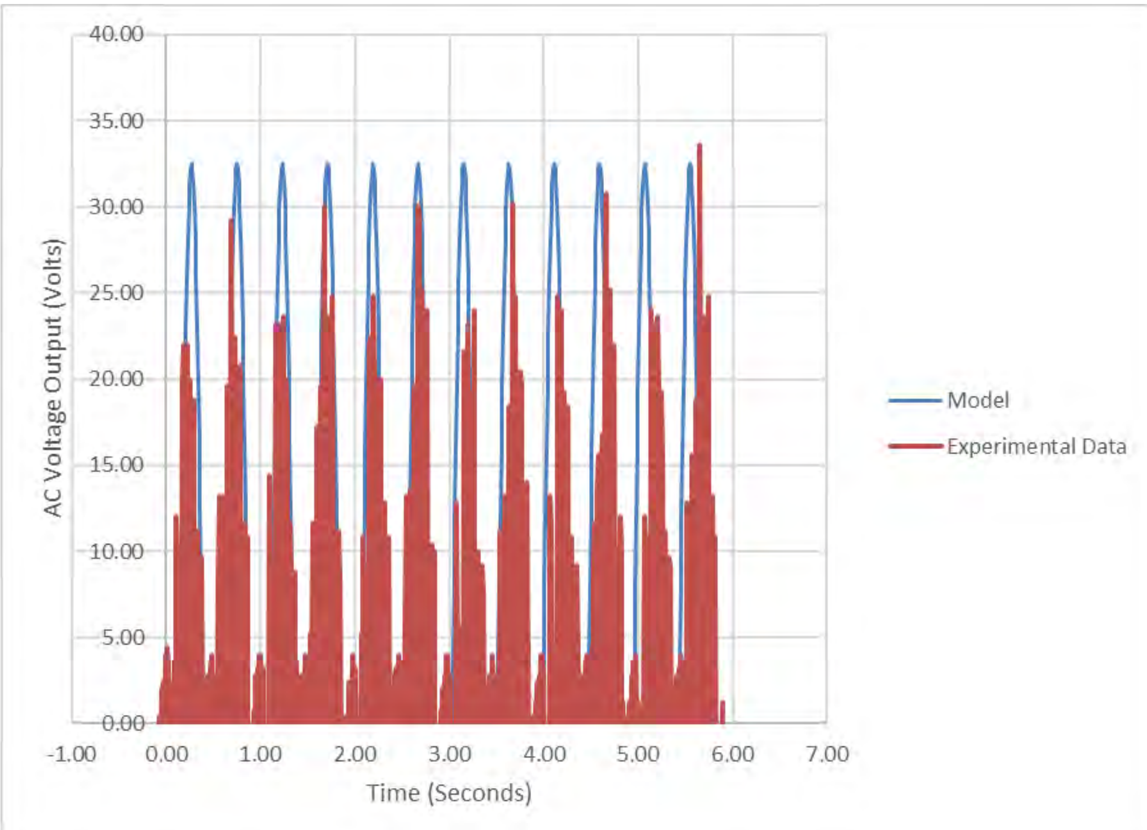

Figure 58. Model to Predict Peak AC Voltage Output of Improved TENG, 2.083 Hertz Frequency, No Additional Weight

As shown in Figure 58, the model was successful in the prediction of the peak AC voltage output of the improved TENG operated at a frequency of 2.083 hertz and no additional weight added. The results from the model compared to the first run, 4.167 hertz frequency TENG testing with no additional weight are shown in Figure 59

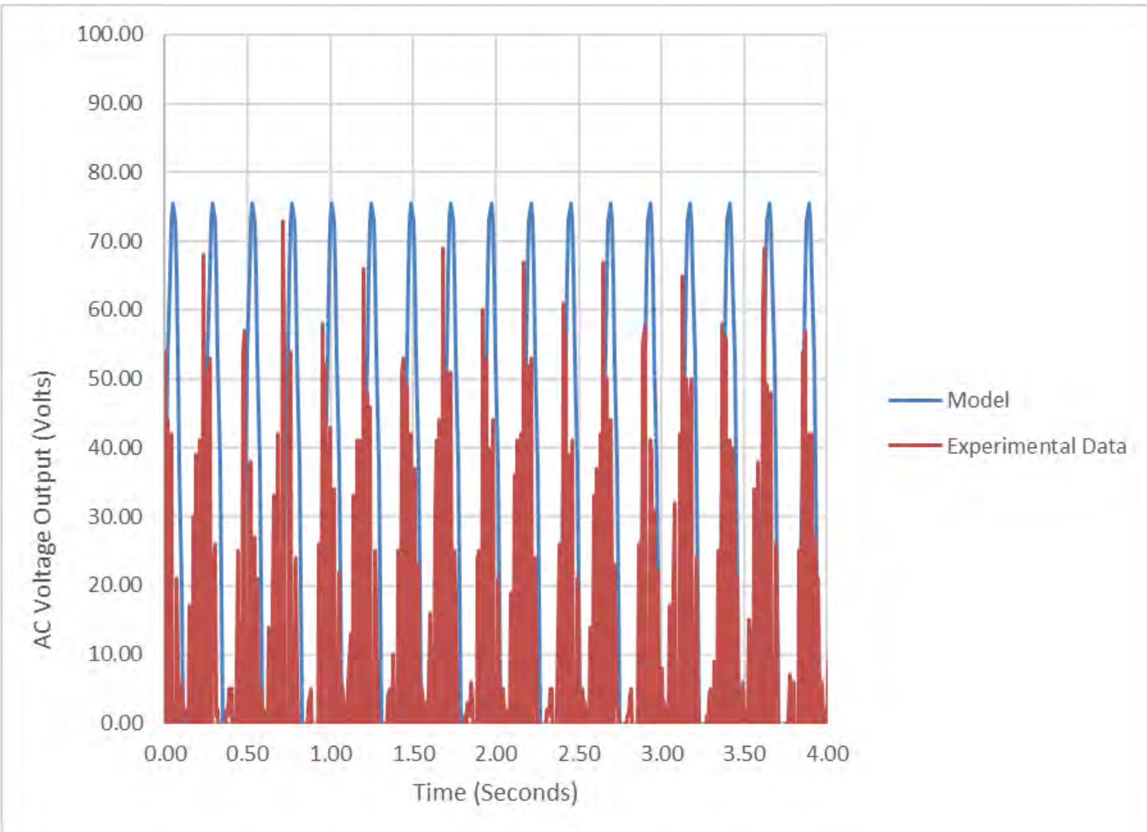

Figure 59. Model to Predict Peak AC Voltage Output of Improved TENG, 4.167 Hertz Frequency, No Additional Weight

This model was also successful at predicting the AC voltage output for the improved TENG at the higher frequency.

THIS PAGE INTENTIONALLY LEFT BLANK

IV. OSCILLATING COLUMN AND TENG

The next step in this research was to combine the TENG with a device that could extract the energy found in water waves. An oscillating column (OC) was the device used for this purpose. The OC is a type of point absorber because the whole column oscillates with the water falling and rising with the wave. The OC was restricted to only be able to operate in the heave (vertical) direction, thus giving the TENG sliding linear motion.

A. COMBINATION OF AN OC AND TENG

An acrylic column with a diameter of 25.4 centimeters and a height of 24.5 centimeters was the main component of the OC. The thickness of the column was 0.397 centimeters. The bottom of the column was closed off, but the top was open. A cap for the column with a height of 12.7 centimeters and a 2.54-centimeter hole in the center was designed to fit inside the column. This cap was designed to make sure the column operated strictly in the heave direction. The cap was built in SolidWorks and the model of it is shown in Figure 60 and Figure 61, the units shown are in centimeters.

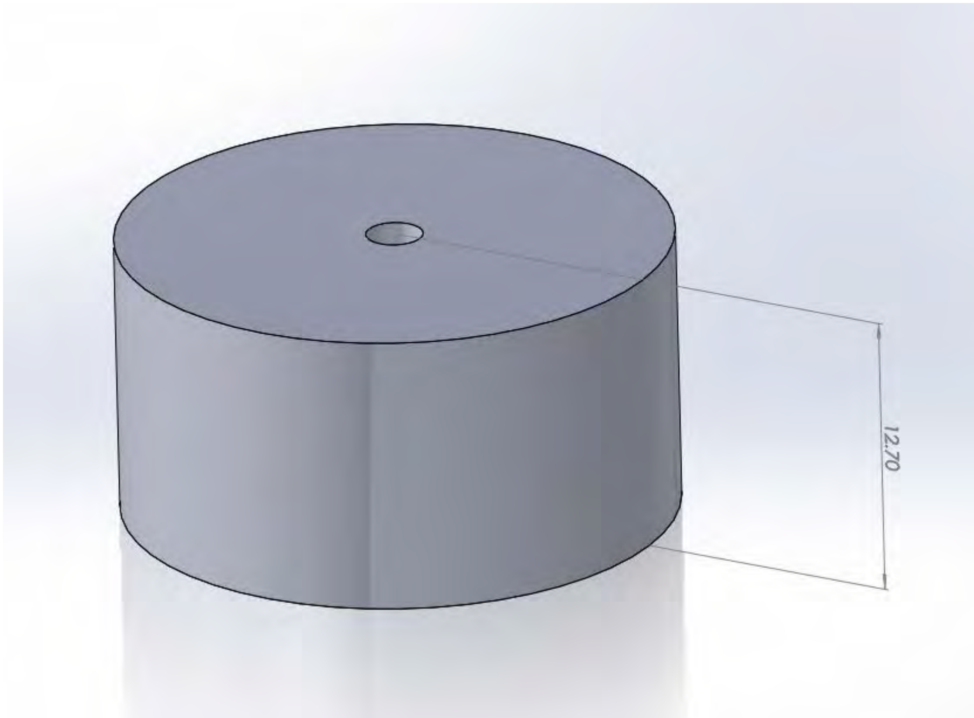

Units in centimeters.

Figure 60. Side View of SolidWorks Model of Cap for the OC

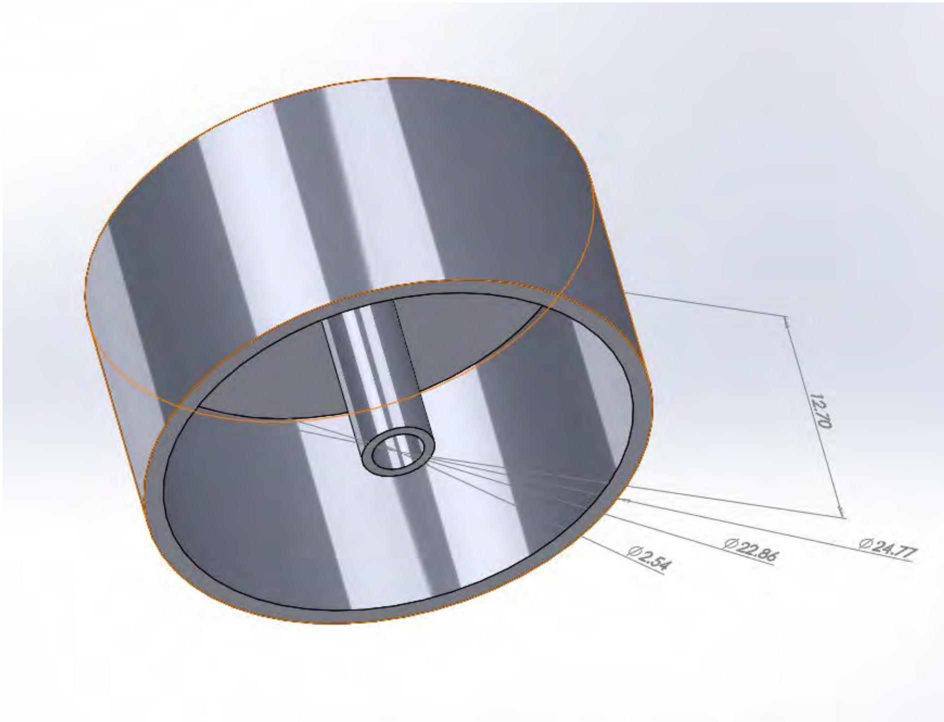

Units in centimeters.

Figure 61. Bottom View of SolidWorks s Model of Cap for OC

This cap was 3D printed on the Fortus 400mc in Bullard Hall at the Naval Postgraduate School in Monterey, California. A block with one flat side and one curved side was then built in SolidWorks to attach the TENG to the OC cap. The SolidWorks model of this block is shown in Figure 62; the units shown are in centimeters.

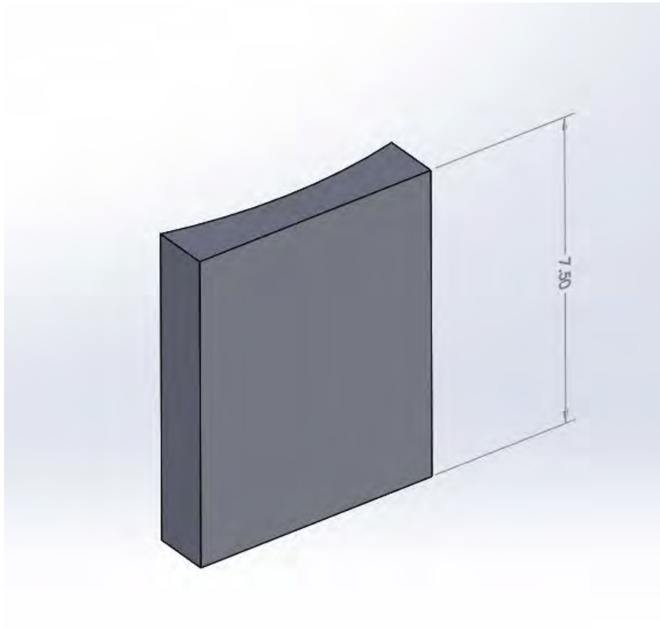

Units in centimeters.

Figure 62. SolidWorks Model of Block to Attach TENG to the OC Cap

This block was printed at the RoboDojo at the Naval Postgraduate School in Monterey, California. The OC cap was then super glued into the column to a depth that would allow the block and TENG to be attached to the side of it. A photo of the final OC with the TENG attached to it is shown in Figure 63.

Figure 63. OC with TENG and Cap Attached, Close Up (left), Overall Experimental Test Article (right)

The overall height of the structure was 33.02 centimeters after the cap was attached. Following the construction of the TENG with the OC, a hole was drilled into a piece of wood to fit across the width of the wave tank. A polyvinyl chloride (PVC) pipe was selected to have a tight fit through the hole in the wood, but have a looser fit through the hole in the cap of the OC. This kept the PVC pipe fixed but allowed the OC to heave along the pipe. In addition, a piece of wood was attached perpendicular to the piece of wood that spanned the width of the tank. This perpendicular piece of wood then had the TENG track attached to it. It was critical that the attachment of the perpendicular piece of wood and TENG track matched up with the TENG block so the triboelectricity could be generated. The final setup of the OC with the TENG attached and matching up with the TENG track in the wave tank is shown in Figure 64.

Figure 64. Full Setup of OC with TENG Attached in Wave Tank

B. TESTING OF TENG WITH AN OC

The OC with the improved TENG attached was tested in the wave tank in Halligan Hall at the Naval Postgraduate School in Monterey, California. It was tested with seven different frequencies of incident waves: 1.716, 1.475, 1.315, 1.2, 1.002, 0.903 and 0.816 hertz. All of these frequencies of waves were set to a wave amplitude of 2.54 centimeters, giving the waves a height of 5.08 centimeters. This wave height was selected to make sure the sliding motion of the TENG stayed within the length of the track. Each of these frequencies was run for two tests to verify the repeatability of the data. The AC voltage outputs were measured with a Keysight DSO1052B digital oscilloscope.

C. EXPERIMENTAL RESULTS OF TENG WITH OC

The highest frequency of wave used was 1.716 hertz. This was run for two tests and created a TENG frequency of about 3.43 hertz because for each wave the TENG had both an up and a down motion. The AC output voltage from these tests is shown in Figure 65.

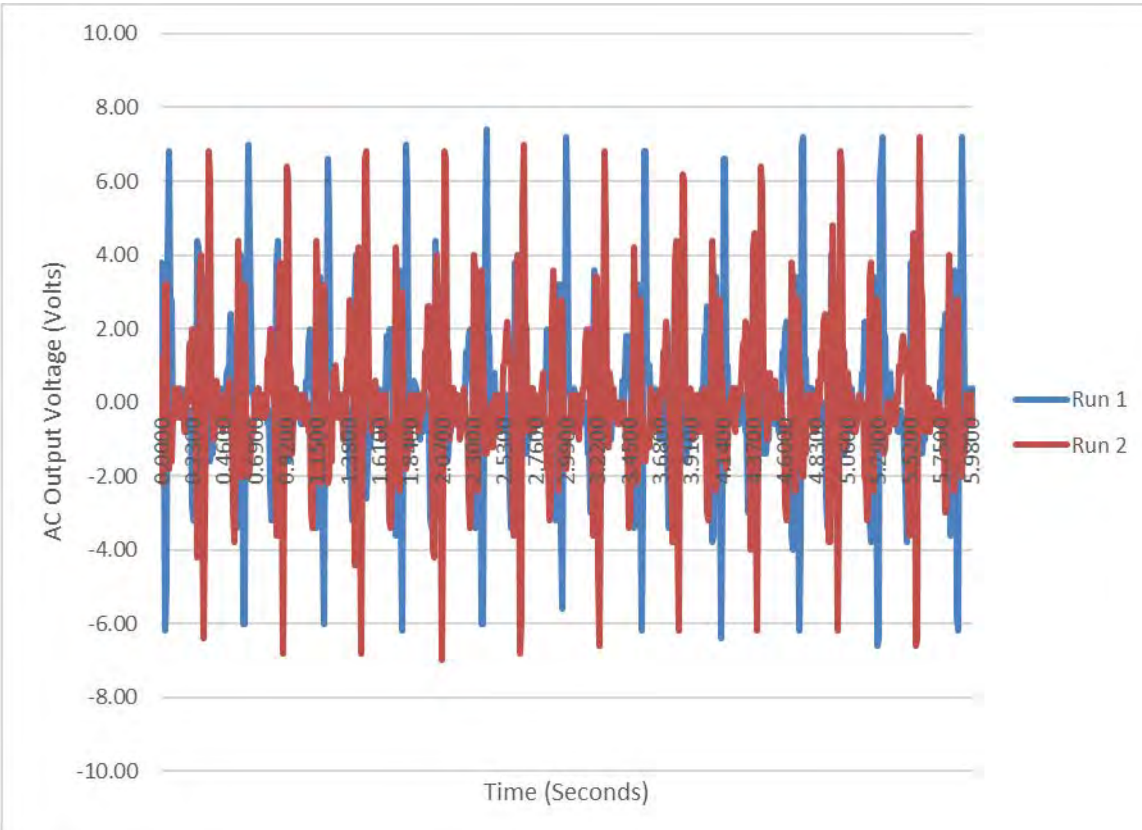

Figure 65. AC Output Voltage of TENG and OC with 1.716 Hertz Frequency of Wave (3.43 Hertz Frequency of TENG)

Similar to the results seen when the TENG was tested with the linear reciprocating motor, the same pulsing of AC output voltage occurred. Yet, with this wave testing, the AC voltage outputs were much less than with the initial experimentation with the motor. The maximum peak-to-peak AC output voltage of run 1 was 14 volts and of run 2 was 14.4 volts.

The next frequency of wave used was 1.475 hertz. This created a TENG frequency of about 2.9 hertz. This was run for two tests and the AC voltage outputs of these tests are shown in Figure 66.

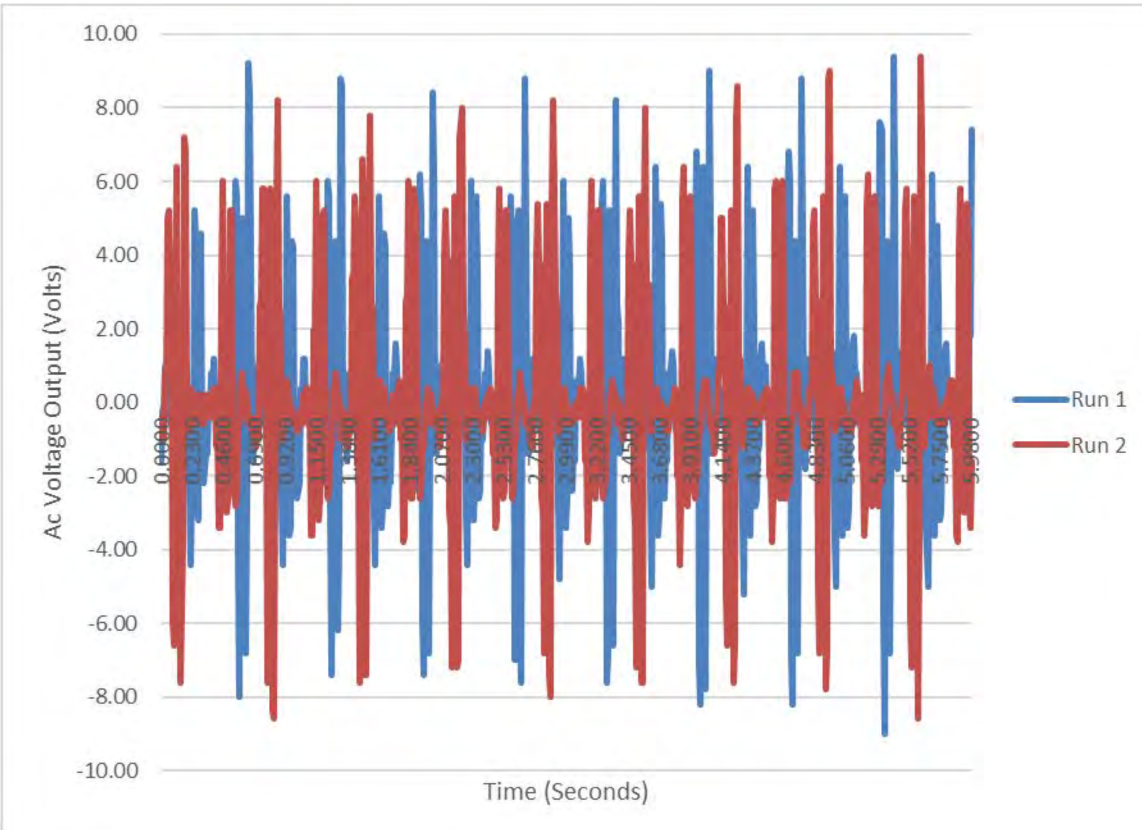

Figure 66. AC Output Voltage of TENG and OC with 1.475 Hertz Frequency of Wave (2.9 Hertz Frequency of TENG)

From the results shown in Figure 66, the wave frequency of 1.475 hertz produced a maximum peak-to-peak AC output voltage of 18.4 volts for run 1 and 18 volts for run 2. The next frequency of wave tested was 1.315 hertz. This created a TENG frequency of about 2.66 hertz. The results from this test are shown in Figure 67.

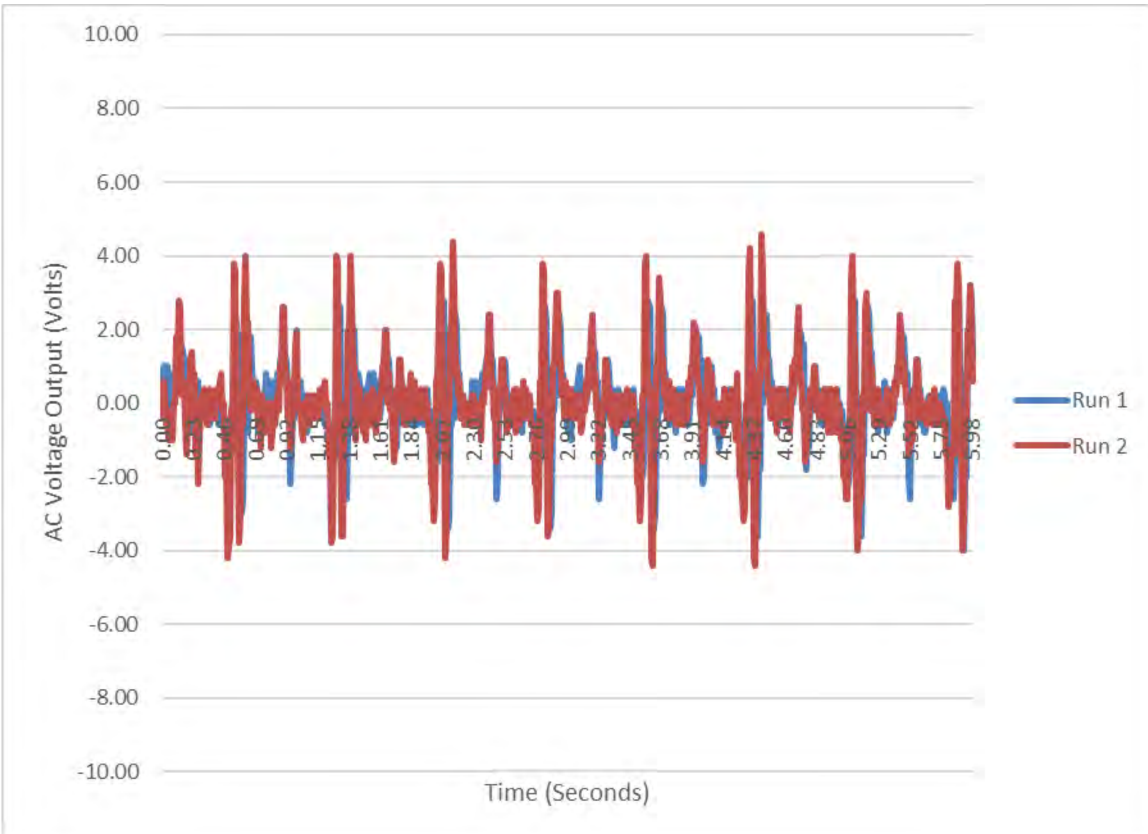

Figure 67. AC Output Voltage of TENG and OC with 1.315 Hertz Frequency of Wave (2.66 Hertz Frequency of TENG)

The maximum peak-to-peak AC output voltage for the 1.315 hertz frequency wave input was found to be particularly lower than any of the previous testing. For run one, the maximum peak-to-peak AC output voltage was 7.2 volts and for run 2 was 9 volts.

The next wave frequency tested was 1.2 hertz. This created a TENG frequency of about 2.4 hertz. The results from this test are shown in Figure 68.

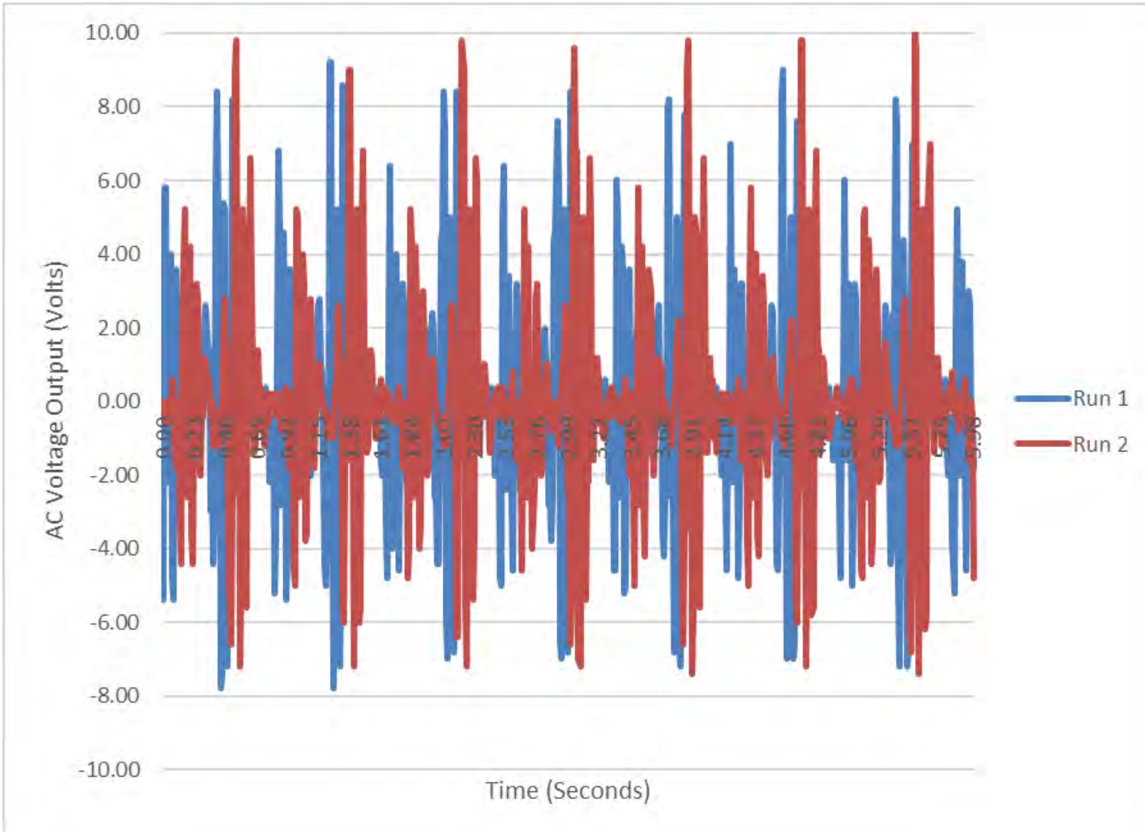

Figure 68. AC Output Voltage of TENG and OC with 1.2 Hertz Frequency of Wave (2.4 Hertz Frequency of TENG)

For the wave frequency of 1.2, the maximum peak-to-peak AC output voltage for run 1 was 17 volts and for run 2 was 17.4 volts. This frequency showed similar properties to the 1.716 hertz frequency and 1.475 hertz frequency testing. The next frequency tested was 1.002 hertz. This created a TENG frequency of about 2 hertz. The result from this test is shown in Figure 69.

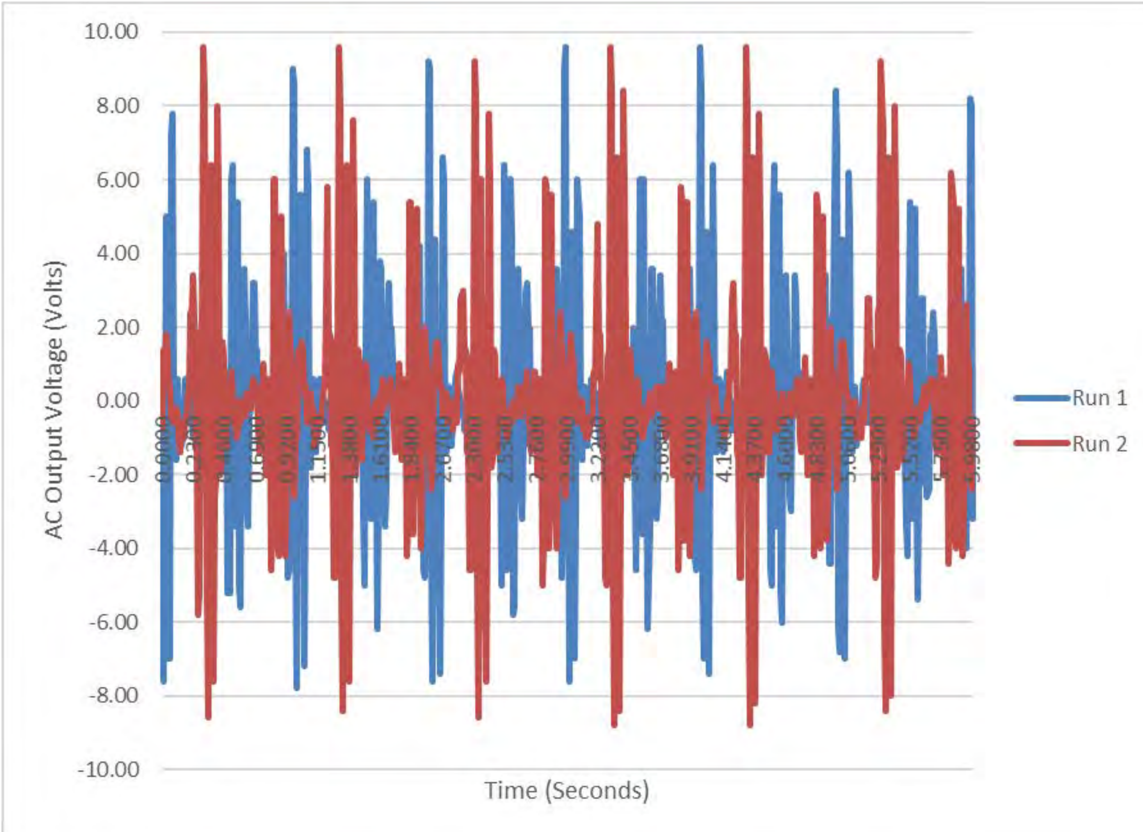

Figure 69. AC Output Voltage of TENG and OC with 1.002 Hertz Frequency of Wave (2.0 Hertz Frequency of TENG)

For the wave frequency of 1.002 hertz, the maximum peak-to-peak output voltages were found to be 17.4 volts for run 1 and 18.4 volts for run 2. The next wave frequency tested was 0.903 hertz. This created a TENG frequency of about 1.8 hertz. The result from this test is shown in Figure 70.

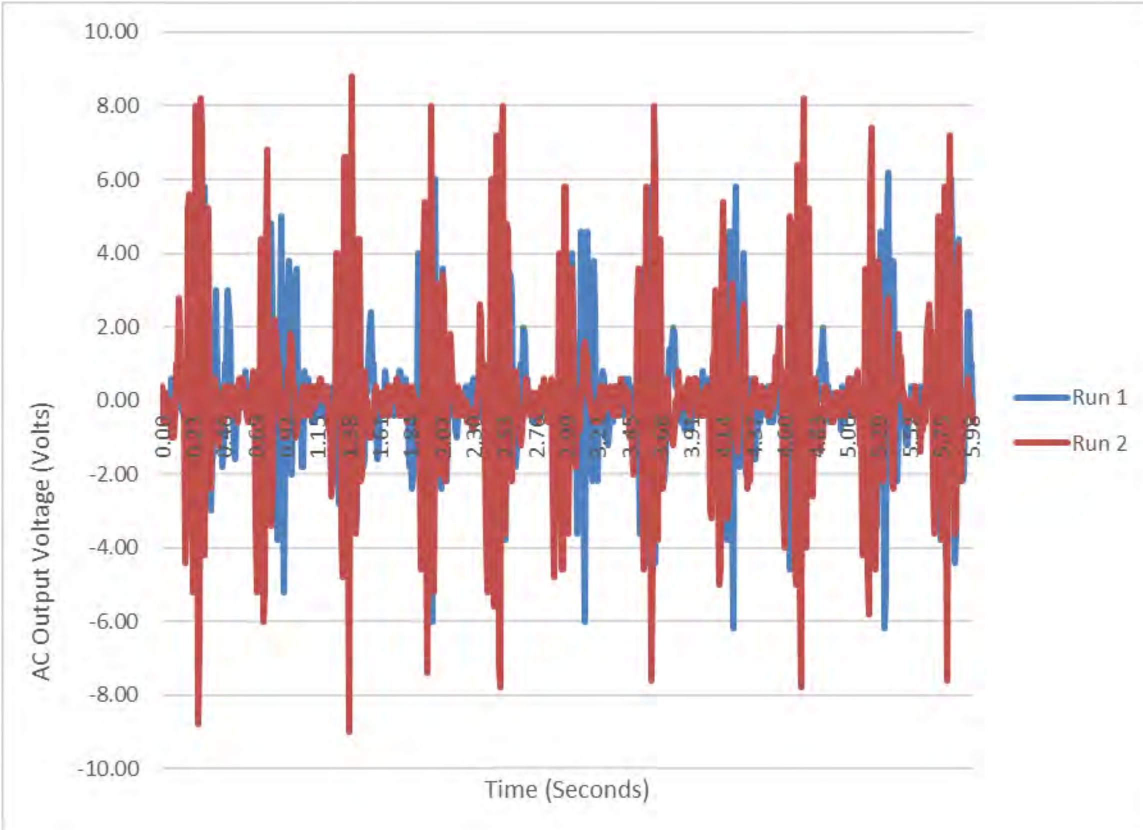

Figure 70. AC Output Voltage of TENG and OC with 0.903 Hertz Frequency of Wave (1.8 Hertz Frequency of TENG)

For the wave frequency of 0.903 hertz, the first run generated a maximum peak-to-peak AC output voltage of 12.4 volts, but the second run generated a much higher maximum peak-to-peak output voltage of 17.8. The final wave frequency tested was 0.816 hertz. This created a TENG frequency of about 1.6 hertz. The result from that test is shown in Figure 71.

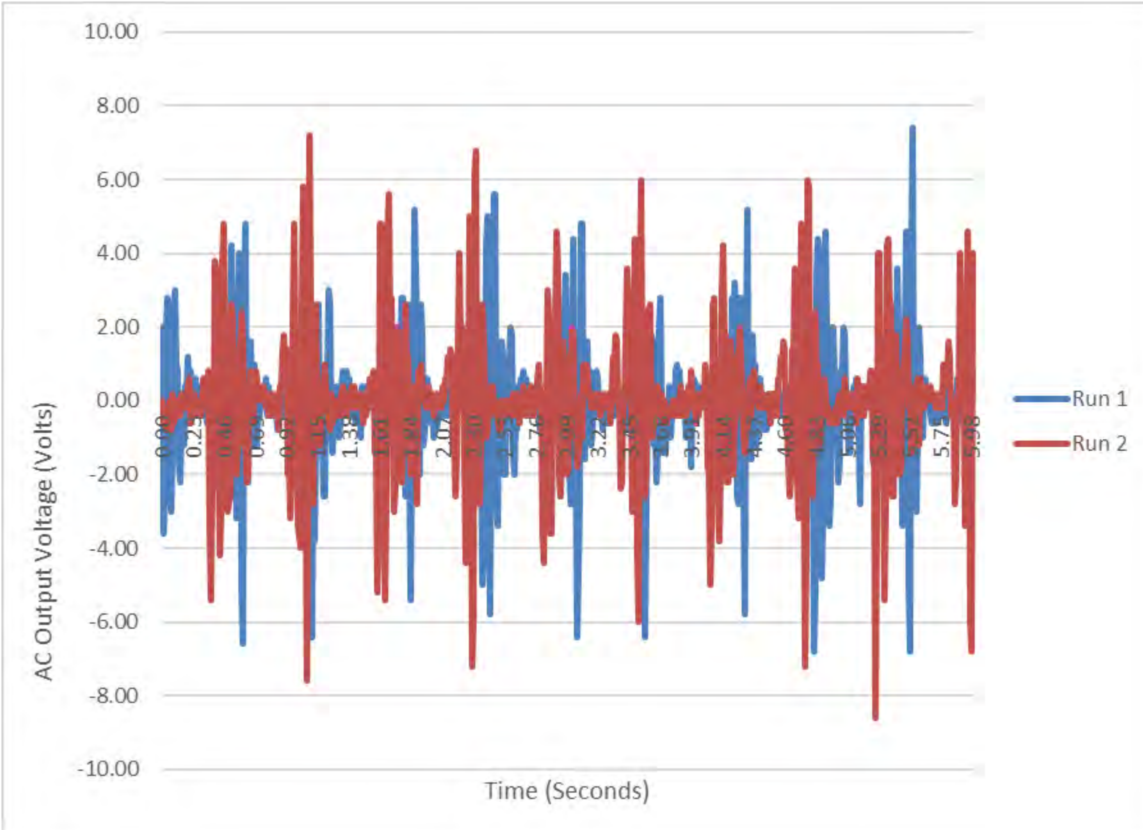

Figure 71. AC Output Voltage of TENG and OC with 0.816 Hertz Frequency of Wave (1.6 Hertz Frequency of TENG)

For this final wave frequency of 0.816 hertz, the maximum peak-to-peak AC output voltage was 14.2 volts for the first run and 15.8 volts for the second run. A summary of all of the wave frequencies run, the corresponding TENG frequency, and the average maximum peak-to-peak AC output voltage are shown in Table 3.

Table 3. Summary of OC and TENG Testing

Wave Frequency	TENG Frequency	Average Max Peak to Peak AC Voltage
1.716	3.4	14.2
1.475	3.0	18.2
1.315	2.6	8.1
1.2	2.4	17.2
1.002	2.0	17.9
0.903	1.8	15.1
0.816	1.6	15

From the results of the testing of the OC and TENG in the wave tank, the TENG maximum peak-to-peak AC voltage outputs did not follow the same pattern with increasing frequency as it did with the linear reciprocating motor. Yet, there are some major operating differences between the linear motor TENG testing and the wave tank TENG testing. One of the major changes is that the TENG is operating in a horizontal motion during the linear motor testing, but during the wave tank testing it is operating in the vertical direction. In the vertical operating direction during the testing in the wave tank, it was difficult to maintain consistent contact forces between the TENG electrode and the TENG track. The TENG relies on the copper electrode and PTFE tape to be in contact to complete the circuit and generate voltage. Nonetheless, it is promising that there was AC voltage produced when the improved TENG was placed in the wave tank and tested, thus triboelectricity was successfully created from waves.

D. MODEL AND EXPERIMENTAL DATA OF TENG WITH OC

Following the testing of the OC with the TENG in the wave tank, it was desired to see if the model developed from the testing with the linear reciprocating motor would be successful in predicting the AC voltage output for the wave tank testing of the TENG. As was discussed, the TENG did not produce as much AC voltage out when operated in the wave tank as when it was operated with the linear reciprocating motor. Therefore, a new plot of TENG frequency versus maximum peak-to-peak AC voltage output was created for the wave tank TENG data. This is shown in Figure 72.

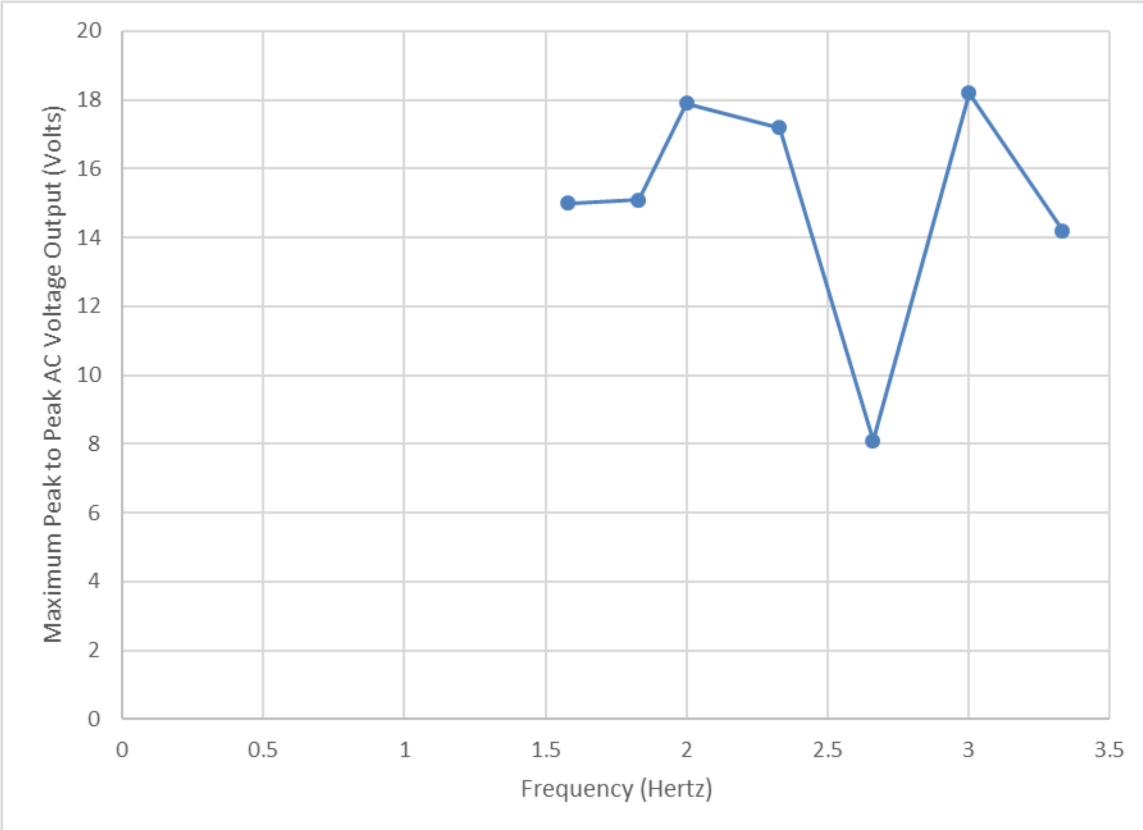

Figure 72. Frequency versus Maximum Peak-to-Peak AC Voltage Output for TENG in Wave Tank

While there was not the same trend that was found with the linear reciprocating motor data, this plot can still be used as a guidance for the peak voltage input into the model to predict the AC voltage output of the TENG.

The model was tested for the wave frequency of 1.002 hertz, giving the TENG a frequency of 2 hertz. A peak voltage, V_{peak}, of 9 volts was used for this model input. This is half of the peak-to-peak voltage of TENG at this frequency. The angular frequency was calculated to be 12.57 radians per second. The results from this model compared to the experimental data are shown in Figure 73.

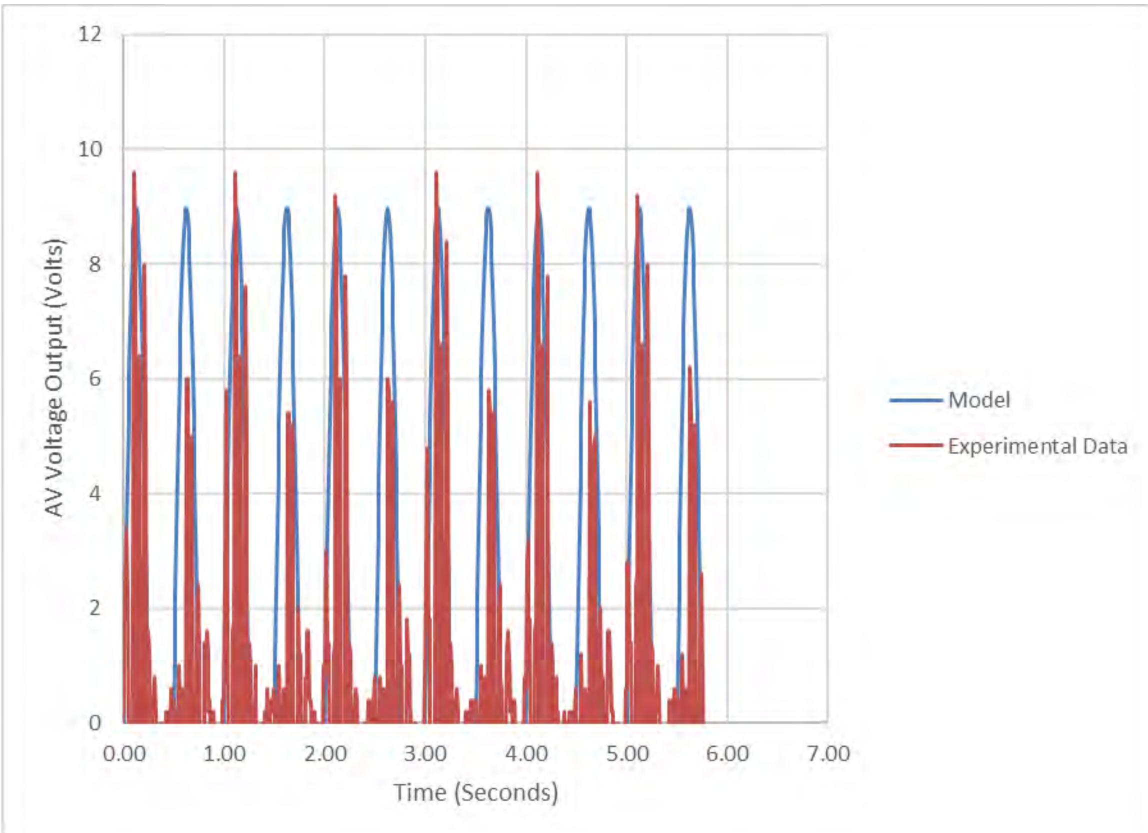

Figure 73. Model vs. Experimental Data from TENG at Frequency of 2 Hertz in Wave Tank

This model was fairly successful at predicting the AC voltage output for the TENG in the wave tank. At some parts, it underestimated the data and at others, it overestimated the data. Yet, the overall trend for the data was successfully represented with the model.

V. CONCLUSION AND FUTURE WORK

A. CONCLUSION

A TENG was successfully constructed and tested with this research project at the Naval Postgraduate School in Monterey, California. This TENG originally had electrodes made out of a copper alloy, but was then improved by using pure copper electrodes. The material on the track that the copper electrode interacted with to complete the TENG circuit was PTFE tape. The original copper alloy TENG and the improved pure copper TENG were both tested with a linear reciprocating motor at two different frequencies and with three different weight conditions. It was found that for both the copper alloy TENG and the pure copper TENG the AC voltage output increased with an increase of the frequency at which the TENG operated. The average maximum peak-to-peak AC output voltage for the copper alloy TENG operated for three tests by hand was found to be 446.67 volts. The average maximum peak-to-peak AC output voltage for the pure copper TENG run for three tests by hand was found to be 641.33 volts. There was no conclusive trend for the impact of the different weights on the original copper alloy TENG. Yet, the improved pure copper TENG was found to have an increase in peak-to-peak AC output voltage with an increase in added weight. The improved TENG made of pure copper was then attached to an OC and tested against 7 different wave frequencies in a wave tank at the Naval Postgraduate School. The improved TENG was successful at generating AC voltage when operating in the wave tank with the OC. The same relationships between frequency and peak-to-peak AC voltage output were not observed with the improved TENG as was the case when it was operated in the wave tank with the linear reciprocating motor. The maximum peak-to-peak AC output voltage for the improved pure copper TENG operating in the wave tank with the OC was 18.4 volts. This maximum of 18.4 volts was found for both the wave frequency of 1.475 hertz and the wave frequency of 1.002 hertz. The TENG was also successfully modeled for both the linear reciprocating motor testing and the wave tank testing using a sine based equation. This sine based equation required inputs of peak voltage, angular frequency, and time.

B. RECOMMENDATIONS

Future testing of a TENG operating in waves should take some things into consideration to improve the AC output voltage. One of these things is to make sure that the TENG is operating in a watertight device. While this experiment was being developed it was learned that it would have been better had the TENG been set up to be protected from the water to prevent any issues that arise when electricity comes into contact with water. In addition, the material selection for the TENG should be a high priority when developing the initial plans for the TENG. This material selection is critical for not only the AC output voltage, but also for the durability of the TENG. Since the TENG is operating on frictional energy there is inevitability going to be wearing down of the materials so more sturdy and durable materials are desirable. Finally, if initial tests outside of the wave tank are completed, they should be tested in the same direction that the TENG will be operating in the wave tank. This will allow any issues that arise with the motion of the TENG operating to be resolved before the TENG is tested in the wave tank.

C. FUTURE WORK

While great strides were made throughout this research project to generate triboelectricity from the energy in ocean waves, there is still a lot more potential and work to be completed with this topic. One thing is that the AC output voltage needs to be collected to charge a capacitor or battery which could then power other devices. This is a very important step so that the electricity generated can be used. In addition, there is a lot of potential to optimize and improve the current TENG operation. While the linearly sliding TENG proved to provide AC output voltage, there are other ways in which the TENG can be utilized with the motion of the waves. It could also be explored what the impact is of having more than one TENG operating at a time, or what happens when the size of the TENG is increased. The TENG could also be tested with more and heavier added weight to see if there are more trends with the increase in contact force. Ultimately, the final step is developing how to get the optimal AC output pulses from an ocean wave. Those output pulses then need to be able to charge a capacitor or battery for use in powering devices, sensors, or lights.

APPENDIX A. ORIGINAL TENG RESULTS RUNS 2 AND 3

The experimental results for the original TENG operated with the linear reciprocating motor with different weight and speed conditions follow.

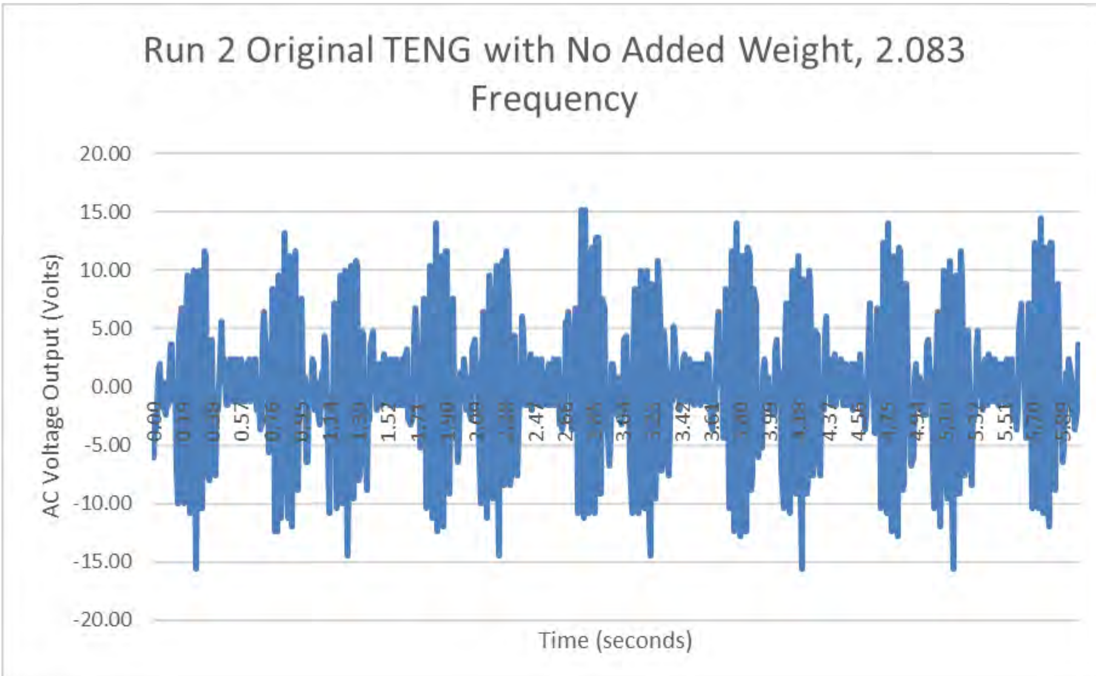

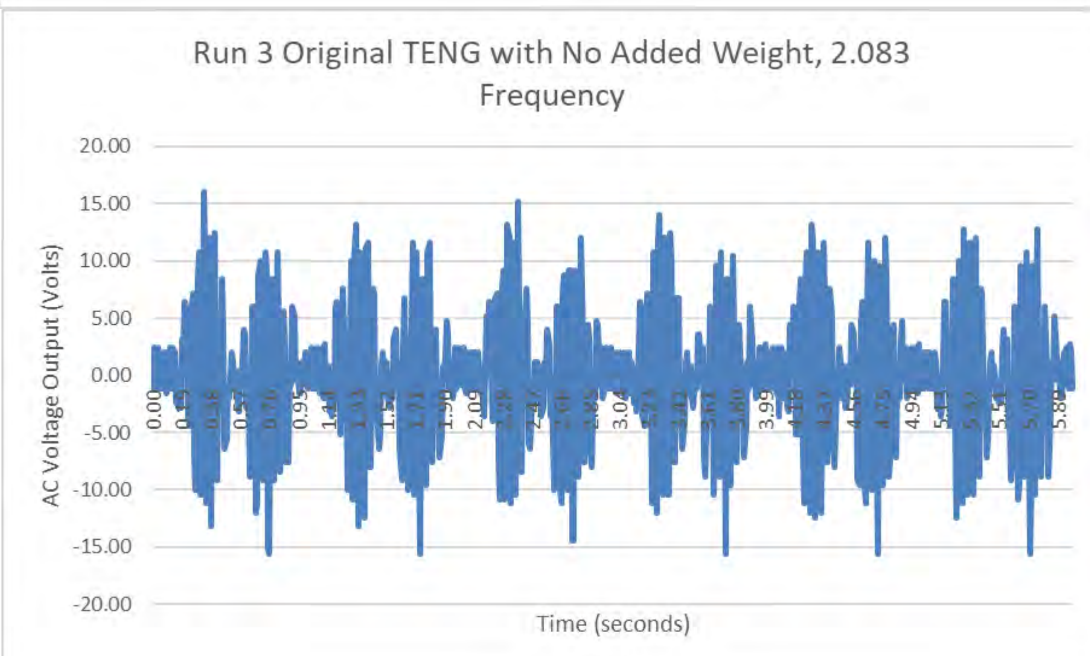

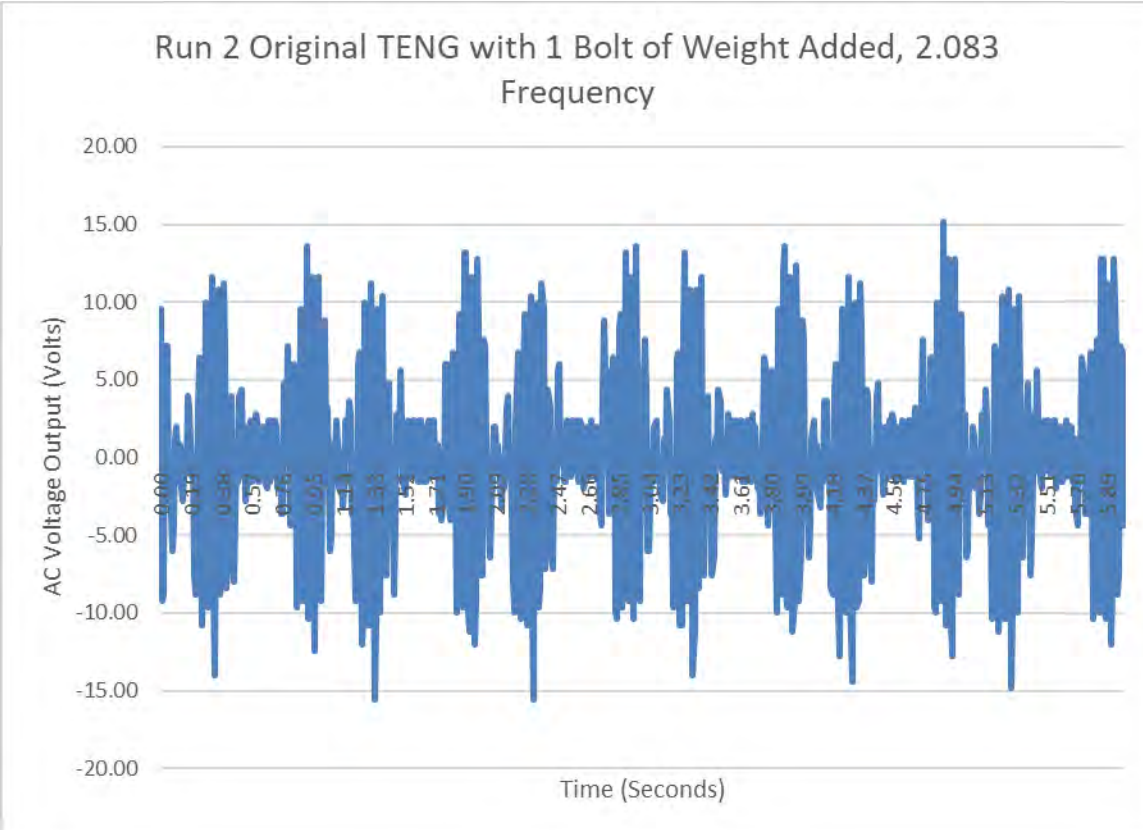
Run 2 Original TENG with 1 Bolt of Weight Added, 2.083 Frequency
AC Voltage Output (Volts)
Time (Seconds)

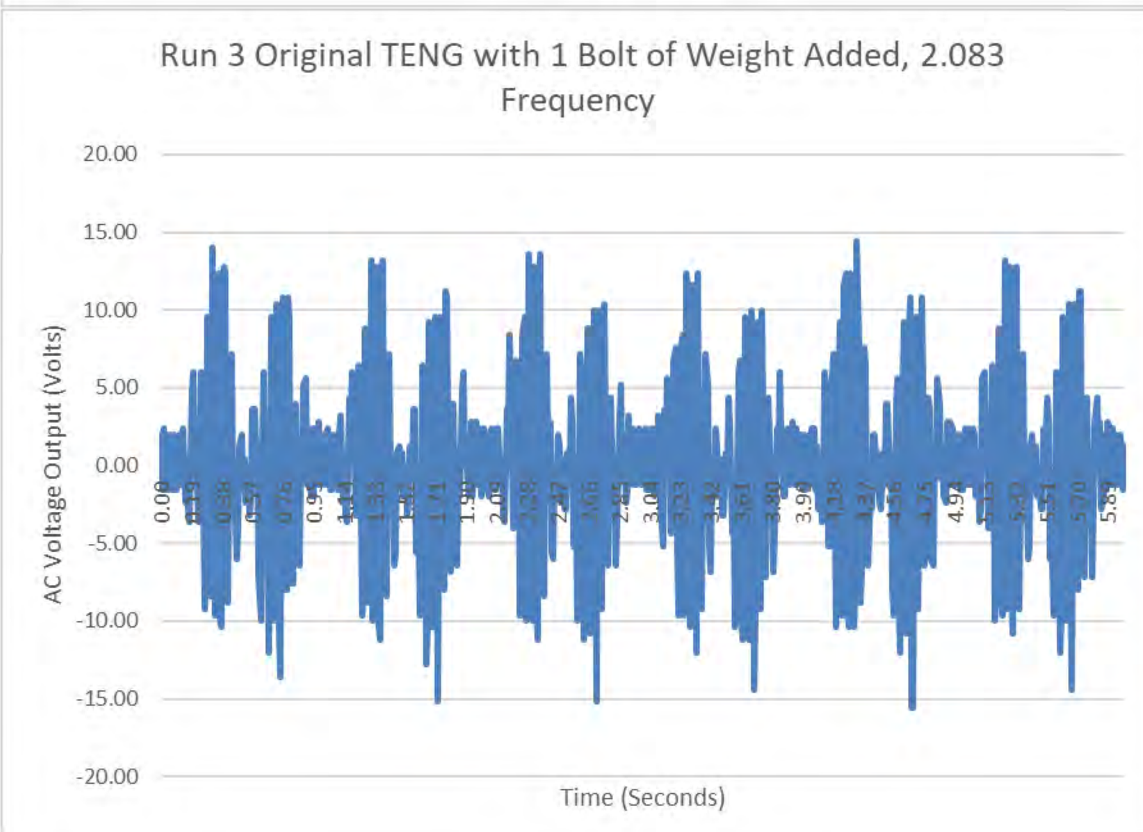
Run 3 Original TENG with 1 Bolt of Weight Added, 2.083 Frequency
AC Voltage Output (Volts)
Time (Seconds)

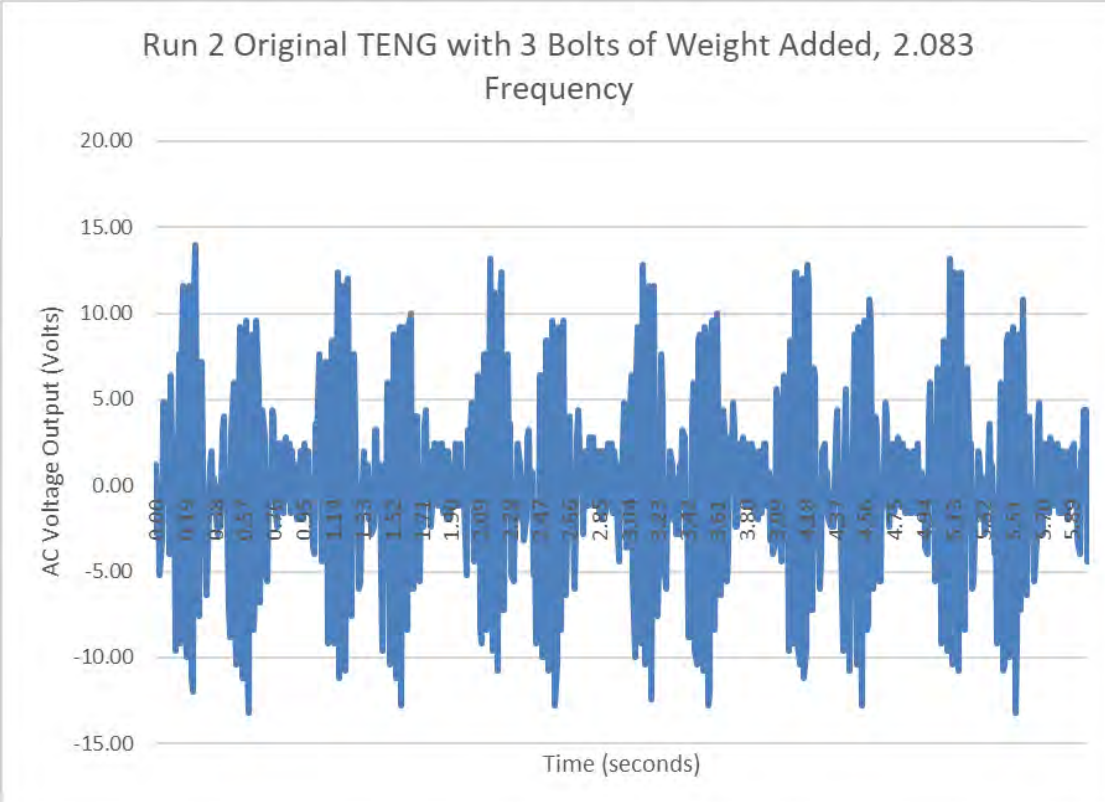
Run 2 Original TENG with 3 Bolts of Weight Added, 2.083 Frequency
20.00
15.00
10.00
5.00
0.00
-5.00
-10.00
-15.00
AC Voltage Output (Volts)
Time (seconds)

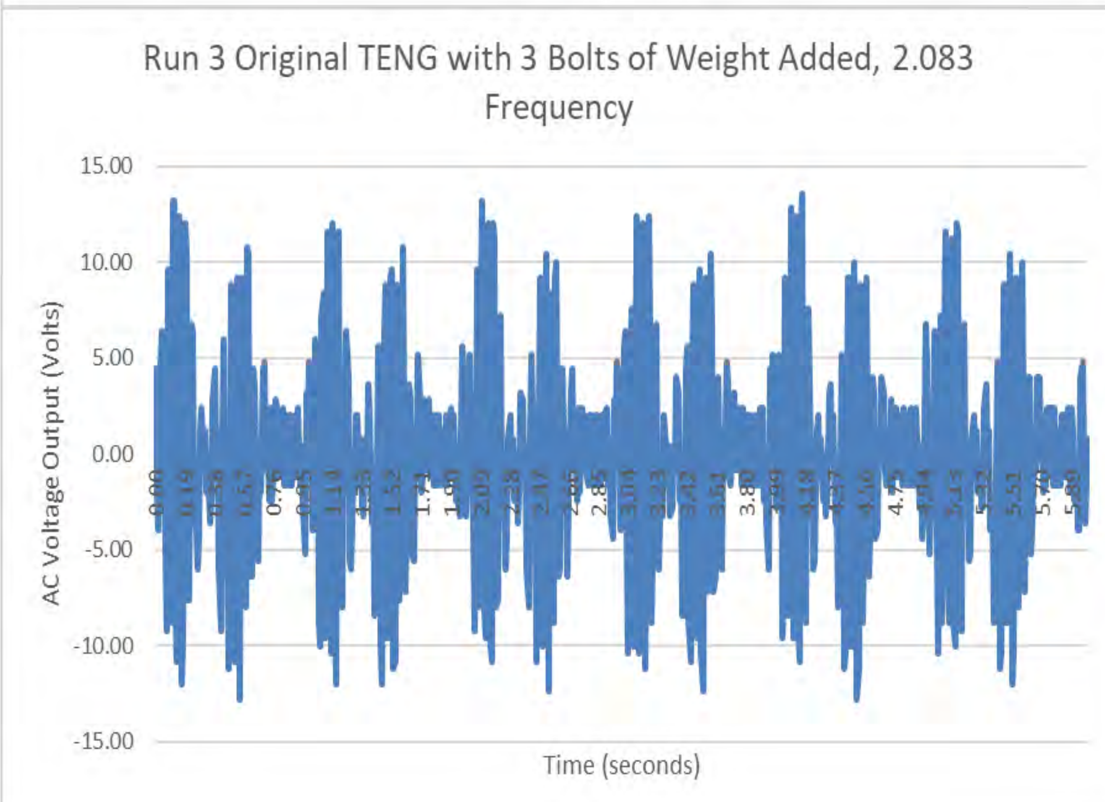
Run 3 Original TENG with 3 Bolts of Weight Added, 2.083 Frequency
15.00
10.00
5.00
0.00
-5.00
-10.00
-15.00
AC Voltage Output (Volts)
Time (seconds)

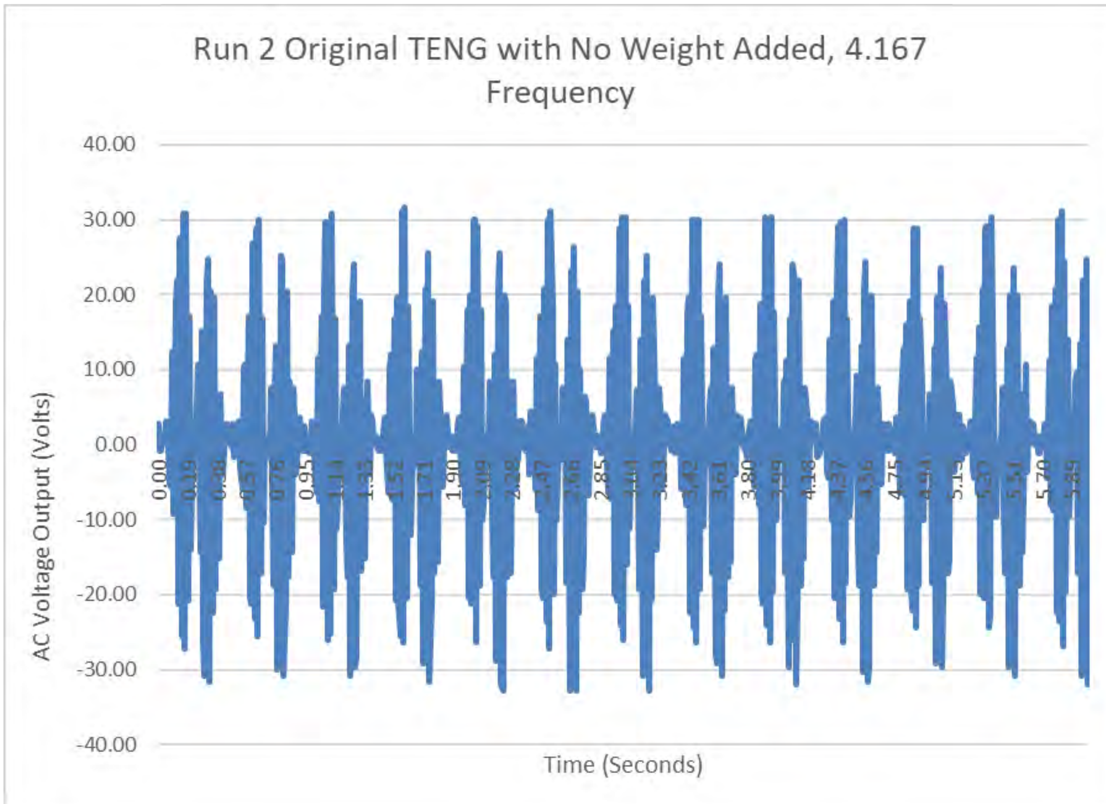
Run 2 Original TENG with No Weight Added, 4.167 Frequency
40.00
30.00
20.00
10.00
0.00
-10.00
-20.00
-30.00
-40.00
AC Voltage Output (Volts)
Time (Seconds)

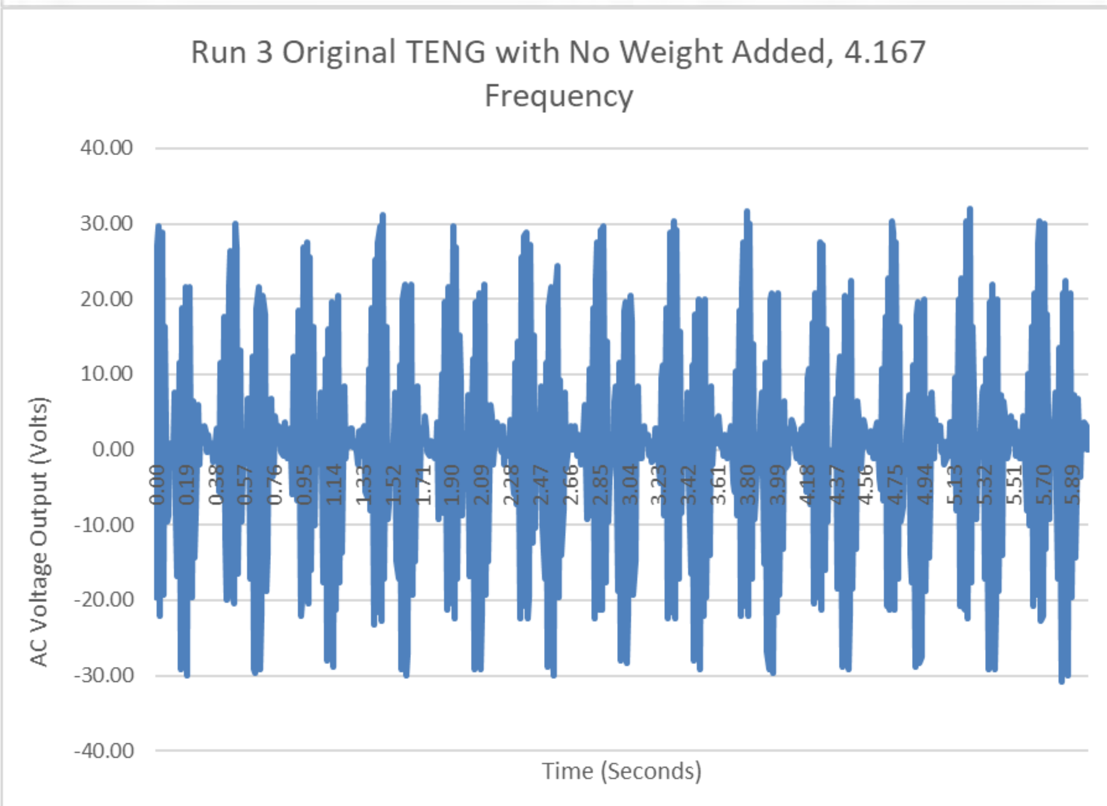
Run 3 Original TENG with No Weight Added, 4.167 Frequency
40.00
30.00
20.00
10.00
0.00
-10.00
-20.00
-30.00
-40.00
AC Voltage Output (Volts)
Time (Seconds)

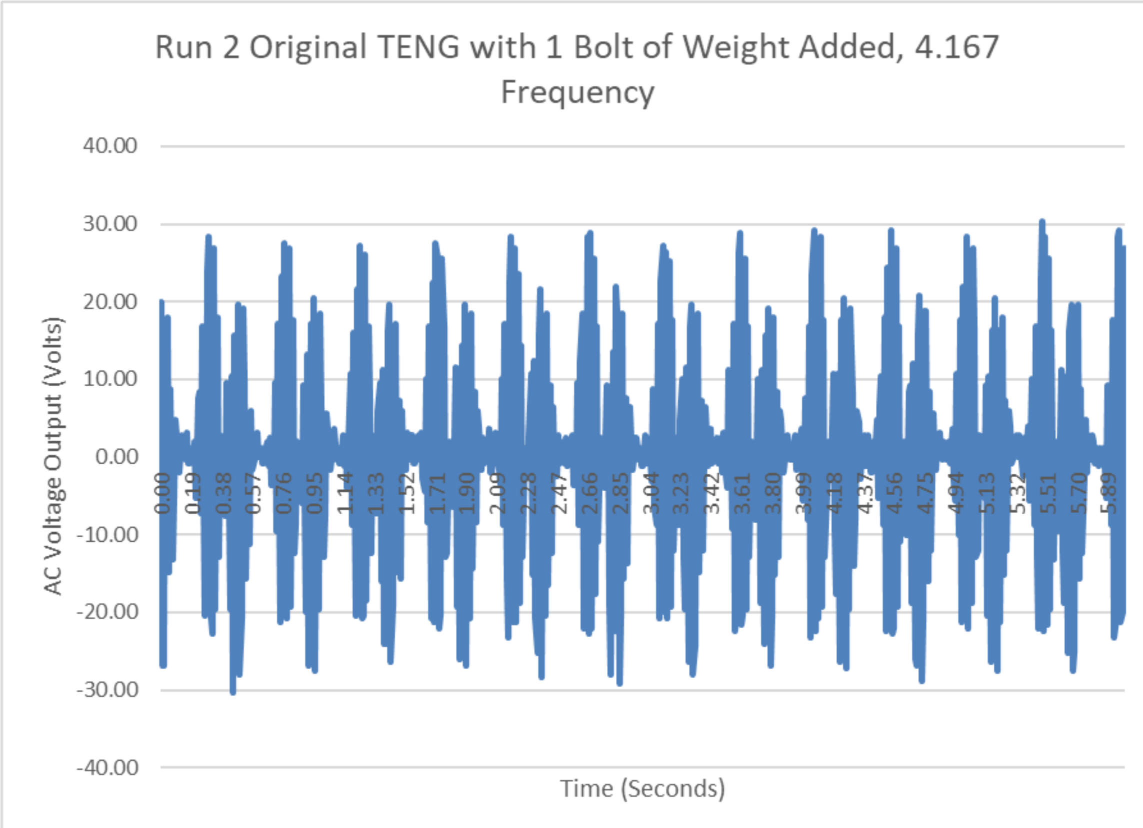
Run 2 Original TENG with 1 Bolt of Weight Added, 4.167 Frequency
AC Voltage Output (Volts)
40.00
30.00
20.00
10.00
0.00
-10.00
-20.00
-30.00
-40.00
0.00 0.19 0.38 0.57 0.76 0.95 1.14 1.33 1.52 1.71 1.90 2.09 2.28 2.47 2.66 2.85 3.04 3.23 3.42 3.61 3.80 3.99 4.18 4.37 4.56 4.75 4.94 5.13 5.32 5.51 5.70 5.89
Time (Seconds)

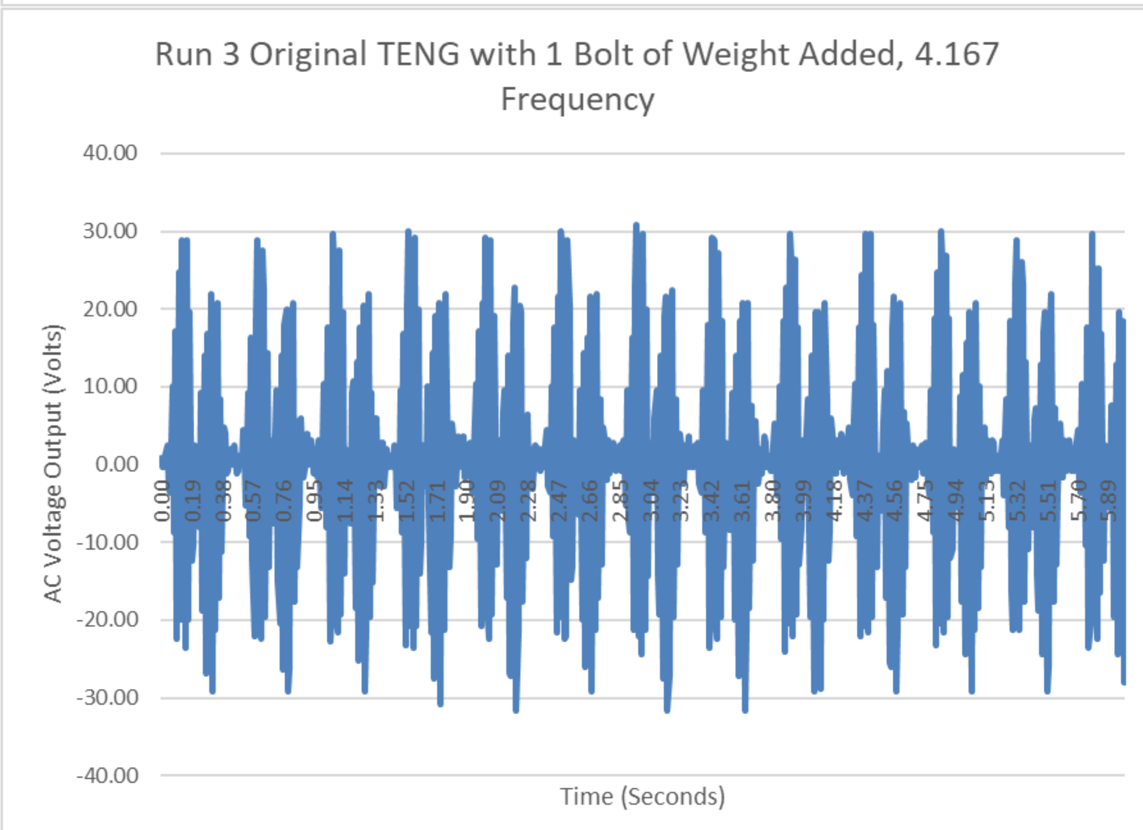
Run 3 Original TENG with 1 Bolt of Weight Added, 4.167 Frequency
AC Voltage Output (Volts)
40.00
30.00
20.00
10.00
0.00
-10.00
-20.00
-30.00
-40.00
0.00 0.19 0.38 0.57 0.76 0.95 1.14 1.33 1.52 1.71 1.90 2.09 2.28 2.47 2.66 2.85 3.04 3.23 3.42 3.61 3.80 3.99 4.18 4.37 4.56 4.75 4.94 5.13 5.32 5.51 5.70 5.89
Time (Seconds)

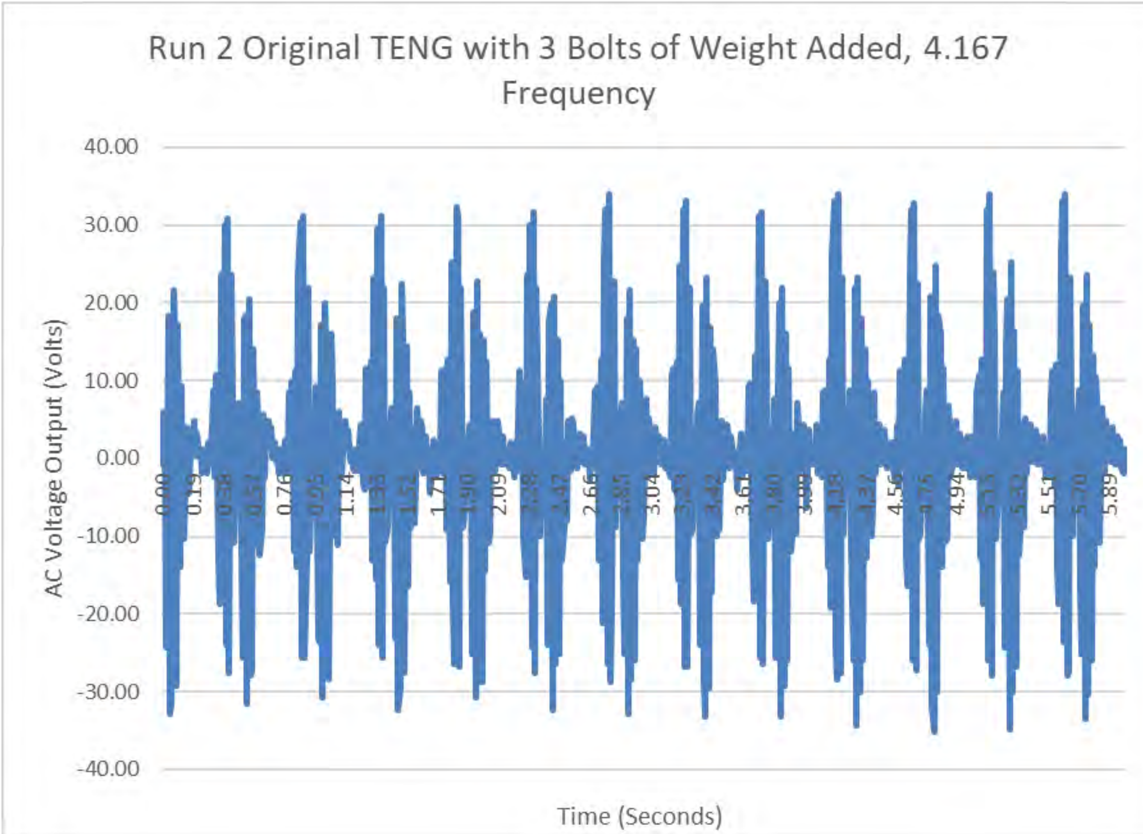
Run 2 Original TENG with 3 Bolts of Weight Added, 4.167 Frequency
AC Voltage Output (Volts)
Time (Seconds)


Run 3 Original TENG with 3 Bolts of Weight Added, 4.167 Frequency
AC Voltage Output (Volts)
Time (Seconds)

APPENDIX B. IMPROVED TENG RESULTS RUNS 2 AND 3

The experimental results for the improved TENG operated with the linear reciprocating motor with different weight and speed conditions follow.

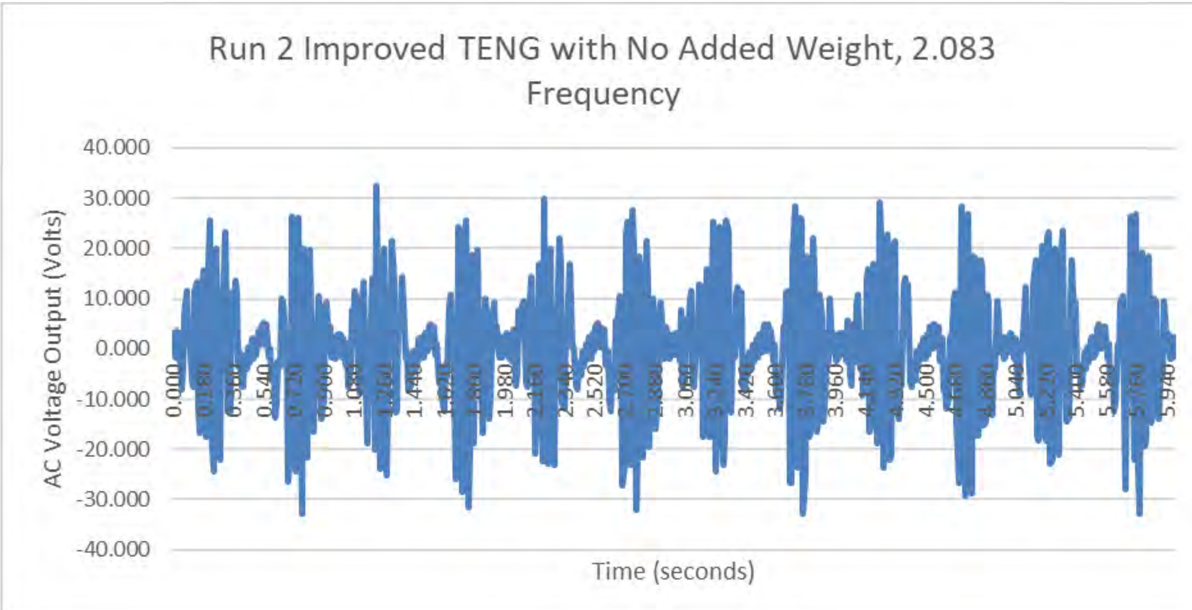

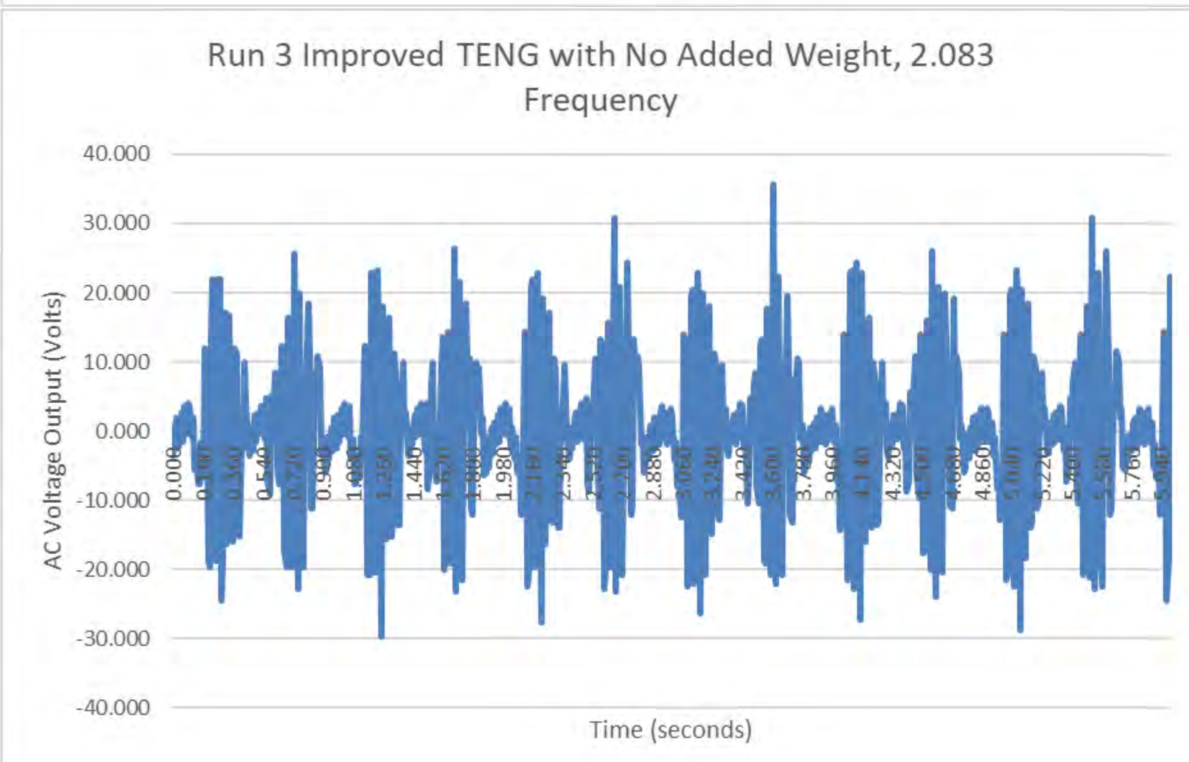

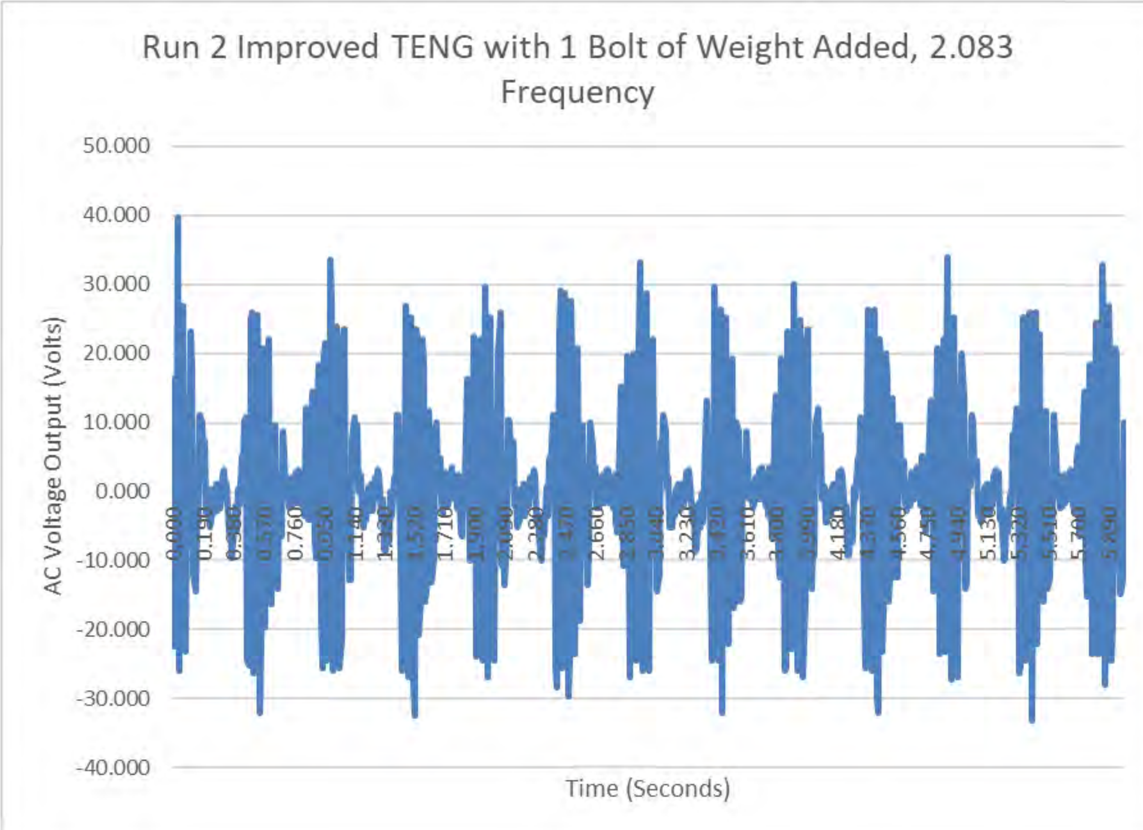
Run 2 Improved TENG with 1 Bolt of Weight Added, 2.083 Frequency
AC Voltage Output (Volts)
50.000
40.000
30.000
20.000
10.000
0.000
-10.000
-20.000
-30.000
-40.000
Time (Seconds)

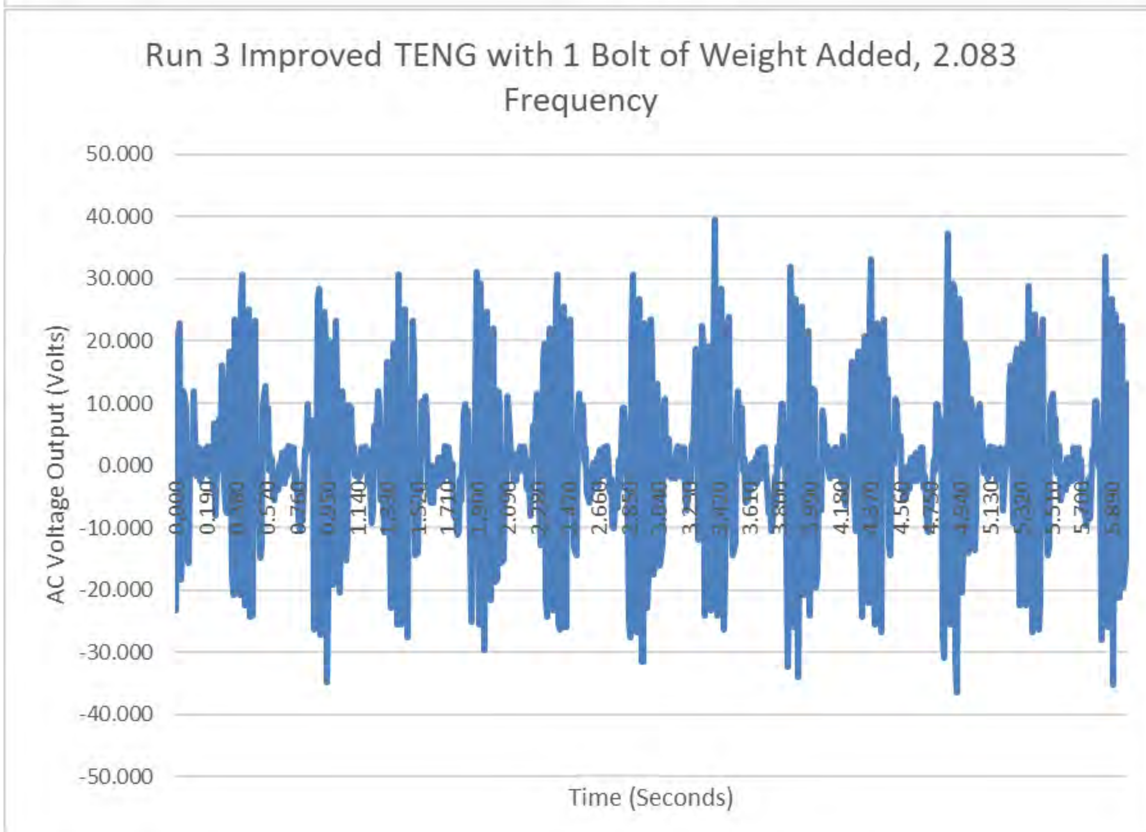
Run 3 Improved TENG with 1 Bolt of Weight Added, 2.083 Frequency
AC Voltage Output (Volts)
50.000
40.000
30.000
20.000
10.000
0.000
-10.000
-20.000
-30.000
-40.000
-50.000
Time (Seconds)

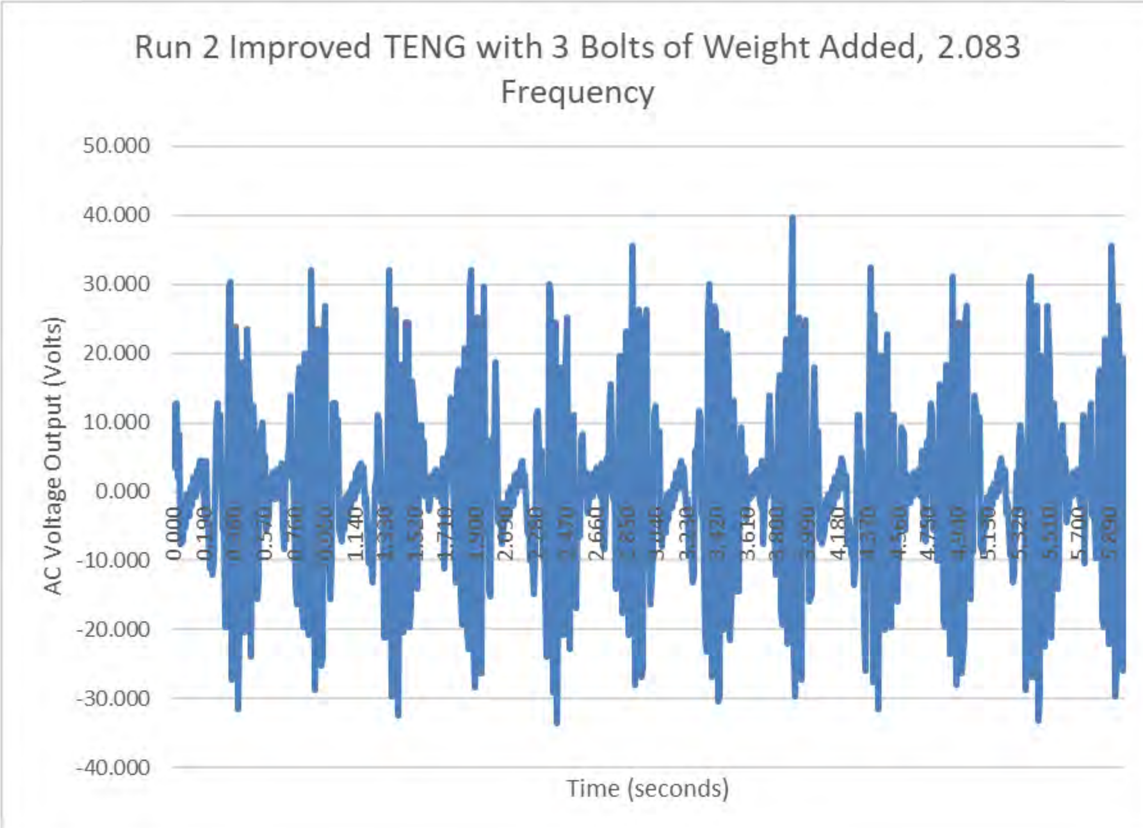
Run 2 Improved TENG with 3 Bolts of Weight Added, 2.083 Frequency
AC Voltage Output (Volts)
Time (seconds)
50.000
40.000
30.000
20.000
10.000
0.000
-10.000
-20.000
-30.000
-40.000


Run 3 Improved TENG with 3 Bolts of Weight Added, 2.083 Frequency
AC Voltage Output (Volts)
Time (seconds)
50.000
40.000
30.000
20.000
10.000
0.000
-10.000
-20.000
-30.000
-40.000
-50.000


Run 2 Improved TENG with No Weight Added, 4.167 Frequency
100.000
80.000
60.000
40.000
20.000
0.000
-20.000
-40.000
-60.000
-80.000
AC Voltage Output (Volts)
Time (Seconds)


Run 3 Improved TENG with No Weight Added, 4.167 Frequency
100.000
80.000
60.000
40.000
20.000
0.000
-20.000
-40.000
-60.000
-80.000
-100.000
AC Voltage Output (Volts)
Time (Seconds)


Run 2 Improved TENG with 1 Bolt of Weight Added, 4.167 Frequency
AC Voltage Output (Volts)
Time (Seconds)
100.000
80.000
60.000
40.000
20.000
0.000
-20.000
-40.000
-60.000
-80.000
-100.000

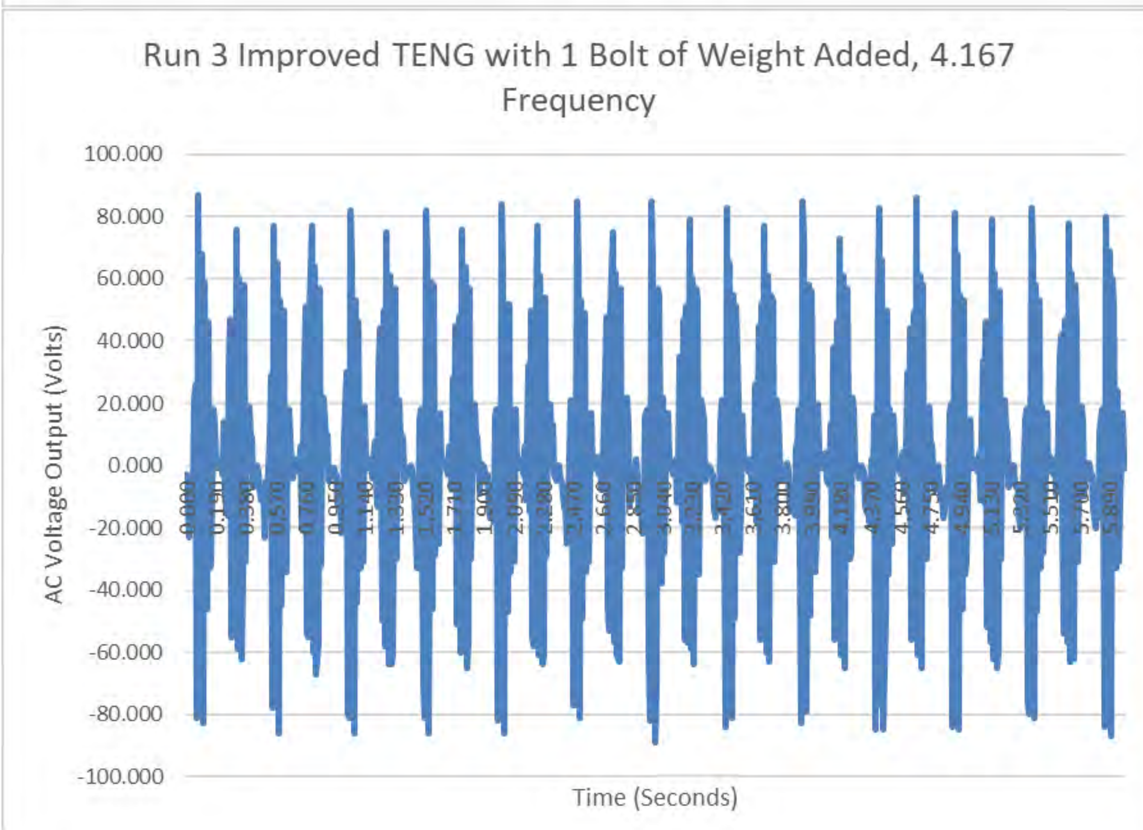
Run 3 Improved TENG with 1 Bolt of Weight Added, 4.167 Frequency
AC Voltage Output (Volts)
Time (Seconds)
100.000
80.000
60.000
40.000
20.000
0.000
-20.000
-40.000
-60.000
-80.000
-100.000

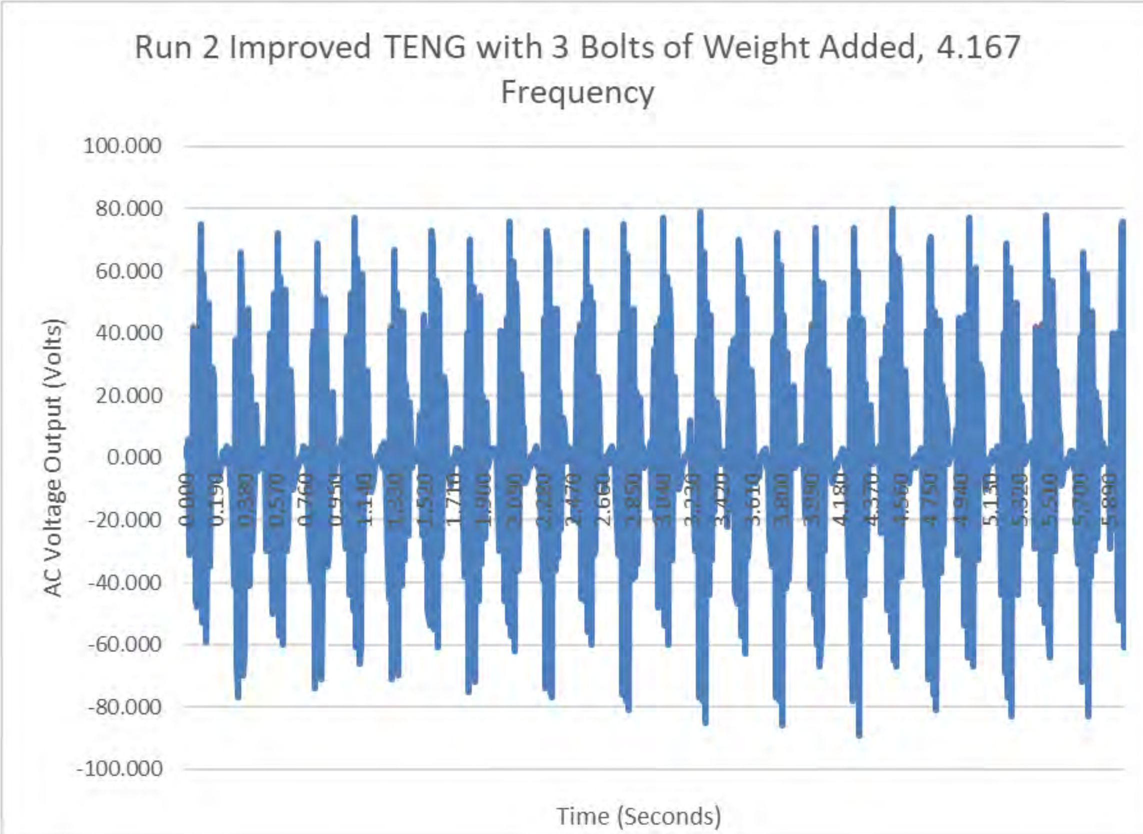
Run 2 Improved TENG with 3 Bolts of Weight Added, 4.167 Frequency
AC Voltage Output (Volts)
Time (Seconds)

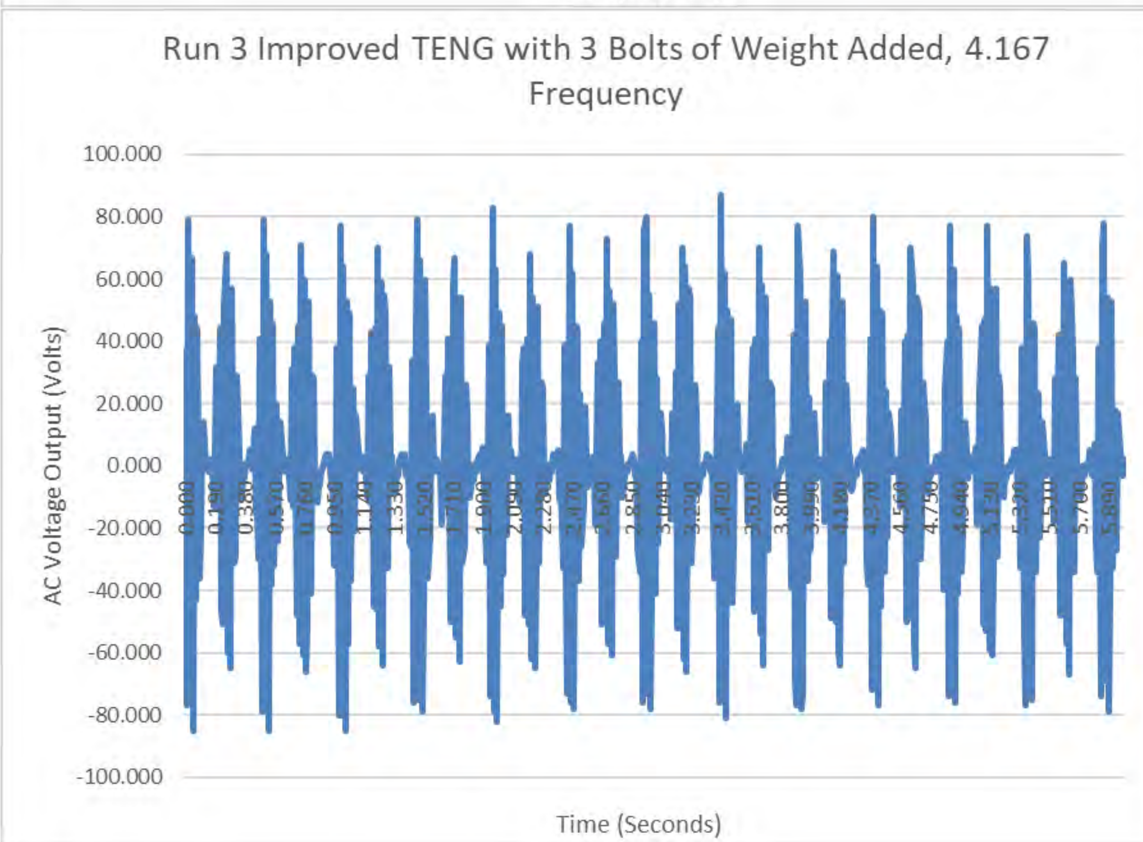
Run 3 Improved TENG with 3 Bolts of Weight Added, 4.167 Frequency
AC Voltage Output (Volts)
Time (Seconds)

APPENDIX C. IMPROVED TENG WITH THINNER PTFE TAPE RUNS 2 AND 3

The experimental results for the improved TENG operated with the linear reciprocating motor and thinner PTFE tape with different weight and speed conditions follow.

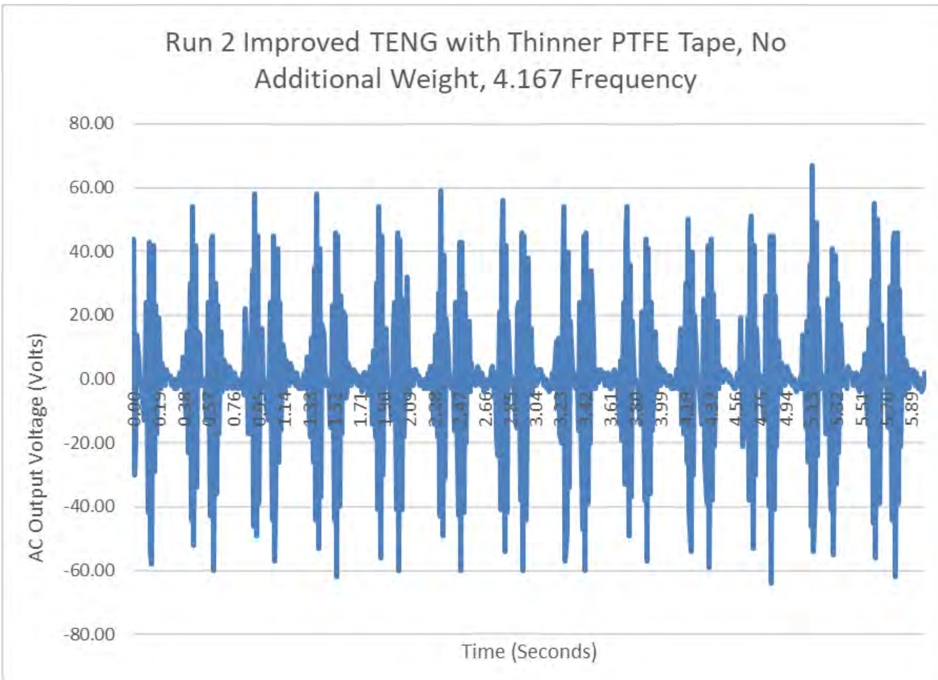

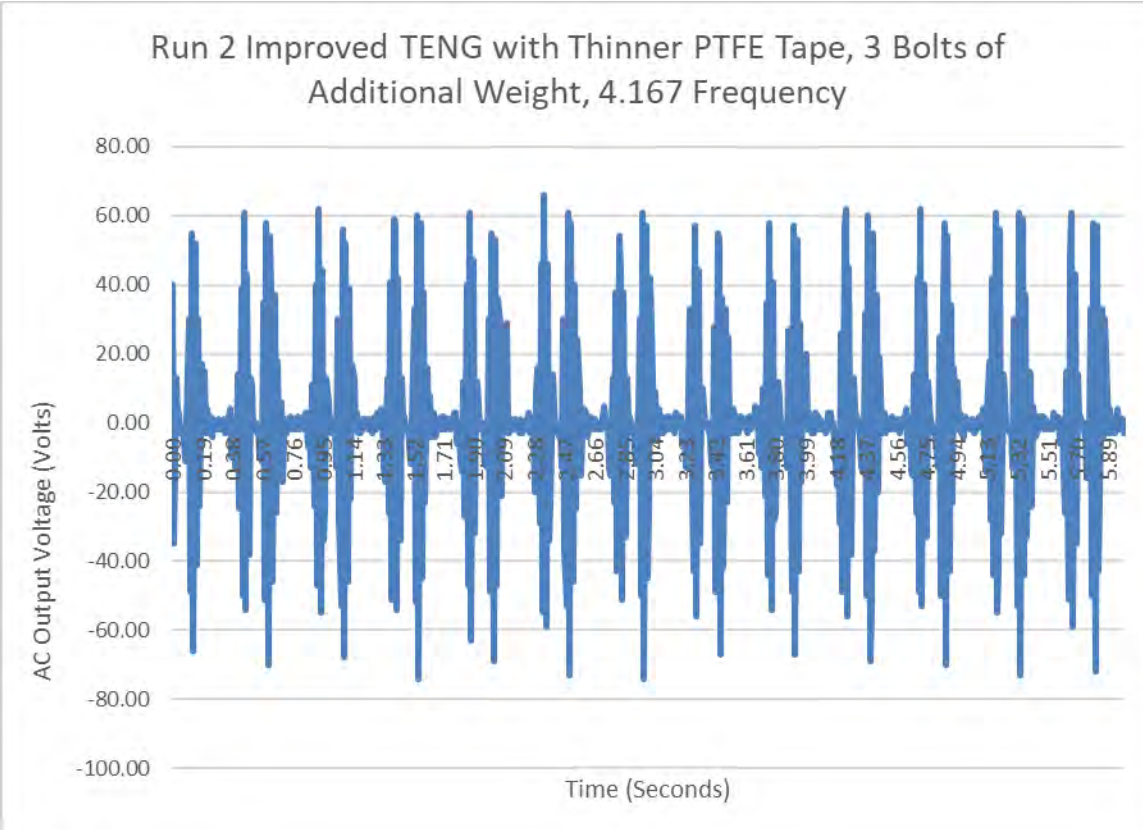
Run 2 Improved TENG with Thinner PTFE Tape, 3 Bolts of Additional Weight, 4.167 Frequency
AC Output Voltage (Volts)
Time (Seconds)

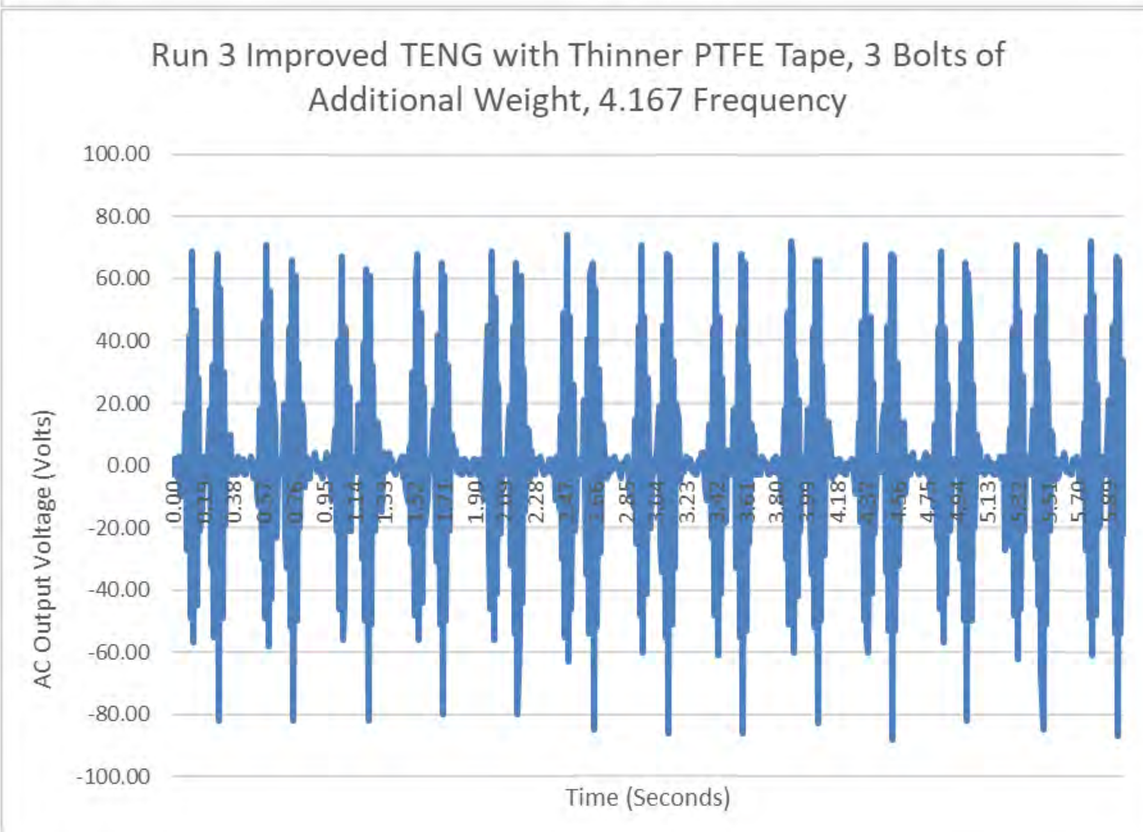
Run 3 Improved TENG with Thinner PTFE Tape, 3 Bolts of Additional Weight, 4.167 Frequency
AC Output Voltage (Volts)
Time (Seconds)

APPENDIX D. MAXIMUM OUTPUTS OF ORIGINAL AND IMPROVED TENGS

The experimental results for the original and improved TENG operated by hand to achieve a maximum AC voltage output follow.

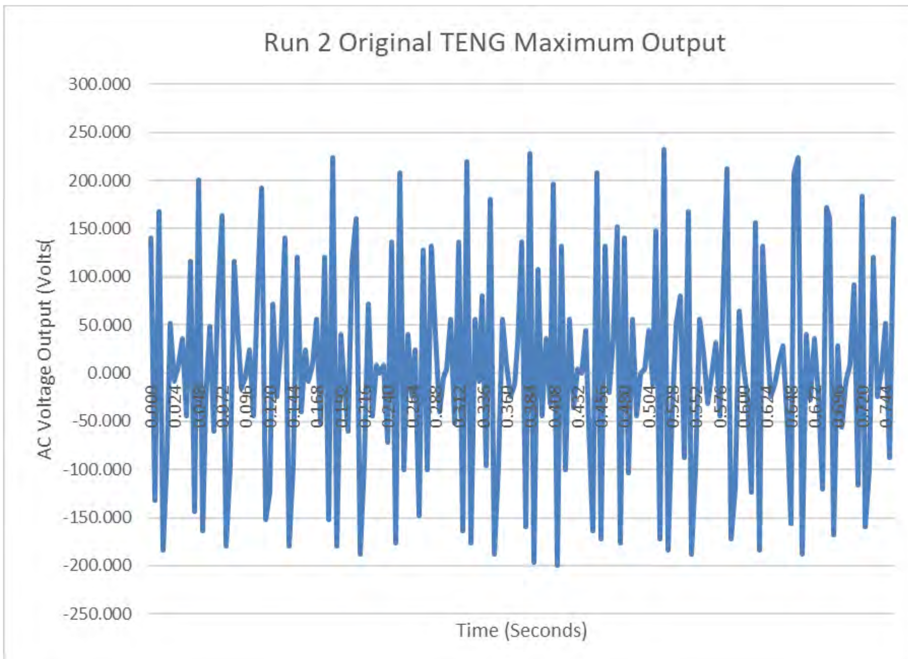

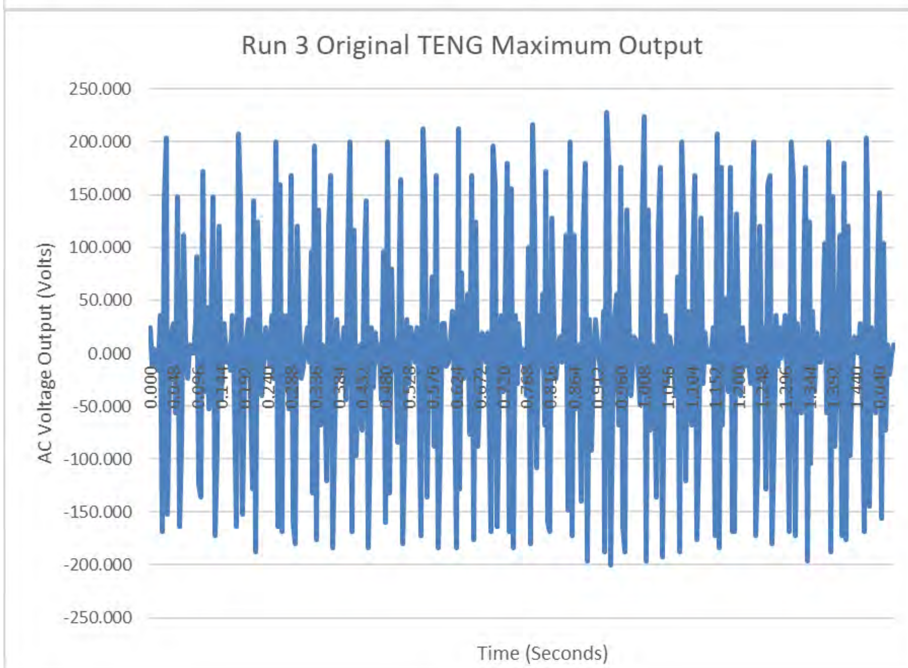


Run 2 Improved TENG Maximum Output
400.000
300.000
200.000
100.000
0.000
-100.000
-200.000
-300.000
-400.000
AC Voltage Output (Volts)
Time (Seconds)

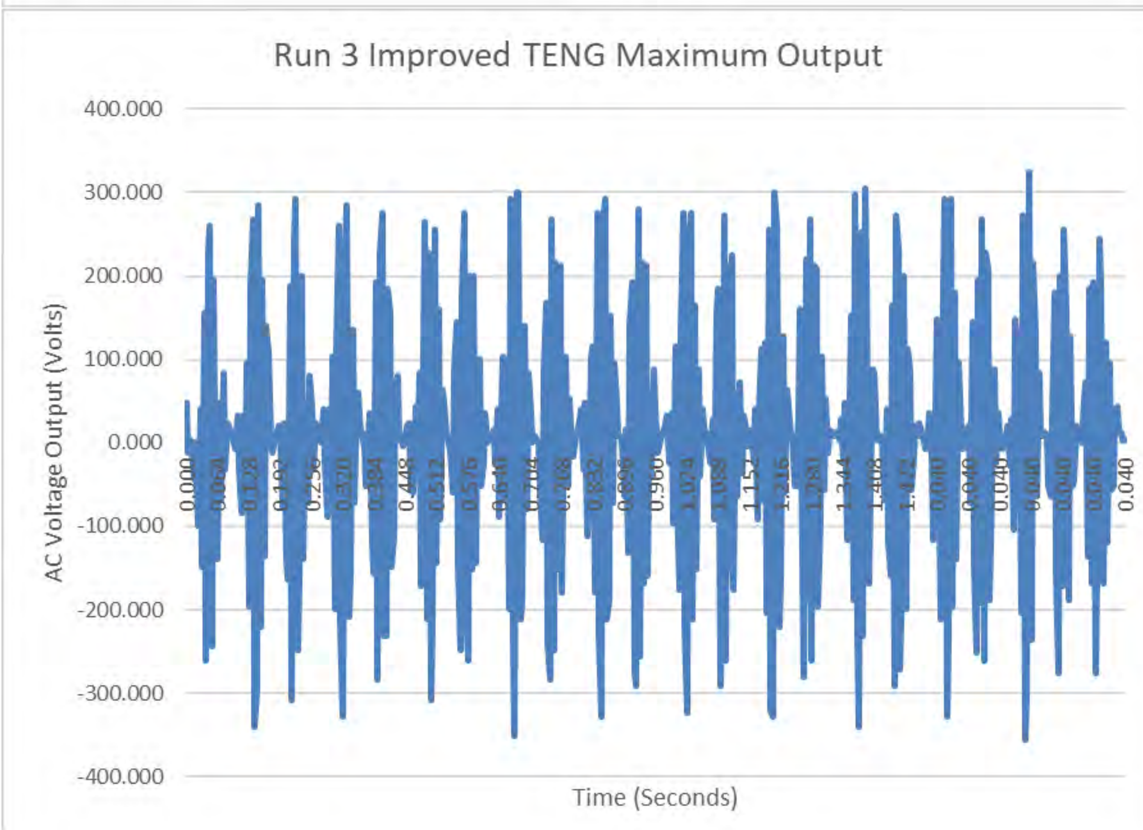
Run 3 Improved TENG Maximum Output
400.000
300.000
200.000
100.000
0.000
-100.000
-200.000
-300.000
-400.000
AC Voltage Output (Volts)
Time (Seconds)

LIST OF REFERENCES

[1] USGS, “How much water is there on Earth?” Accessed November 8, 2018. [Online]. Available: https://water.usgs.gov/edu/earthhowmuch.html

[2] J. Tollefson, “Power from the oceans: Blue energy,” *Nature*, vol. 508, no. 7496, pp. 302–304, Apr. 17, 2014.

[3] National Ocean Service, “How important is the ocean to our economy?” Accessed November 8, 2018. [Online]. Available: https://oceanservice.noaa.gov/facts/oceaneconomy.html

[4] A. Clément, P. McCullen, A. Falcão, A. Fiorentino, F. Gardner, K. Hammarlund, G. Lemonis, T. Lewis, K. Nielsen, S. Petroncini, M. Pontes, P. Schild, B. Sjöström, H.C. Sørensen, and T. Thorpe, “Wave energy in Europe: Current status and perspectives,” *Renewable and Sustainable Energy Reviews*, vol. 6, no. 5, pp. 405–431, Feb. 26, 2002.

[5] B. Drew, A.R. Plummer, and M.N. Sahinkaya, “A review of wave energy converter technology,” *Proceedings of the Institution of Mechanical Engineers, Part A: Journal of Power and Energy*, vol. 223, no. 8, pp. 887–902, Mar. 26, 2009.

[6] A. F. Falcão, “Wave energy utilization: A review of the technologies,” *Renewable and Sustainable Energy Reviews*, vol. 14, no. 3, pp. 899–918, Oct. 22, 2008.

[7] C. Sun, J. Shang, Z. Luo, Z. Lu, and R. Wang, “A review of wave energy extraction technology,” *IOP Conference Series: Materials Science and Engineering*, vol. 394, pp. 042038, 2018.

[8] Z. L. Wang, and J. Song, “Piezoelectric Nanogenerators based on zinc oxide nanowire arrays,” *Science*, vol. 312, no. 5771, pp. 242–246, Apr. 14, 2006.

[9] F. Fan, Z. Tian, and Z. Lin Wang, “Flexible triboelectric generator,” *Nano Energy*, vol. 1, no. 2, pp. 328–334, Jan. 20, 2012.

[10] C. Wu, A. C. Wang, W. Ding, H. Guo, and Z. L. Wang, “Triboelectric nanogenerator: A foundation of the energy for the new era,” *Advanced Energy Materials*, vol. 9, no. 1, pp. 1802906, 2019.

[11] Z. L. Wang, “Triboelectric nanogenerators as new energy technology and self-powered sensors – Principles, problems and perspectives,” *Faraday Discuss.*, vol. 176, pp. 447–458, Sept. 8, 2014.

[12] Z. L. Wang, “On Maxwell’s displacement current for energy and sensors: the origin of nanogenerators,” *Materials Today*, pp. 1–9, Jan. 2017.

[13] S. Niu, Y. Liu, S. Wang, L. Lin, Y. Zhou, Y. Hu, and Z. L. Wang, "Theory of sliding-mode triboelectric nanogenerators," *Advanced Materials*, vol. 25, no. 43, pp. 6184–6193, 2013.

[14] G. Zhu, J. Chen, Y. Liu, P. Bai, Y. S. Zhou, Q. Jing, C. Pan, and Z. L Wang, "Linear-grating triboelectric generator based on sliding electrification.," *Nano Letters*, vol. 13, no. 5, pp. 2282–2289, Apr. 11, 2013.

[15] H. Guo, Q. Leng, X. He, M. Wang, J. Chen, C. Hu, and Y. Xi, "A Triboelectric Generator based on checker-like interdigital electrodes with a sandwiched pet thin film for harvesting sliding energy in all directions," *Advanced Energy Materials*, vol. 5, no. 1, pp. 1400790, 2015.

[16] M. Ma, Z. Kang, Q. Liao, Q. Zhang, F. Gao, X. Zhao, Z. Zhang, and Y. Zhang, "Development, applications, and future directions of triboelectric nanogenerators," *Nano Research*, vol. 11, no. 6, pp. 2951–2969, Jan. 16 2018.

[17] Y. Xi, H. Guo, Y. Zi, X. Li, J. Wang, J. Deng, S. Li, C. Hu, X. Cao, and Z. L. Wang "Multifunctional TENG for Blue energy scavenging and self-powered wind speed sensor," *Advanced Energy Materials*, vol. 7, no. 12, pp.1602397, 2017.

[18] G. Cheng, Z-H Lin, Z-I. Du, and Z. L. Wang, "Simultaneously harvesting electrostatic and mechanical energies from flowing water by a hybridized triboelectric nanogenerator," *ACS Nano*, vol. 8, no. 2, pp. 1932–1939, Jan. 27, 2014.

[19] Q. J. Liang, X. Yan, X. Liao, S. Cao, X. Zheng, H. Si, S. Lu, and Y. Zhang, "Multi- unit hydroelectric generator based on contact electrification and its service behavior," *Nano Energy*, vol.16, pp. 329–338, Jul. 18, 2015.

[20] Q. Liang, X. Yan, X. Liao, and Y. Zhang, "Integrated multi-unit transparent triboelectric nanogenerator harvesting rain power for driving electronics," *Nano Energy*, vol. 25, pp. 18–25, Apr. 20, 2016.

[21] Q. Liang, X. Yan, Y. Gu, K. Zhang, M. Liang, S. Lu, X. Zheng, and Y. Zhang, "Highly transparent triboelectric nanogenerator for harvesting water- related energy reinforced by antireflection coating," *Sci. Rep.*, vol. 5, pp. 9080, Mar. 13, 2015.

[22] Z-H. Lin, G. Cheng, L. Lin, S. Lee, and Z. L Wang, "Water-solid surface contact electrification and its use for harvesting liquid-wave1 energy," *Angew. Chem.*, vol. 52, pp. 12545– 12549, 2013.

[23] Q. Zhang, Q. L. Liang, Q. Liao, F. Yi, X. Zheng, M. Ma, and F. Gao, Y. Zhang, "Service behavior of multifunctional triboelectric nanogenerators.," *Adv. Mater.* vol. 29, pp. 1606703, 2017.

[24] X. Wang, Z. Wen, H. Guo, C. Wu, X. He, L. Lin, X. Cao, X. and Z. L. Wang, "Fully packaged blue energy harvester by hybridizing a rolling triboelectric nanogenerator and an electromagnetic generato," *ACS Nano*, vol. 10, no. 12, pp. 11369-11376, Nov. 22, 2016.

[25] S. Lee, J. Chung, D. Y. Kim, J-Y. Jung, S. H. Lee, and S. Lee, "Cylindrical water triboelectric nanogenerator via controlling geometrical shape of anodized aluminum for enhanced electrostatic induction," *ACS Applied Materials & Interfaces*, vol. 8, no. 38, pp. 25014-25018, Sept. 13, 2016.

[26] T. X. Xiao, T. Jiang, J. X. Zhu, X. Liang, L. Xu, J. J. Shao, C. L. Zhang, J. Wang, and Z. L. Wang, "Silicone-based triboelectric nanogenerator for water wave energy harvesting," *ACS Applied Materials & Interfaces*, vol. 10, no. 4, pp. 3616-3623, Jan. 2, 2018.

[27] L. Xu, T. Jiang, P. Lin, J. Shao, C. He, W. Zhong, X. Y. Chen, and Z. L. Wang, "Coupled triboelectric nanogenerator networks for efficient water wave energy harvesting," ACS *Nano*, vol. 12, no. 2, pp. 1849–1858, Jan. 12, 2018.

[28] Z. Wen, H. Guo, Y. Zi, M-H. Yeh, X. Wang, J. Deng, J. Wang, S. Li, C. Hu, L. Zhu, and Z. L. Wang, "Harvesting broad frequency band blue energy by a triboelectric–electromagnetic hybrid nanogenerator," *ACS Nano*, vol. 10, no. 7, pp. 6526–6534, Jun. 6, 2016.

[29] K. Lee, J-W. Lee, K. Kim, D. Yoo, D.S. Kim, W. Hwang, I. Song, and J-Y. Sim, "A spherical hybrid triboelectric nanogenerator for enhanced water wave energy harvesting," *Micromachines*, vol. 9, no. 11, p. 598, Nov. 15, 2018.

[30] Y. Su, X. Wen, G. Zhu, J. Yang, J. Chen, P. Bai, Z. Wu, Y. Jiang, and Z. L. Wang, "Hybrid triboelectric nanogenerator for harvesting water wave energy and as a self-powered distress signal emitter," *Nano Energy*, vol. 9, pp. 186–195, Aug. 6, 2014.

[31] J. Chen, J. Yang, Z. Li, X. Fan, Y. Zi, Q. Jing, H. Guo, Z. Wen, K. Pradel, S. Niu, and Z. L Wang, "Networks of triboelectric nanogenerators for harvesting water wave energy: A potential approach toward blue energy," *ACS Nano*, vol. 9, no. 3, pp. 3324–3331, Feb. 26, 2015.

[32] L. Xu, Y. Pang, C. Zhang, T. Jiang, X. Chen, J. Luo, W. Tang, X. Cao, and Z. L. Wang, "Integrated triboelectric nanogenerator array based on air-driven membrane structures for water wave energy harvesting," *Nano Energy*, vol. 31, pp.351-358, Nov. 17, 2016.

[33] G. Zhu, Y. Su, P. Bai, J. Chen, Q. Jing, W. Yang, and Z. L. Wang, "Harvesting water wave energy by asymmetric screening of electrostatic charges on a nanostructured hydrophobic thin-film surface. *ACS Nano*, vol. 8, no. 6, pp. 6031–6037, Apr. 18, 2014.

[34] Z. Saadatnia, E. Asadi, H. Askari, J. Zu and E. Esmailzadeh, “Modeling and performance analysis of duck-shaped triboelectric and electromagnetic generators for water wave energy harvesting,” *International Journal of Energy Research*, vol. 41, no. 14, pp. 2392–2404, 2017.

[35] M-L. Seol, J-W. Han, D_I. Moon, K. J. Yoon, C. S. Hwang, and M. Meyyappan, “All-printed triboelectric nanogenerator,” *Nano Energy*, vol. 44, pp. 82–88, Nov. 28, 2017.

[36] A. F. Diaz, and R. M. Felix-Navarro, “A semi-quantitative tribo-electric series for polymeric materials: the influence of chemical structure and properties,” *Journal of Electrostatics*, vol. 62, pp. 277–290, May 12, 2004.

[37] K. Xia, Z. Zhu, H. Zhang, C. Du, R. Wang, Z. Xu, “Cost-effective triboelectric nanogenerator based on Teflon tape and conductive copper foil tape,” *Microelectronic Engineering*, vol. 199, pp. 114–117, Aug. 14, 2018.

INITIAL DISTRIBUTION LIST

1. Defense Technical Information Center
   Ft. Belvoir, Virginia

2. Dudley Knox Library
   Naval Postgraduate School
   Monterey, California